

Prom. Nr. 3442

**Investigation
of a thyatron- or thyristor-controlled synchronous
motor by simulation on an analog computer**

THESIS

presented to

THE SWISS FEDERAL INSTITUTE OF TECHNOLOGY, ZURICH

for the degree of
Doctor of Technical Sciences

by

Mohamed Mahmoud Bayoumi

B.Sc. Electrical Engineering
Citizen of Egypt

Accepted on the recommendation of
Prof. ED. GERECKE and Prof. A. DUTOIT

Buchdruckerei Berichthaus

Zurich 1963

Leer - Vide - Empty

**Investigation
of a thyatron- or thyristor-controlled synchronous
motor by simulation on an analog computer**

Leer - Vide - Empty

To my Parents and to my wife

Leer - Vide - Empty

ACKNOWLEDGMENT

I am greatly indebted to Professor ED. GERECKE for his valuable suggestions and helpful guidance that enabled me to accomplish this research.

My thanks are also due to Professor A. DUTOIT for his consent to examine this thesis.

CONTENTS

Notations	10
<i>1. Introduction</i>	16
<i>2. Preliminary experimentation</i>	18
2.1 Machines and instruments used	18
2.2 Single-phase investigation	18
2.2.1 Connection diagram	18
2.2.2 Oscillograms	21
2.2.3 External characteristics	23
2.3 Three-phase investigation	24
2.3.1 Connection diagram	24
2.3.2 Oscillograms	27
<i>3. Mathematical analysis of the synchronous machine</i>	30
3.1 The machine equations expressed in the per-unit form	34
<i>4. Determination of the machine constants</i>	36
4.1 Stator resistance and leakage reactance	36
4.2 Field time constant	36
4.3 Direct and quadrature axis synchronous reactances	36
4.4 Determination of the leakage coefficients in the direct axis direction	37
4.5 Direct axis transient and subtransient reactances and time constants	39
4.6 Determination of the leakage coefficient and time constant in the quadrature axis direction	42
<i>5. Machine as a synchronous generator</i>	47
<i>6. Analog Computation of the single-phase controlled synchronous machine</i>	53
6.1 Mathematical formulation	53

6.2	Simulation of the inverter effect	59
6.3	Analog set-up	60
6.4	Analog Computer results	60
6.4.1	Oscillograms	60
6.4.2	External characteristics	63
6.4.3	Current locus	66
7.	<i>Analog computation of the three-phase controlled synchronous machine</i>	69
7.1	The mathematical formulation	69
7.2	Machine with variable speed	82
7.3	The thyatron simulator	83
7.3.1	Block diagram	87
7.3.2	The "saw-tooth" generators	87
7.3.3	The coinciding voltages	89
7.3.4	The Schmitt trigger	89
7.3.5	The pulses determining the end-points of the currents	90
7.3.6	The bistable multivibrator	90
7.3.7	The gate	90
7.3.8	Advantages of the thyatron simulator	94
8.	<i>Analog investigation</i>	95
9.	<i>Simulation of the system on the PACE analog computer</i>	100
9.1	The mathematical formulation	100
9.2	Oscillograms	112
9.3	Characteristic curves	124
9.3.1	External characteristics	124
9.3.2	Current locus	124
9.4	Behaviour of the air gap flux vector	124
9.5	Transient behaviour	128
10.	<i>Summary and conclusion</i>	139
	Zusammenfassung	141
	Literature	143

NOTATIONS

- i_1, i_2, i_3 = the stator currents flowing in phases No. 1, 2 and 3 respectively (in ampere)
- i_1^r = the stator current flowing in phase No. 1 when it is expressed in the per-unit system
 All the currents, voltages, fluxes and resistances are characterized by the letter r when they are expressed in their relative form
- i_f = the current flowing in the field winding
- i_D = the current flowing in the damper winding in the direct axis direction
- i_Q = the current flowing in the damper winding in the quadrature axis direction
- i_α = the current flowing through the hypothetical winding in the α direction to replace the stator. The α direction coincides with the direction of the phase No. 1, i.e. it is fixed with respect to the stator
- i_β = the current flowing through the hypothetical winding in the β direction that is also fixed with respect to the stator windings. The β direction advances that of phase No. 1 by 90°
- i_0 = the zero sequence current
- i_d = the current flowing through the hypothetical winding in the d direction to replace the stator. The d direction coincides with the axis of the rotor
- i_q = the current flowing through the hypothetical winding in the q direction which advances the d direction by 90°
- $I_n \sqrt{2}$ = the amplitude of the stator current at normal load
- $i_{d.c.}$ = the current flowing from the d.c. voltage U_d through the smoothing inductance (refer to *Fig. 1*)
- $I_{d.c.}$ = the average value of the current $i_{d.c.}$
- I_{1s} = the fundamental component of the stator current i_1 in phase with $\sin \gamma$

I_{1c}	= the fundamental component of the stator current i_1 in phase with $\cos \gamma$
U_d	= a d.c. voltage source used to feed the stator of the synchronous machine through thyratrons
u_1, u_2, u_3	= the phase voltages of the synchronous machine in volts
u'_1, u'_2, u'_3	= the voltages between the three terminals of the stator of the synchronous machine and the middle point of the d.c. power supply
u'_0	= the voltage of the star point with respect to the middle point of the battery
u'_{0k}	= the voltage of the star point with respect to the negative pole of the battery
U_f	= a d.c. voltage source used to feed the field winding of the synchronous machine
$U_n \sqrt{2}$	= the amplitude of the normal phase voltage
U_{1s}	= the fundamental component of the phase voltage u_1 in phase with $\sin \gamma$
U_{1c}	= the fundamental component of the phase voltage u_1 in phase with $\cos \gamma$
R	= resistance of the stator winding in ohms
R_f	= resistance of the field winding
R_D	= resistance of the damper winding in the direct axis direction
R_Q	= resistance of the damper winding in the quadrature axis direction
T_f	= the field time constant
T_D	= the damper winding time constant (coil D)
T_Q	= the damper winding time constant (coil Q)
L_{dd}	= the direct axis synchronous inductance
X_d	= the direct axis synchronous reactance in ohms
x_d	= the direct axis synchronous reactance in per unit
L_{qq}	= the quadrature axis synchronous inductance
X_q	= the quadrature axis synchronous reactance in ohms
x_q	= the quadrature axis synchronous reactance in per unit
L_{fd}	= the mutual inductance between the field coil and the d coil
L_{Dd}	= the mutual inductance between the D coil and the d coil
L_{Df}	= the mutual inductance between the D coil and the field coil

L_{DD}	= the self-inductance of the D coil
L_{ff}	= the self-inductance of the field winding
L_{QQ}	= the self-inductance of the Q coil
L_{Qq}	= the mutual inductance between the Q coil and the q coil
μ_d	$= 1 - \frac{L_{dD} L_{fd}}{L_{dd} L_{fD}}$
μ_f	$= 1 - \frac{L_{fD} L_{df}}{L_{ff} L_{dD}}$
μ_D	$= 1 - \frac{L_{Df} L_{dD}}{L_{DD} L_{df}}$
σ_{df}	$= 1 - \frac{L_{df} L_{fd}}{L_{ff} L_{dd}}$
σ_{dD}	$= 1 - \frac{L_{dD} L_{Dd}}{L_{DD} L_{dd}}$
σ_{Df}	$= 1 - \frac{L_{Df} L_{fD}}{L_{DD} L_{ff}}$
σ_q	$= 1 - \frac{L_{qQ} L_{Qq}}{L_{QQ} L_{qq}}$
x_d''	= the direct axis subtransient synchronous reactance in per unit
x_d'	= the direct axis transient synchronous reactance in per unit
X_l	= the leakage reactance in ohms
x_q''	= the quadrature axis subtransient synchronous reactance in per unit
L_q''	= the quadrature axis subtransient synchronous inductance
ψ_1, ψ_2, ψ_3	= the flux linking the stator coils 1, 2 and 3 respectively
ψ_f	= the flux linking the field winding
ψ_D, ψ_Q	= the flux linking the D and Q coils respectively
ψ_α, ψ_β	= the flux linking the α and β coils respectively
ψ_d, ψ_q	= the flux linking the d and q coils respectively
ψ_0	= the zero sequence flux
t	= time in seconds
τ	= the per-unit value of the time

- f_n = the normal frequency of the synchronous machine
 n_s = the synchronous speed
 P_{sn} = $3 U_n I_n$
 α' = the firing angle measured as the angle between the axis of the phase No. 1 and the rotor axis at the point of begin of the current flowing in phase No. 1 (see Fig. 19)
 ξ = conduction angle
 γ = the angle between the axis of the phase No. 1 and the rotor axis
 $\omega_m = \dot{\gamma}$ = the instantaneous value of the angular speed
 ω_n = $2 \pi f_n$
 ω_s = the angular synchronous speed
 N_p = the number of pairs of poles
 ρ = friction coefficient
 J = moment of inertia
 T_m = mechanical time constant
 M_a = mechanical torque
 M_e = electromagnetic torque

$$[u] = \begin{bmatrix} u_d \\ 0 \\ U_f \\ u_q \\ 0 \end{bmatrix}, \quad [i] = \begin{bmatrix} i_d \\ i_D \\ i_f \\ i_q \\ i_Q \end{bmatrix}$$

$$[R] = \begin{bmatrix} R & 0 & 0 & 0 & 0 \\ 0 & 1 & 0 & 0 & 0 \\ 0 & 0 & 1 & 0 & 0 \\ 0 & 0 & 0 & R & 0 \\ 0 & 0 & 0 & 0 & 1 \end{bmatrix}, \quad [L'] = \begin{bmatrix} 0 & 0 & 0 & -x_q & -1 \\ 0 & 0 & 0 & 0 & 0 \\ 0 & 0 & 0 & 0 & 0 \\ x_d & 1 & 1 & 0 & 0 \\ 0 & 0 & 0 & 0 & 0 \end{bmatrix}$$

$$[L] = \begin{bmatrix} x_d & 1 & 1 & 0 & 0 \\ T_D \cdot x_d(1-\sigma_{dD}) & T_D & T_D(1-\mu_D) & 0 & 0 \\ T_f \cdot x_d(1-\sigma_{df}) & T_f(1-\mu_f) & T_f & 0 & 0 \\ 0 & 0 & 0 & x_q & 0 \\ 0 & 0 & 0 & T_Q \cdot x_q(1-\sigma_q) & T_Q \end{bmatrix}$$

The reference quantities taken by LAIBLE [3] are used throughout the whole of this thesis. The following table gives the physical quantities and their corresponding reference values.

Physical value	Reference value
(a) stator voltages	$U_n \sqrt{2}$
(b) stator currents	$I_n \sqrt{2}$
(c) stator flux linkages	$\psi_n = \frac{U_n \sqrt{2}}{\omega_n}$
(d) stator impedances	$R_n = \frac{U_n}{I_n}$
(e) active, reactive and total power	$3 U_n \cdot I_n$
(f) torque	$\frac{P_{sn}}{\omega_s} = \frac{3 U_n \cdot I_n}{\omega_n / N_p}$
(g) speeds	n_s
angular speeds	$\frac{\omega_n}{N_p} = \omega_s$
(h) time t	$\tau = 2 \pi t$
(i) field current	$\frac{U_n \sqrt{2}}{\omega_n \cdot L_{fd}}$
(j) field flux linkage	$\frac{U_n \sqrt{2}}{\omega_n} \cdot \frac{L_{ff}}{L_{fd}}$
(k) current in the damper winding in the direct axis	$\frac{U_n \sqrt{2}}{\omega_n \cdot L_{Dd}}$
(l) flux linking the damper winding in the direct axis	$\frac{U_n \sqrt{2}}{\omega_n} \cdot \frac{L_{DD}}{L_{Dd}}$
(m) current in the damper winding in the quadrature axis	$\frac{U_n \sqrt{2}}{\omega_n \cdot L_{Qq}}$
(n) flux linking the damper winding in the quadrature axis	$\frac{U_n \sqrt{2}}{\omega_n} \cdot \frac{L_{QQ}}{L_{Qq}}$

Where the per-unit system is not applied, the Giorgi system of units has been used. The recommendations for mercury arc vapour of the International Electrotechnical Commission (IEC) [19] and the list of symbols suggested by the Association of the Swiss Electrical Engineers (SEV) [18] have been adopted, especially:

[V]	volts
[mV]	millivolt
[A]	ampere
[mA]	milliamperere
[VA]	volt-ampere
[kVA]	kilovolt-ampere
[HP]	horsepower
[s]	seconds
[ms]	milliseconds
[Hz]	Hertz = cycle/second
[rev/min]	revolutions per minute

1. INTRODUCTION

Since the invention of the first electric motor, one of the aims was to control the speed of that motor. It is possible to vary the speed of the d.c. motor smoothly and at will, however it has some disadvantages. One of these disadvantages is that there is a maximum limit on its power and on the applied voltage. The voltage is limited because it is mostly applied on the rotor through brushes and segments. On the other hand, the synchronous motor has a fixed speed, namely the synchronous speed, while the maximum limit put on its power and on the applied voltage is much greater than those corresponding to the d.c. motor.

It is desirable to combine the advantages of the synchronous motor and those of the d.c. motor. This can be achieved by the noncommutator motor, being a synchronous machine in construction and fed either from a d.c. supply through inverters or from an a.c. supply through a set of rectifiers and another of inverters. Thyratrons or silicon-controlled rectifiers can be used as inverters or rectifiers. The speed control is fairly easy, while the limit put on the maximum applied voltage and on its power is high. There are no troubles resulting from the commutation as those involved with the d.c. motors.

Another advantage presented by the noncommutator motor operating from a d.c. supply is that the thyatron tubes can be located at any convenient place and when silicon-controlled rectifiers are used, then a very small volume is necessary.

The noncommutator motor offers advantages of simplified construction and improved insulation over the conventional d.c. motor. It shows great promise as an adjustable speed motor of great flexibility against classical a.c. motors. In its behaviour, the motor is analogous to a commutator motor, where the group of thyatron tubes (or silicon-controlled rectifiers) takes the place of the commutator.

The speed variation of this type of motors can be executed by changing:

- (a) the firing angle of the inverter tubes,
- (b) the magnitude of the field current,
- (c) the amplitude of the applied d.c. voltage, which is effectively done by changing the firing angle of the rectifier tubes when the motor is fed from an a.c. supply, or by

(d) changing the triggering frequency of the source controlling the inverter tubes.

The aim of this thesis is to investigate this type of motors experimentally and mathematically. The Park's equations of the synchronous machine is the basis of the mathematical analysis. It is assumed that the damper coils will be replaced by two windings, one in the direction of the direct axis and the other in that of the quadrature axis. The assumption of neglecting the effect of saturation is also made. A salient pole machine is considered and the variation of the permeance over the average value is assumed to follow a cosine function of the rotor position angle γ . The stator windings are assumed to be sinusoidally distributed in space.

2. PRELIMINARY EXPERIMENTATION

2.1 *Machines and instruments data*

DSM

three-phase synchronous machine

- serial number 383075 MFO
- 145/250 V, 8 A, 3.5 kVA
- 1500 rev/min, 50 Hz

The machine is provided with 4 salient poles. The stator can be connected either in star or in delta.

GMn

- 125 V, 97 A, 14 HP
- 1400 rev/min
- serial number 313966 MFO

Three-phase tachometer

- 220/380 V, 0.5/0.29 A, 190 VA
- 1500 rev/min, 50 Hz
- serial number 27673 Hübner

Thyratrons

- AEG, ASG 5155 A; mercury vapour, 12.5 A

2.2 *Single-phase investigation*

2.2.1 Connection diagram

Fig. 1 shows the connection diagram of a synchronous machine, one of its phases being fed from a d.c. power supply through thyratrons. Starting is performed with the help of a d.c. machine which is made to run at a speed so high that, when the field winding of the synchronous machine is fed, a back voltage may be available at its stator.

One phase of the three-phase tachometer is used to feed the thyatron controller. Thus it is possible to switch on the voltage U_d and to disconnect the driving d.c. machine.

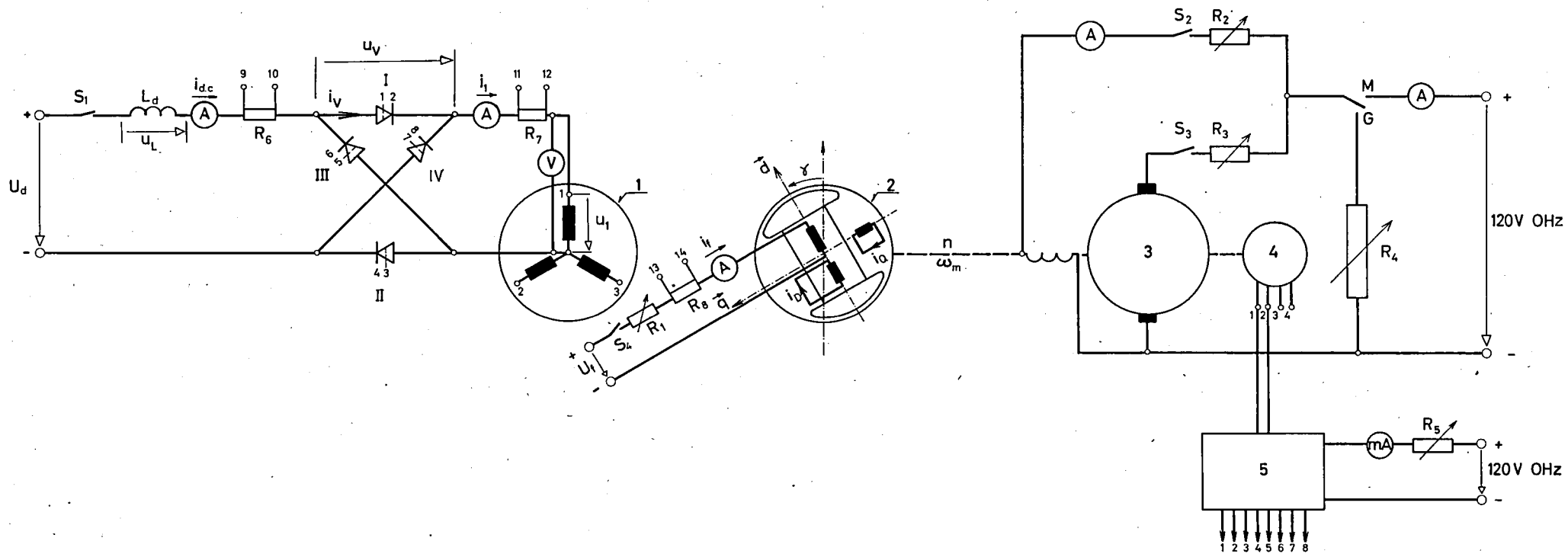


Fig. 1 Connection diagram of the single-phase controlled synchronous machine

- 1 = stator
 2 = rotor
 3 = d.c. machine used for starting or loading the synchronous machine
 4 = three-phase tachometer
 5 = thyristron controller
 L_d = smoothing inductance
 I...IV = thyristrons
 U_d = d.c. voltage source for feeding the stator
 u_L = voltage drop across the smoothing inductance
 u_v = voltage across one of the thyristrons
 u_1 = phase voltage
 U_f = d.c. voltage source for feeding the field winding of the synchronous machine
 $i_{d.c.}$ = current flowing in the smoothing inductance

- i_v = current flowing in one of the thyristrons
 i_1 = phase current
 γ = angle between the axis of the phase No. 1 and the rotor axis
 $R_6 \dots R_8$ = shunts
 \vec{d} = direct axis
 \vec{q} = quadrature axis
 $R_1 \dots R_5$ = variable resistors
 $S_1 \dots S_4$ = switches
 9-10, 11-12, 13-14 = connected to CRO

Leer - Vide - Empty

2.2.2 Oscillograms

Fig. 2 shows oscillograms of the stator current i_1 , phase voltage u_1 , field current i_f , the voltage across the smoothing inductance u_L and the voltage across one of the thyratrons u_v . It is to be noted that the induced voltage in the stator winding is no more a sine wave and that the distortion appears only during the interval at which current flows in the stator winding. Also during this interval, the field current i_f will be affected, but it is unaffected in the interval at which no current flows in the stator winding.

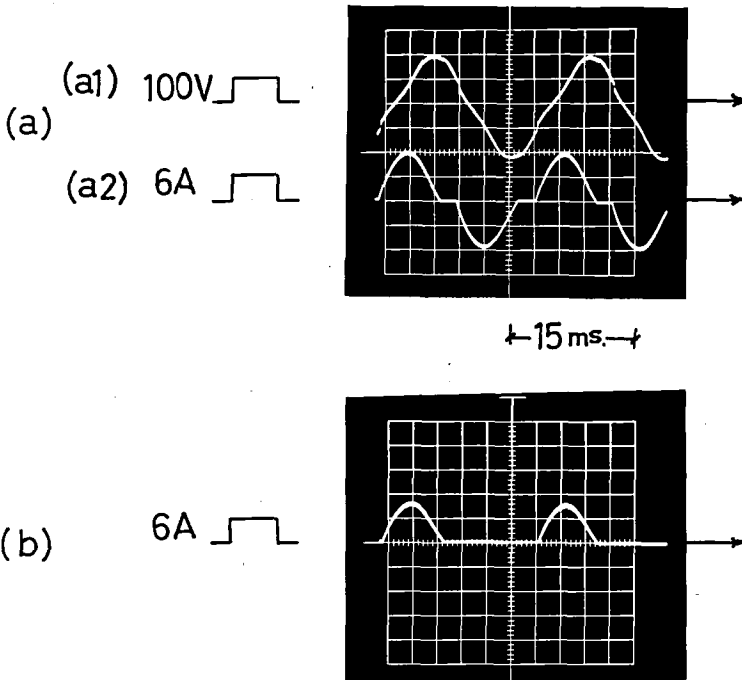
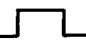
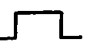
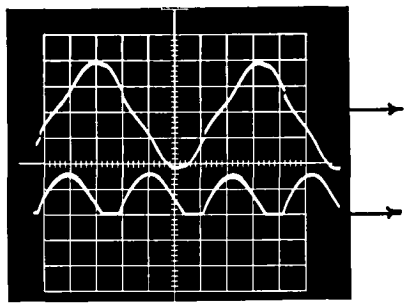


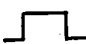

Fig. 2 Oscillograms of the single-phase controlled synchronous machine

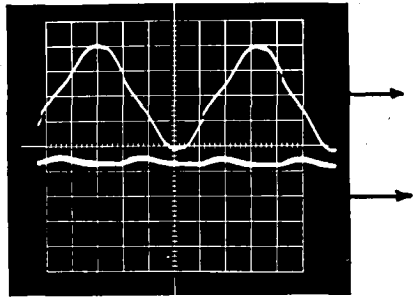
$$U_d = 127 \text{ V} \quad \alpha' = 140^\circ \quad i_f = 2.18 \text{ A}$$

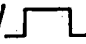
- (a1) = phase voltage u_1 (a2) = phase current i_1
 (b) = thyratron current i_{v1}
 (c1) = phase voltage u_1 (c2) = d.c. current $i_{d.c.}$
 (d1) = phase voltage u_1 (d2) = field current i_f
 (e) = voltage u_{v1} across the thyratron
 (f) = voltage u_L across the smoothing inductance

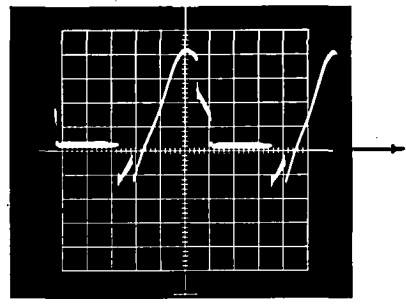
(c1) 100V 
 (c) (c2) 6A 

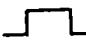


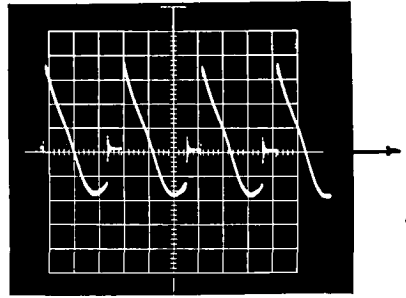
(d1) 100V 
 (d) (d2) 1.5A 



(e) 50V 



(f) 50V 



2.2.3 External characteristics

Fig. 3 shows the external characteristics of the single-phase machine at normal speed (1500 rev/min). The applied voltage U_a and the d.c. current $i_{d.c.}$ are plotted with the firing angle α' as parameter. A voltmeter and an ammeter (Siemens) whose class of accuracy is ± 0.2 and whose pointer possesses an accuracy of 0.1% were used for the measurement. The firing angle was measured on a Tektronix CRO, using the 5X magnifier in order to increase the accuracy of measurement. The definition of the firing angle α' is given in the notations on page 13.

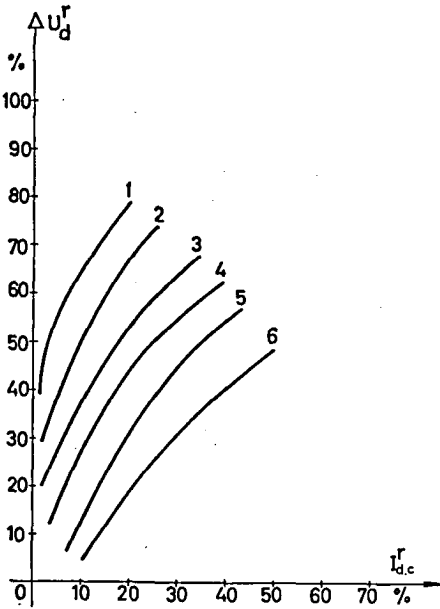


Fig. 3 External characteristics of the single-phase controlled synchronous machine

1 $\alpha' = 170^\circ$	4 $\alpha' = 140^\circ$
2 $\alpha' = 160^\circ$	5 $\alpha' = 130^\circ$
3 $\alpha' = 150^\circ$	6 $\alpha' = 120^\circ$

2.3 Three-phase investigation

2.3.1 Connection diagram

Fig. 4 shows the connection diagram of a synchronous machine, with the three phases fed from a d.c. power supply through 6 thyratrons connected in a bridge circuit. Starting is performed as explained in 2.2.1, where the three-phase tachometer feeds the thyratron controllers. Since no two conducting pulses come at the same time, a provision should be made so that the current finds a closed path at the moment the switch S_1 is closed. This was achieved by constructing the circuit shown in Fig. 5. This allows the thyratron controller which feeds the grid of thyratron No. 2 to provide another pulse at the same time as the pulse No. 1 is produced.

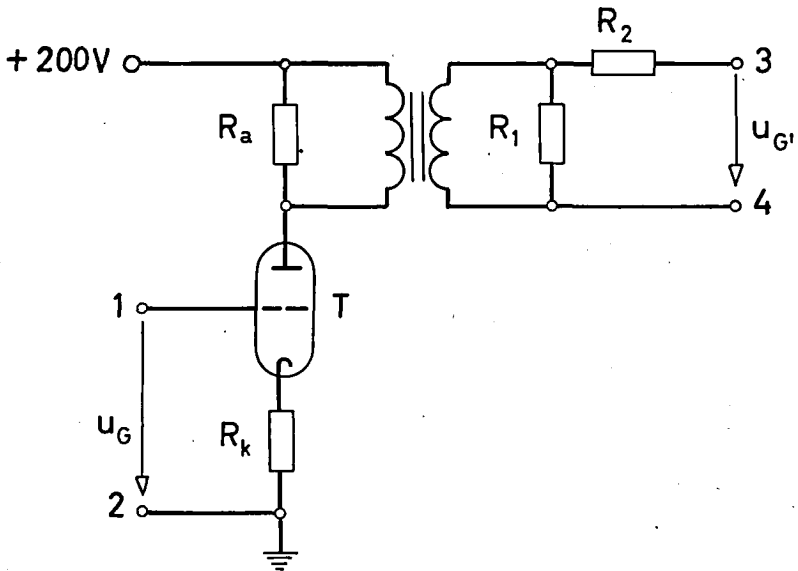


Fig. 5 Circuit producing pulses at the grid of thyratron No. 2 at the same time as the pulses controlling thyratron No. 1

u_G = the output of thyratron controller No. 1

$u_{G'}$ = connected to the grid-cathode of thyratron No. 2

$T = \frac{1}{2} \text{Ecc82}$ $R_k = 1.5 \text{ k}\Omega$ $R_a = 39 \text{ k}\Omega$

$R_1 = 47 \text{ k}\Omega$ $R_2 = 47 \text{ k}\Omega$

1 = from grid of thyratron No. 1

2 = from cathode of thyratron No. 1

3 = to grid of thyratron No. 2

4 = to cathode of thyratron No. 2

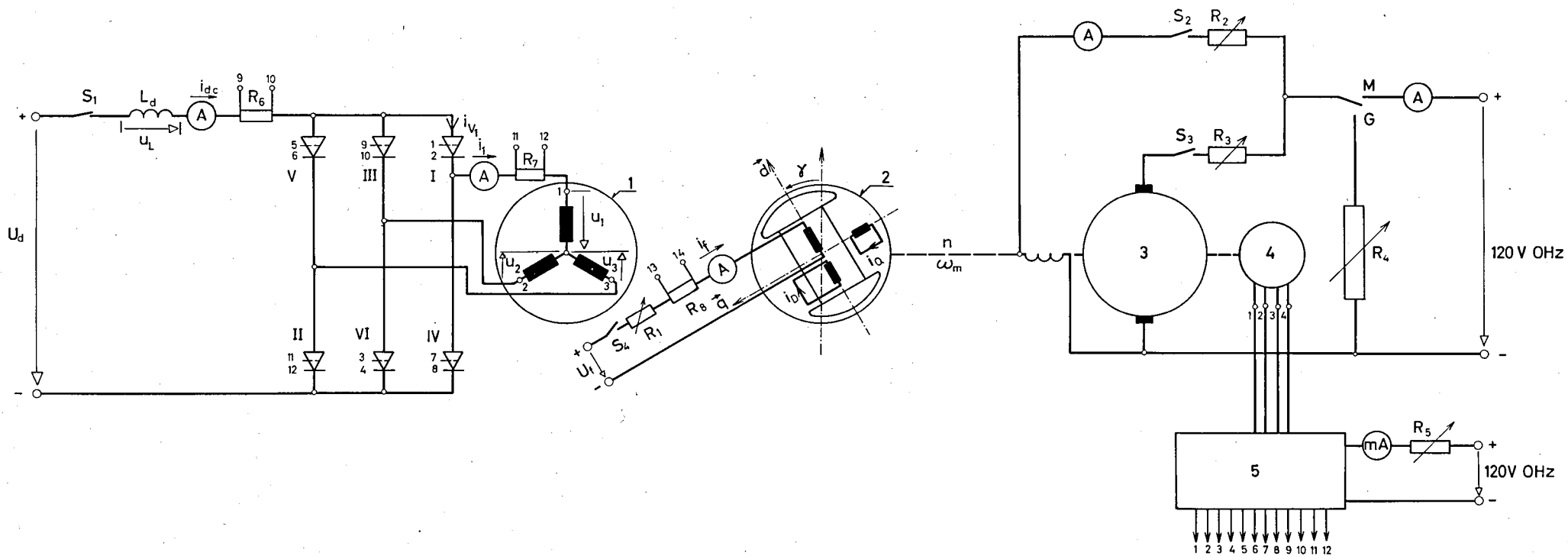


Fig. 4 Connection diagram of the three-phase controlled synchronous machine

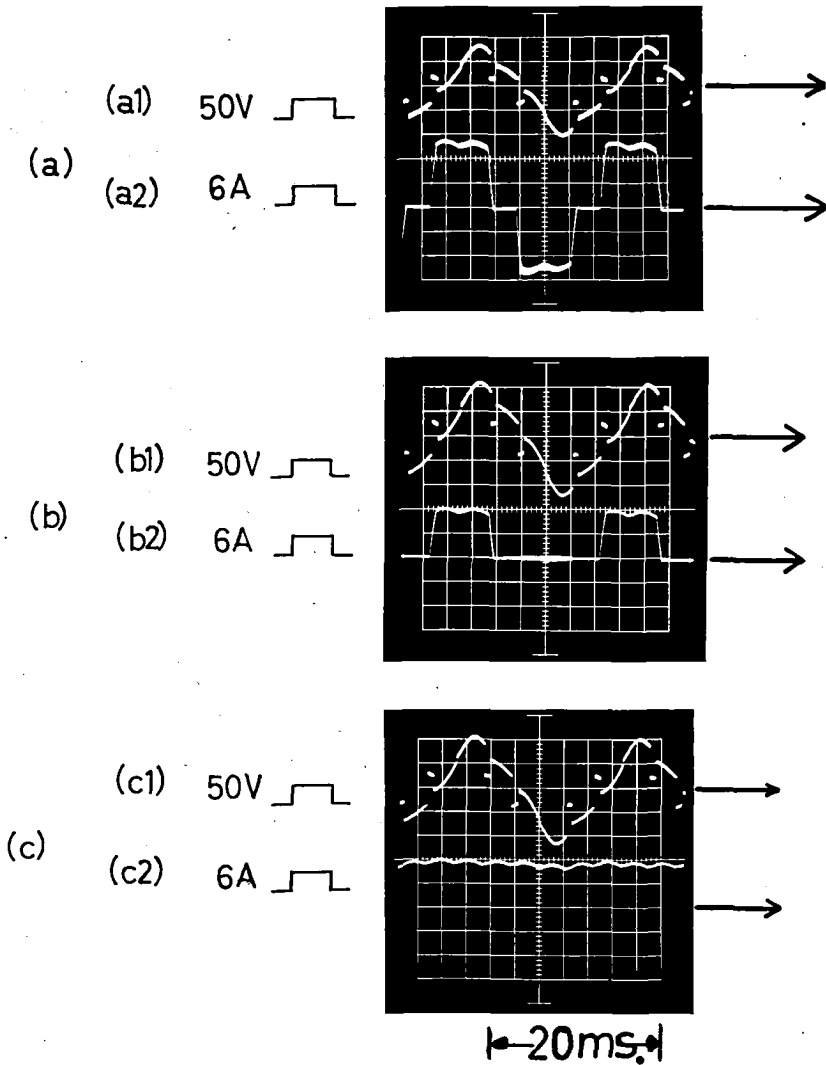
- 1 = stator
- 2 = rotor
- 3 = d.c. machine used for starting or loading the synchronous machine
- 4 = three-phase tachometer
- 5 = thyristor controller
- L_d = smoothing inductance
- I...VI = thyristors
- U_d = d.c. voltage source for feeding the stator
- u_L = voltage drop across the smoothing inductance
- u_v = voltage across one of the thyristors
- u_1, u_2, u_3 = phase voltages
- U_f = d.c. voltage source for feeding the field winding of the synchronous machine
- $i_{d.c.}$ = current flowing in the smoothing inductance

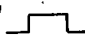

- i_v = current flowing in one of the thyristors
- i_1 = phase current
- γ = angle between the axis of the phase No. 1 and the rotor axis
- $R_6 \dots R_8$ = shunts
- \vec{d} = direct axis
- \vec{q} = quadrature axis
- $R_1 \dots R_5$ = variable resistors
- $S_1 \dots S_4$ = switches
- 9-10, 11-12, 13-14 = connected to CRO

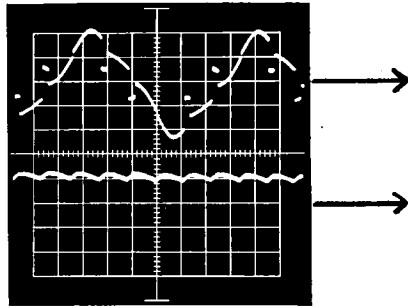
Leer - Vide - Empty

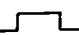
2.3.2 Oscillograms

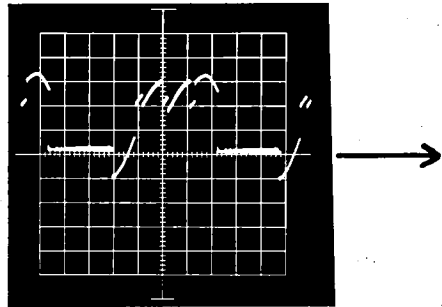
Fig. 6 shows oscillograms of the currents and voltages of the three-phase controlled synchronous machine. It is to be noted that the voltage u'_0 of the star point with respect to the mid-point of the d.c. supply is a pulsating voltage whose fundamental frequency is equal to three times that of the phase voltage.



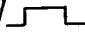
(d) (d1) 50V 
(d2) 15A 

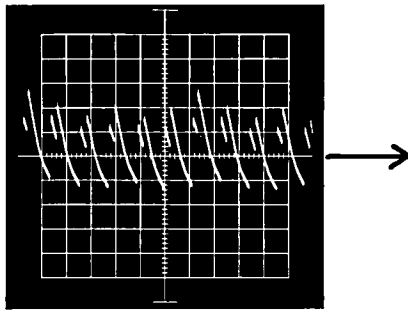


(e) 50V 




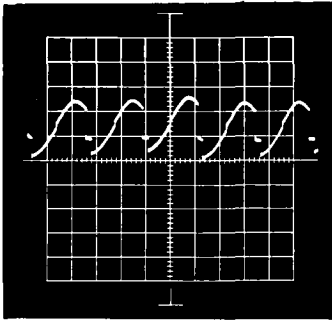
← 20ms →

(f) 20V 



(g)

50V 



←20ms→

Fig. 6 Oscillograms of the different currents and voltages of the three-phase controlled synchronous machine

$$U_d = 150 \text{ V}$$

$$i_f = 1.75 \text{ A}$$

$$\alpha' = 140^\circ$$

(a1) = phase voltage u_1

(a2) = phase current i_1

(b1) = phase voltage u_1

(b2) = thyatron current i_{v1}

(c1) = phase voltage u_1

(c2) = the d.c. current $i_{d.c.}$

(d1) = phase voltage u_1

(d2) = field current i_f

(e) = voltage across the thyatron u_{v1}

(f) = voltage across the smoothing inductance

(g) = the voltage u'_{0k} of the star point measured with respect to the negative pole of the battery U_d

3. MATHEMATICAL ANALYSIS OF THE SYNCHRONOUS MACHINE

The general theory and mathematical description of the synchronous machine were founded in 1929 by PARK and others [1]. They established the two-axis theory used for handling rotating machines in general, where all the currents, voltages and fluxes are transformed along two axes. These two axes may be fixed in space or they may be rotating with the rotor. The choice of the first type of axes proves to be advantageous when applied to cylindrical rotor machines and to induction machines. The movable axes are adequate to apply on machines with salient pole rotors. In general, the fixed axes are used when there is an unsymmetry in the stator and the movable axes when the unsymmetry lies in the rotor. In the case when both the rotor and the stator are symmetric, either type of axes may be used.

The stator of the synchronous motor is composed of three phases displaced around the stator at 120° interval, whereas the rotor comprises the field winding and the damper coils, the axis of the field being in line with that of the rotor, while the damper coil may be resolved into two windings, one in the direct axis direction and the other in the quadrature axis direction.

The three stator windings (1, 2, 3) will be replaced by two fictitious windings (α , β) which are fixed in space, the first (the α coil) being in line with the stator coil No. 1, the second (the β coil) being perpendicular to it as shown in *Fig. 7*.

In addition to the α , β directions, there is the zero sequence direction along the rotor axis. Thus all the stator quantities will be transformed along the α , β and zero sequence directions. The next step is to transform from the α , β directions to the d , q directions. Hence it is possible to reduce the machine into two sets of coils, one along the d direction and the other along the q direction. The following equations are valid for transient or steady state currents and voltages, and whether these currents and voltages are sinusoidal or not. The voltage equations of the armature are:

$$u_1 = R \cdot i_1 + \frac{d\psi_1}{dt} \quad (1)$$

$$u_2 = R \cdot i_2 + \frac{d\psi_2}{dt} \quad (2)$$

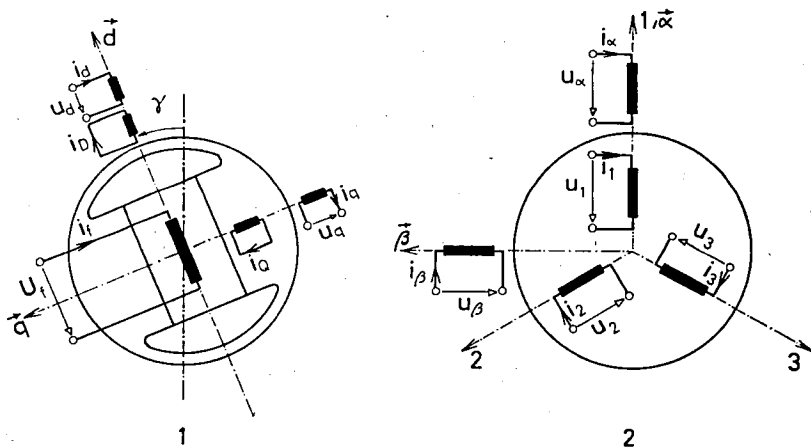


Fig. 7 Transformation of a three-phase stationary system into two-phase stationary system and to two-phase rotating system

- $\vec{\alpha}, \vec{\beta}$ = axes fixed with respect to the stator
 \vec{d}, \vec{q} = axes moving with the rotor
 u_1, u_2, u_3 = stator phase voltages
 i_1, i_2, i_3 = stator phase currents
 u_α, u_β = equivalent voltages in the fixed axes coordinates
 u_d, u_q = equivalent voltages in the moving axes coordinates
 i_α, i_β = equivalent currents in the fixed axes coordinates
 i_d, i_q = equivalent currents in the moving axes coordinates
 i_D = current in the damper winding in the direct axis direction
 i_Q = current in the damper winding in the quadrature axis direction
 U_f = d.c. voltage source used to supply the field winding
 i_f = field current
 γ = angle between the axis of the phase No. 1 and the rotor axis

$$u_3 = R \cdot i_3 + \frac{d\psi_3}{dt} \quad (3)$$

Those of the rotor windings are:

$$U_f = R_f \cdot i_f + \frac{d\psi_f}{dt} \quad (4)$$

$$0 = R_D \cdot i_D + \frac{d\psi_D}{dt} \quad (5)$$

$$0 = R_Q \cdot i_Q + \frac{d\psi_Q}{dt} \quad (6)$$

The transformation from the 1, 2, 3 directions into the α , β directions takes place according to the following equations:

$$i_\alpha = \frac{2}{3} \left(i_1 - \frac{i_2 + i_3}{2} \right) \quad (7)$$

$$i_\beta = \frac{1}{\sqrt{3}} (i_2 - i_3) \quad (8)$$

$$i_0 = \frac{1}{3} (i_1 + i_2 + i_3) \quad (9)$$

$$\psi_\alpha = \frac{2}{3} \left(\psi_1 - \frac{\psi_2 + \psi_3}{2} \right) \quad (10)$$

$$\psi_\beta = \frac{1}{\sqrt{3}} (\psi_2 - \psi_3) \quad (11)$$

$$\psi_0 = \frac{1}{3} (\psi_1 + \psi_2 + \psi_3) \quad (12)$$

In order to transform the currents and fluxes from the α , β directions into the d , q directions, the following equations are used:

$$i_d = i_\alpha \cdot \cos \gamma + i_\beta \cdot \sin \gamma \quad (13)$$

$$i_q = -i_\alpha \cdot \sin \gamma + i_\beta \cdot \cos \gamma \quad (14)$$

$$\psi_d = \psi_\alpha \cdot \cos \gamma + \psi_\beta \cdot \sin \gamma \quad (15)$$

$$\psi_q = -\psi_\alpha \cdot \sin \gamma + \psi_\beta \cdot \cos \gamma \quad (16)$$

Now the flux linkages ψ_d , ψ_f , ψ_D are related to the currents i_d , i_f , i_D by the equations:

$$\psi_d = L_{dd} \cdot i_d + L_{fd} \cdot i_f + L_{Dd} \cdot i_D \quad (17)$$

$$\psi_f = L_{df} \cdot i_d + L_{ff} \cdot i_f + L_{Df} \cdot i_D \quad (18)$$

$$\psi_D = L_{dD} \cdot i_d + L_{fD} \cdot i_f + L_{DD} \cdot i_D \quad (19)$$

The corresponding equations in the quadrature axis direction are:

$$\psi_q = L_{qq} \cdot i_q + L_{Qq} \cdot i_Q \quad (20)$$

$$\psi_Q = L_{qQ} \cdot i_q + L_{QQ} \cdot i_Q \quad (21)$$

The inverse transformation from the d, q directions into the α, β directions will take place according to:

$$i_\alpha = i_d \cdot \cos \gamma - i_q \cdot \sin \gamma \quad (22)$$

$$i_\beta = i_d \cdot \sin \gamma + i_q \cdot \cos \gamma \quad (23)$$

$$\psi_\alpha = \psi_d \cdot \cos \gamma - \psi_q \cdot \sin \gamma \quad (24)$$

$$\psi_\beta = \psi_d \cdot \sin \gamma + \psi_q \cdot \cos \gamma \quad (25)$$

In order to transform from the α, β directions to the original 1, 2, 3 directions, we have the following relations:

$$i_1 = i_\alpha + i_0 \quad (26)$$

$$i_2 = -\frac{1}{2} i_\alpha + \frac{\sqrt{3}}{2} i_\beta + i_0 \quad (27)$$

$$i_3 = -\frac{1}{2} i_\alpha - \frac{\sqrt{3}}{2} i_\beta + i_0 \quad (28)$$

$$\psi_1 = \psi_\alpha + \psi_0 \quad (29)$$

$$\psi_2 = -\frac{1}{2} \psi_\alpha + \frac{\sqrt{3}}{2} \psi_\beta + \psi_0 \quad (30)$$

$$\psi_3 = -\frac{1}{2} \psi_\alpha - \frac{\sqrt{3}}{2} \psi_\beta + \psi_0 \quad (31)$$

We note that the transformation is made from the original axes to the rotating d, q directions with the aid of the transformation along the fixed α, β directions. This has the advantage of greatly reducing the necessary number of multipliers necessary in the simulation on the analog computer.

Another method for calculating the different currents may be done if all machine voltages, currents, fluxes, resistances and inductances are put in a matrix form. This method was also applied in a later chapter when the problem was simulated on the PACE analog computer.

3.1 The machine equations expressed in the per-unit form

It is the general practice, when analyzing synchronous machines to specify all machine quantities in relative form rather than to use the absolute values. The relative value of any physical quantity is obtained by dividing its absolute value by the corresponding reference one. A list showing all reference values used in this thesis is to be found on page 10. Transforming equation (1) into the relative form yields:

$$u_1^r = R^r \cdot i_1^r + \frac{d\psi_1^r}{d\tau} \quad (32)$$

Its general form is not changed, however, all values are expressed in relative form. Applying this on the equations (1)...(31), we get the corresponding ones in their relative form. The equations (1)...(3), (7)...(16), (22)...(31) will not change the general appearance, but the equations (4), (5), (6) will be reduced to:

$$U_f^r = i_f^r + T_f^r \frac{d\psi_f^r}{d\tau} \quad (33)$$

$$0 = i_D^r + T_D^r \frac{d\psi_D^r}{d\tau} \quad (34)$$

$$0 = i_Q^r + T_Q^r \frac{d\psi_Q^r}{d\tau} \quad (35)$$

The equations (17)...(21) will be reduced to:

$$\psi_a^r = x_d \cdot i_d^r + i_D^r + i_f^r \quad (36)$$

$$\psi_f^r = x_d \cdot (1 - \sigma_{df}) \cdot i_d^r + (1 - \mu_f) \cdot i_D^r + i_f^r \quad (37)$$

$$\psi_D^r = x_d \cdot (1 - \sigma_{dD}) \cdot i_d^r + i_D^r + (1 - \mu_D) \cdot i_f^r \quad (38)$$

$$\psi_q^r = x_q \cdot i_q^r + i_Q^r \quad (39)$$

$$\psi_Q^r = x_q \cdot (1 - \sigma_q) \cdot i_q^r + i_Q^r \quad (40)$$

where

$$T_f^r = \frac{\omega_n L_{ff}}{R_f} \quad x_d = \frac{\omega_n L_{dd}}{R_n}$$

$$T_D^r = \frac{\omega_n L_{DD}}{R_D} \quad x_q = \frac{\omega_n L_{qq}}{R_n}$$

$$T_Q^r = \frac{\omega_n L_{QQ}}{R_Q}$$

The leakage coefficients are:

$$\sigma_q = 1 - \frac{L_{qQ} L_{Qq}}{L_{qq} L_{QQ}} \quad (41)$$

$$\sigma_{df} = 1 - \frac{L_{df} L_{fd}}{L_{ff} L_{dd}} \quad (42)$$

$$\sigma_{dD} = 1 - \frac{L_{dD} L_{Dd}}{L_{dd} L_{DD}} \quad (43)$$

$$\mu_f = 1 - \frac{L_{fD} L_{fD}}{L_{ff} L_{dD}} \quad (44)$$

$$\mu_D = 1 - \frac{L_{Df} L_{dD}}{L_{df} L_{DD}} \quad (45)$$

$$\mu_d = 1 - \frac{L_{dD} L_{fd}}{L_{dd} L_{fD}} \quad (46)$$

These values are related to one another by the following equations:

$$(1 - \sigma_{dD}) = \frac{L_{dD} L_{Dd}}{L_{dd} L_{DD}} = (1 - \mu_d) (1 - \mu_D) \quad (47)$$

$$(1 - \sigma_{df}) = \frac{L_{df} L_{fd}}{L_{ff} L_{dd}} = (1 - \mu_d) (1 - \mu_f) \quad (48)$$

4. DETERMINATION OF THE MACHINE CONSTANTS

4.1 Stator resistance and leakage reactance

The stator resistance was measured using the voltmeter-ammeter method and it was transformed to the value corresponding to 75 °C.

Thus $R = 1.03 \Omega$

$$R' = 0.0571$$

The leakage reactance of the stator winding (x_l) was measured using the Potier triangle method and was found to be,

$$X_l = 1.18 \Omega$$

$$x_l' = 0.0653$$

4.2 Field time constant

The machine was made to run at synchronous speed and the field winding excited so that the stator phase voltage is equal to half the rated voltage at no load. The armature is left unloaded and the field winding is suddenly short circuited on itself, and the armature voltage recorded. T_f was determined from a semi-log. plot of the armature voltage.

$$T_f = 0.37 \text{ s}$$

$$T_f' = 116.18$$

4.3 Direct and quadrature axis synchronous reactances

The measurement of the reactances and time constants was made according to the American Institute of Electrical Engineers test codes [7]. A short description of the measurement of each quantity is given in the following. As for the direct and quadrature axis synchronous reactances, the slip test was made. The machine was driven at a very small slip, in our case the speed was adjusted to be 1470 rev/min. Subnormal sinusoidal voltage was applied to the armature terminals with the field open. The

current flowing in the stator winding is modulated, attaining a minimum value when the rotor axis comes to be in line with the axis of that winding, and reaching a maximum value when the field axis is in quadrature with respect to that of that stator winding.

The direct axis synchronous reactance is obtained when the armature current is minimum,

$$x_d = \frac{\text{per-unit armature voltage}}{\text{per-unit armature current}} = 0.5805$$

$$X_d = 10.47 \Omega$$

The quadrature axis synchronous reactance is obtained when the armature current is maximum,

$$x_q = \frac{\text{per-unit armature voltage}}{\text{per-unit armature current}} = 0.2684$$

$$X_q = 4.84 \Omega$$

4.4 Determination of the leakage coefficients in the direct axis direction

It is required to calculate the coefficients σ_{dD} , σ_{df} , μ_f , μ_D and the time constant T'_D out of the knowledge of the reactances x_d , x'_d , x''_d , x_l and the time constant T''_d . The method of measurement of these reactances and the time constant T''_d will be given in section 4.5.

For the sake of simplicity in deriving expressions for these leakage coefficients, it was assumed that the three coils d , D , f have no resistances, or that the frequency is so high that their effect will be neglected compared with the inductances [3]. Now at sudden short circuit, we have:

$$\psi'_d = x'_d \cdot i'_d$$

$$\psi'_D = \psi'_f = 0$$

After a while, the damper coils are assumed to be open while the field winding is still short circuited, i.e.,

$$\psi'_f = 0$$

$$\psi'_d = x'_d \cdot i'_d$$

$$i'_D = 0$$

then,

$$\begin{aligned}x'_d \cdot i_d^r &= x_d \cdot i_d^r + i_f^r \\0 &= x_d(1 - \sigma_{df}) i_d^r + i_f^r\end{aligned}$$

substituting, $(1 - \sigma_{df}) = (1 - \mu_f)(1 - \mu_d)$,

$$\text{and } \mu_d = \frac{x_l}{x_d}$$

then by eliminating i_f^r , and dividing by i_d^r , we obtain the following formula for μ_f :

$$\mu_f = \frac{x'_d - x_l}{x_d - x_l} \quad (49)$$

As mentioned above, just at the moment after the sudden short circuit, we have:

$$\begin{aligned}x''_d \cdot i_d^r &= x_d \cdot i_d^r + i_D^r + i_f^r \\0 &= x_d(1 - \sigma_{df}) \cdot i_d^r + (1 - \mu_f) \cdot i_D^r + i_f^r \\0 &= x_d(1 - \sigma_{dD}) \cdot i_d^r + i_D^r + (1 - \mu_D) \cdot i_f^r\end{aligned}$$

substituting $(1 - \sigma_{dD}) = (1 - \mu_d)(1 - \mu_D)$, and

$$\mu_f = \frac{(x'_d - x_l)}{(x_d - x_l)}$$

and eliminating i_f^r , i_D^r , i_d^r , we get:

$$\mu_D = \frac{(x'_d - x_l)(x''_d - x_l)}{[x_l^2 + x'_d \cdot x_d - 2 \cdot x_l \cdot x'_d + x''_d(x'_d - x_d)]} \quad (50)$$

As for σ_{df} , σ_{dD} , they can be calculated according to equations (47) and (48) since μ_d , μ_f , μ_D are now known as a function of x_l , x_d , x'_d , x''_d , thus,

$$\sigma_{df} = \mu_f + \mu_d - \mu_d \mu_f \quad (51)$$

$$\sigma_{dD} = \mu_D + \mu_d - \mu_d \mu_D \quad (52)$$

As for the time constant T_D^r , it is possible to prove that [3]; the sub-transient time constant $T_d^r = T_D^r(\sigma_{dD})$,

hence,

$$T_D^r = \frac{T_d^r}{\sigma_{dD}} = \frac{T_d^r}{\mu_D + \mu_d - \mu_D \mu_d} \quad (53)$$

Thus knowing the reactances x_l , x_d , x'_d , x''_d and the time constant T_d^r , and applying the equations (49)...(53) we should be able to calculate the different leakage coefficients. The experimental determination of these quantities will be given in the next chapter.

4.5 Direct axis transient and subtransient reactances and time constants

The machine was driven at rated speed (1500 rev/min), the field was excited so that the output phase voltage is equal to the rated voltage [7]. A sudden short circuit was made on the three phases instantaneously. The resulting currents are recorded by a "bifilar oscillograph" and are shown in *Fig. 8*.

The peaks are determined from the oscillogram, the median line drawn, and the a.c. component calculated. This a.c. component was plotted on a semi-log. paper (shown in *Fig. 9*). Also the a.c. component minus the sustained value was plotted in the same figure (curve *C*). The two curves are then extrapolated to the point of zero time. It is clear that curve *C* is composed of a straight line and a curve which extends for some cycles beginning at the point of zero time. The difference *E* between the curve *C* and the extension of the straight part is again plotted on the semi-log. paper, being itself a straight line.

The per-unit direct axis transient reactance x'_d is,

$$x'_d = \frac{\text{per-unit open circuit voltage of the machine immediately before the s.c.}}{\text{per-unit current from transient component plus sustained value at } t = 0}$$

$$x'_d = 0.1193 \quad (\text{see Fig. 9})$$

The per-unit direct axis subtransient reactance x''_d is

$$x''_d = \frac{\text{per-unit open circuit voltage of the machine immediately before the s.c.}}{\text{per-unit current from the a.c. component curve at } t = 0}$$

$$x''_d = 0.0841 \quad (\text{see Fig. 9})$$

The direct axis subtransient time constant T''_d is the time required for the curve *E* (*Fig. 9*) to decrease to 0.368 of its initial value.

T''_d was found to be equal to 23.5 ms, i.e. $T''_d = 7.379$ per unit.

Knowing the reactances x_d , x'_d , x''_d , x_l and the subtransient time constant T''_d , and applying the equations (49)...(53) led to the calculation of the following coefficients:

$$\begin{array}{ll} \mu_d = 0.1125 & \sigma_{dD} = 0.1308 \\ \mu_f = 0.1049 & \sigma_{df} = 0.2056 \\ \mu_D = 0.0206 & T'_D = 56.4196 \end{array}$$

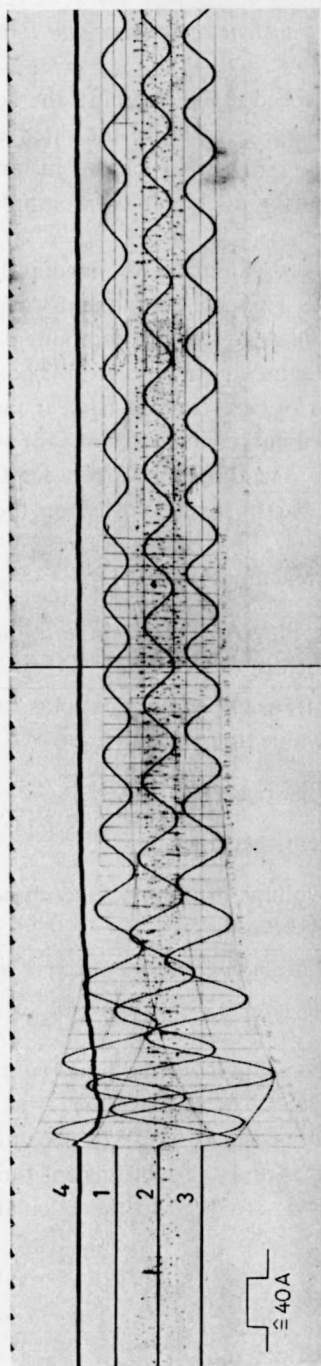


Fig. 8 The three-phase stator currents resulting from the sudden application of a short circuit on the stator windings

- 1 = current flowing in phase No. 1
- 2 = current flowing in phase No. 2
- 3 = current flowing in phase No. 3
- 4 = current flowing in the field winding

The 4 digits after the point do not mean that the accuracy of the measurement is up to that position, but it is maintained in order to avoid any inaccuracy that can result from the calculations.

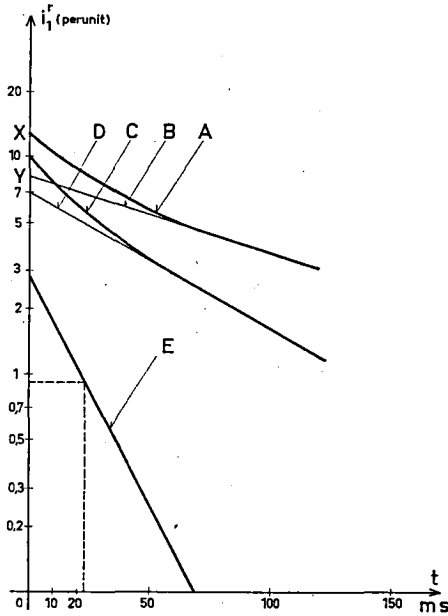


Fig. 9 Analysis of the a.c. component of the short circuit current

- A = a.c. component
- B = transient component plus sustained value
- C = a.c. component minus sustained value
- D = transient component
- E = subtransient component

$$OX = \frac{U_1^r}{x_d''} = \frac{1}{x_d''}$$

$$OY = \frac{U_1^r}{x_d'} = \frac{1}{x_d'}$$

U_1^r = phase voltage just before the short circuit

4.6 Determination of the leakage coefficient and time constant in the quadrature axis direction

Now it is required to determine and measure the leakage coefficient in the quadrature axis direction. The machine is to be manually rotated until the axis of phase No. 1 becomes perpendicular to the rotor axis as shown in Fig. 10. A reduced d.c. voltage was suddenly applied to phase 1, and the current was recorded by a "bifilar oscillograph". Hence we have two magnetically coupled coils, one of which is short circuited. Applying a d.c. voltage U_d on the stator winding No. 1, the voltage equations will be:

$$U_d = R i_1 + \frac{d\psi_1}{dt} \quad (54)$$

$$0 = R_Q \cdot i_Q + \frac{d\psi_Q}{dt} \quad (55)$$

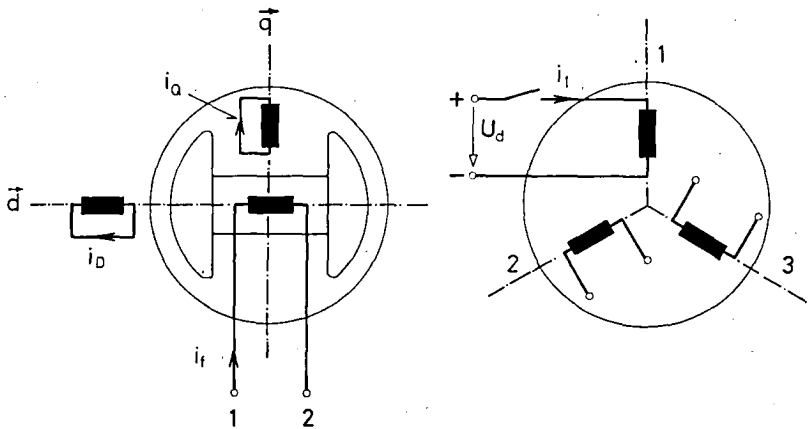


Fig. 10 Sudden application of a d.c. voltage U_d on phase No. 1, the rotor being in quadrature with respect to it

1, 2, 3 = directions of the stator windings

\vec{d} = direct axis

\vec{q} = quadrature axis

U_d = d.c. voltage suddenly applied to the stator winding No. 1

i_1 = current flowing in phase No. 1

i_Q = current flowing in the damper winding in the quadrature axis direction

And the flux linking each of the two coils will be given by:

$$\psi_1 = L_{qq} \cdot i_1 + L_{qQ} \cdot i_Q \quad (56)$$

$$\psi_Q = L_{Qq} \cdot i_1 + L_{QQ} \cdot i_Q \quad (57)$$

Applying the Laplace-Transform to the equations (54)...(57) and solving for $i_1(p)$, we get:

$$i_1(p) = \frac{U_d}{T''_{q0} L''_q} \cdot \frac{(1 + p T''_{q0})}{p \cdot (p^2 + 2\sigma p + \omega_0^2)} \quad (58)$$

where,

$$2\sigma = \frac{L_{qq} + R \cdot T''_{q0}}{T''_{q0} \cdot L''_q}$$

$$\omega_0^2 = \frac{R}{T''_{q0} \cdot L''_q}$$

$$L''_q = L_{qq} - \frac{L_{qQ}^2}{L_{QQ}}, \quad \text{and} \quad T''_{q0} = \frac{L_{QQ}}{R_Q}$$

Resolving in partial fractions to get the time response, we assume:

$$i_1(p) = \frac{A}{p} + \frac{B_1}{(p - p_1)} + \frac{B_2}{(p - p_2)}$$

An approximate pole for p_1 is given by:

$$p_1 \approx -\frac{1}{T''_q} = \frac{-L_{qq}}{L''_q \cdot T''_{q0}} = \frac{-L_{qq} \cdot R_Q}{L''_q \cdot L_{QQ}} = -\frac{1}{\tau_1} \quad (59a)$$

since the sum of these two roots $(p_1 + p_2) = \frac{-L_{qq}}{T''_{q0} \cdot L''_q} - \frac{R}{L''_q}$

then,

$$p_2 \approx -\frac{R}{L''_q} = -\frac{1}{\tau_2} \quad (59b)$$

Thus it is possible to calculate A , B_1 , B_2 .

$$A = \frac{U_d}{R} \quad (59c)$$

$$B_1 \approx \frac{U_d \cdot \left(\frac{L_{qQ}^2}{L_{qq}} \right)}{L_{QQ} \cdot R - L_{qq} \cdot R_Q} \quad (59d)$$

$$B_2 \approx \frac{U_d \cdot \left(\frac{R_Q \cdot L_q''}{R} - L_{QQ} \right)}{(L_{QQ} \cdot R - L_{qq} \cdot R_Q)} \quad (59e)$$

Hence the inverse Laplace-Transform was calculated and found to be:

$$i_1 \approx A + B_1 \cdot e^{-\frac{t}{\tau_1}} + B_2 \cdot e^{-\frac{t}{\tau_2}} \quad (60)$$

where $\tau_1, \tau_2, A, B_1, B_2$ are given by the equations (59a)...(59e).

An oscillogram of this curve is shown in *Fig. 11* which is photographed with a "bifilar oscillograph". It is to be noted that the transient part possesses two time constants, one of which is very small compared to the other. Accordingly, it is possible to separate them. The current $U_d/R - i_1 = i_1'$ was plotted on a semi-log. paper that is shown in *Fig. 12*. It is clear that, except for the first 10 ms, the curve is a straight line. The time which elapses until this straight line falls to 0.368 from its initial value was found to be 44 ms. The difference between i_1' and the straight line portion is once more plotted on the same graph. It was also found to be a straight line. The time elapsing in order that this last straight line falls to 0.368 of its initial value was measured and found to be 4.2 ms.

Equation (59b) enables us to calculate L_q'' since R and τ_2 are known. With the help of L_q'', L_{qq} and τ_1 ; T_{qo}'' can be calculated according to equation (59a).

$$\frac{L_{qQ}^2}{L_{qq} \cdot L_{QQ}} = 1 - \sigma_q \text{ can be calculated using equation (59d).}$$

$$T_{qo}'' \text{ was found to be } 0.155 \text{ s; thus } T_Q^r = \frac{\omega_n \cdot L_{QQ}}{R_Q} = \omega_n \cdot T_{qo}'' = 48.67$$

σ_q was found to be 0.2825.

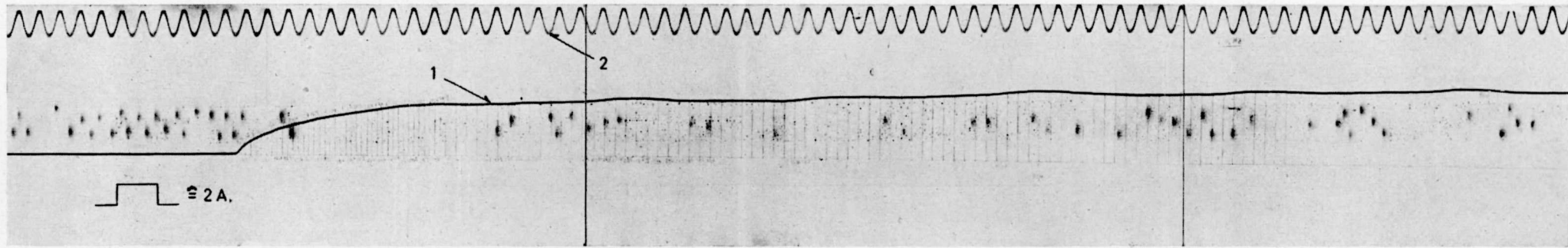


Fig. 11 Stator current resulting from the sudden application of a d.c. voltage U_d to the phase No. 1

- 1 = current flowing in phase No. 1
- 2 = timing wave $\cong 1 \text{ kHz}$

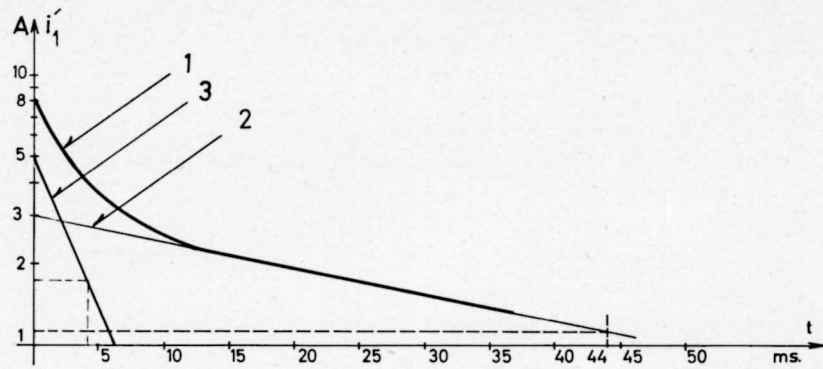


Fig. 12 Representation of the stator current of Fig. 11 on a semi-log. scale

- 1 = $i'_1 = \frac{U_d}{R} - i_1$
- 2 = the straight line portion of the current i'_1 after the attenuation of the subtransient phenomenon
- 3 = the difference between the current i'_1 and the straight line portion denoted by curve 2

Leer - Vide - Empty

5. MACHINE AS A SYNCHRONOUS GENERATOR

As a preliminary check, the equations of the short circuited synchronous generator were written, and then simulated on an analog computer of the Donner type. The analog scheme is given in *Fig. 14* which contains 22 amplifiers, 8 multipliers and 19 potentiometers.

A curve showing the relation between armature current and field current—as obtained from the computer—was plotted.

For the sake of comparison, the corresponding curve—taken from the actual machine—was also plotted. *Fig. 13* shows these two curves.

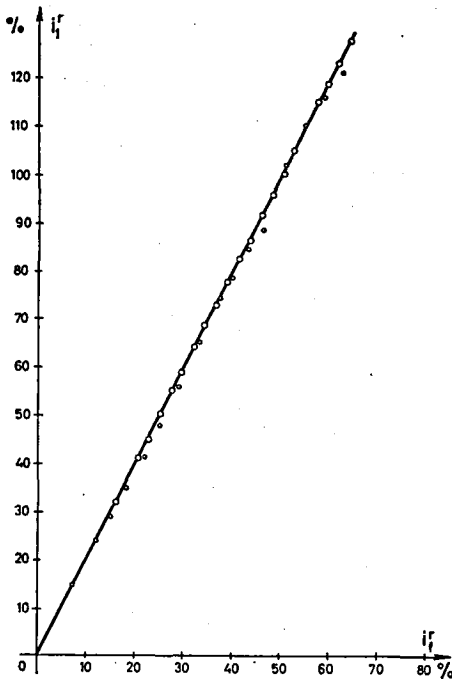


Fig. 13 Steady state short circuit characteristics

- = from the machine
- ◻ = from the computer

The voltage equations of the three-phase short circuited generator are:

$$0 = -0.0571 i_{\alpha}^r + \frac{d\psi_{\alpha}^r}{d\tau} \quad (61)$$

$$0 = -0.0571 i_{\beta}^r + \frac{d\psi_{\beta}^r}{d\tau} \quad (62)$$

$$U_f^r = i_f^r + 116.2 \frac{d\psi_f^r}{d\tau} \quad (63)$$

$$0 = i_D^r + 56.42 \frac{d\psi_D^r}{d\tau} \quad (64)$$

$$0 = i_Q^r + 48.90 \frac{d\psi_Q^r}{d\tau} \quad (65)$$

The flux linkage equations of the different coils of this generator are given by:

$$\psi_d^r = 0.5805 i_d^r + i_f^r + i_D^r \quad (66)$$

$$\psi_f^r = 0.4611 i_d^r + i_f^r + 0.8951 i_D^r \quad (67)$$

$$\psi_D^r = 0.5045 i_d^r + 0.9794 i_f^r + i_D^r \quad (68)$$

$$\psi_q^r = 0.2684 i_q^r + i_Q^r \quad (69)$$

$$\psi_Q^r = 0.1926 i_q^r + i_Q^r \quad (70)$$

The transformation equations are:

$$\psi_d^r = \psi_{\alpha}^r \cdot \cos \gamma + \psi_{\beta}^r \cdot \sin \gamma \quad (71)$$

$$\psi_q^r = -\psi_{\alpha}^r \cdot \sin \gamma + \psi_{\beta}^r \cdot \cos \gamma \quad (72)$$

$$i_{\alpha}^r = i_d^r \cdot \cos \gamma - i_q^r \cdot \sin \gamma \quad (73)$$

$$i_{\beta}^r = i_d^r \cdot \sin \gamma + i_q^r \cdot \cos \gamma \quad (74)$$

Before these equations can be simulated on the analog computer, we have to introduce the suitable amplitude and time scales. As for the amplitude scale, it was assumed that every 100 V correspond to 100% of the reference value of each quantity, e.g. $U_f^r \cong 100$ V, when $U_f^r = 100\%$ of its reference value.

As for the time scale, the relation between the per-unit time τ and the time w.r.t. the analog computer t_c was chosen according to the relation:

$$\tau = 5 t_c \quad (75)$$

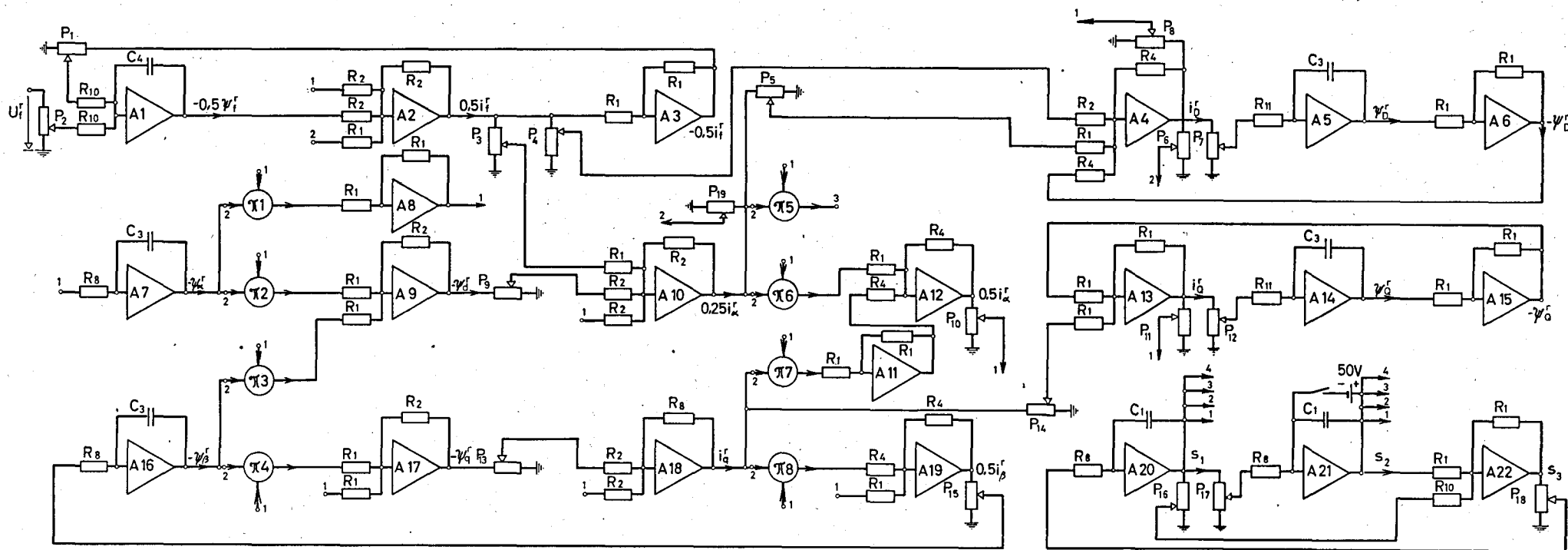


Fig. 14 Analog computer scheme for the short circuited synchronous generator driven at constant speed

$A4.1 = A2.1$	$A4.2 = A10.1$	$A8.1 = A17.1$
$A10.2 = A2.2$	$A5.3 = A19.1$	$A12.1 = A7.1$
$A13.1 = A18.1$	$A20.1 = \pi 1.1$	$A20.2 = \pi 3.1$
$A20.3 = \pi 5.1$	$A20.4 = \pi 7.1$	$A21.1 = \pi 2.1$
$A21.2 = \pi 4.1$	$A21.3 = \pi 6.1$	$A21.4 = \pi 8.1$
$P_1 = 0.3443$	$P_2 = 0.1722$	$P_3 = 0.4307$
$P_4 = 0.9794$	$P_5 = 0.5045$	$P_6 = 0.4307$
$P_7 = 0.4431$	$P_8 = 0.4475$	$P_9 = 0.4307$
$P_{10} = 0.5709$	$P_{11} = 0.7452$	$P_{12} = 0.5112$
$P_{13} = 0.7452$	$P_{14} = 0.1926$	$P_{15} = 0.5709$
$P_{16} = 0.0040$	$P_{17} = 0.5 \omega_m^r = 0.5$	
$P_{18} = 0.5 \omega_m^r = 0.5$	$P_{19} = 0.4611$	

$$s_1 = 50 \sin \gamma$$

$$s_2 = 50 \cos \gamma$$

$$s_3 = -50 \cos \gamma$$

Leer - Vide - Empty

This means that the relation between the time on the actual synchronous machine t and the time on the analog computer t_c is given by:

$$t_c = 20 \pi t$$

The speed of the synchronous generator was assumed to be constant and equal to that of synchronism. Hence the $\sin \gamma$ and $\cos \gamma$ were obtained by solving the differential equation:

$$\frac{d^2 y}{dt_c^2} = -25 y \quad (76)$$

The analog set-up for solving this equation is done by means of the two integrators $A20$ and $A21$ and inverter $A22$ of Fig. 14.

Due to the very small phase shift encountered in the amplifiers, there is a tendency for the sine wave to be decreased slightly in amplitude. With the course of time this change in amplitude can be dangerous. To compensate this effect, a part of the output of integrator $A20$ is given to the input of the amplifier $A22$, by means of the potentiometer $P16$ and an input resistance of $4 \text{ M}\Omega$. With the potentiometer $P16$ adjusted to the value of 0.004 , the sine wave having an amplitude of 50 V has decreased by 1 V in a period of 10 minutes. The results were, however, taken within 3 minutes of computation.

Introducing the mentioned time scale in the equations (61)...(74), and making the necessary alterations, we obtain the following equations which are ready for the simulation on the analog computer:

$$-\psi'_\alpha = - \int 0.2854 i'_\alpha dt_c \quad (77)$$

$$-\psi'_\beta = - \int 0.2854 i'_\beta dt_c \quad (78)$$

$$-0.5 \psi'_f = -0.0215 \int (U'_f - i'_f) dt_c \quad (79)$$

$$\psi'_D = -0.0886 \int i'_D dt_c \quad (80)$$

$$\psi'_Q = -0.1022 \int i'_Q dt_c \quad (81)$$

$$-\psi'_d = -(\psi'_\alpha \cdot \cos \gamma + \psi'_\beta \cdot \sin \gamma) \quad (82)$$

$$-\psi'_q = -(-\psi'_\alpha \cdot \sin \gamma + \psi'_\beta \cdot \cos \gamma) \quad (83)$$

$$0.25 i'_d = -0.4307 (i'_D + i'_f - \psi'_d) \quad (84)$$

$$0.5 i'_f = -(0.2306 i'_d + 0.4475 i'_D - 0.5400 \psi'_f) \quad (85)$$

$$i_D^r = -(0.5045 i_d^r + 0.9794 i_f^r - \psi_D^r) \quad (86)$$

$$i_q^r = -3.7261 (i_Q^r - \psi_q^r) \quad (87)$$

$$i_Q^r = -(0.1926 i_q^r - \psi_Q^r) \quad (88)$$

$$0.5 i_a^r = -(0.5 i_q^r \cdot \sin \gamma - 0.5 i_d^r \cdot \cos \gamma) \quad (89)$$

$$0.5 i_b^r = -(-0.5 i_q^r \cdot \cos \gamma - 0.5 i_d^r \cdot \sin \gamma) \quad (90)$$

The analog scheme representing these equations is shown in *Fig. 14*. U_f^r was varied in magnitude, then the amplitude of the field current i_f^r and the i_a^r were measured. Since $i_0^r = 0$, as the machine is connected in star, then $i_a^r = i_1^r$. The armature current i_1^r was plotted against the field current i_f^r and is shown in *Fig. 13*. This shows that the experimental results agree with the calculated ones.

The following values are valid for *Fig. 14, 17, 19, 21, 24, 25, 32 and 34*.

$R_1 = 100 \text{ k}\Omega$	$R_7 = 800 \text{ k}\Omega$	$R_{13} = 10 \text{ k}\Omega$
$R_2 = 200 \text{ k}\Omega$	$R_8 = 1 \text{ M}\Omega$	$R_{14} = 15 \text{ k}\Omega$
$R_3 = 300 \text{ k}\Omega$	$R_9 = 2 \text{ M}\Omega$	$C_1 = 0.1 \text{ }\mu\text{F}$
$R_4 = 400 \text{ k}\Omega$	$R_{10} = 4 \text{ M}\Omega$	$C_2 = 0.2 \text{ }\mu\text{F}$
$R_5 = 500 \text{ k}\Omega$	$R_{11} = 5 \text{ M}\Omega$	$C_3 = 1 \text{ }\mu\text{F}$
$R_6 = 600 \text{ k}\Omega$	$R_{12} = 10 \text{ M}\Omega$	$C_4 = 2 \text{ }\mu\text{F}$

6. ANALOG COMPUTATION OF THE SINGLE-PHASE CONTROLLED SYNCHRO- NOUS MACHINE

6.1 Mathematical formulation

The aim of this chapter is to investigate the case shown in *Fig. 1*, where only one phase of the stator of the synchronous machine is fed from a d.c. power supply through 4 thyratrons. The calculation will be done by obtaining a mathematical expression for the voltage drop across the smoothing inductance L_d . Integrating this voltage over the period from α' to β' and from $(\alpha' + \pi)$ to $(\beta' + \pi)$ (where α' is the ignition angle and β' the extinction angle), and forcing the input of the integrator to be zero in the period from β' to $(\alpha' + \pi)$ and from $(\beta' + \pi)$ to $(\alpha' + 2\pi)$, the thyatron action is thus realized.

Fig. 15a represents the equivalent circuit of the stator when current flows in the forward direction. Neglecting the voltage drop across the conducting thyratrons 1 and 2, then the voltage drop across the smoothing inductance is the difference between the applied d.c. voltage U_d and the sum of the induced voltage from the synchronous machine in the phase No. 1 plus the voltage drop across the stator resistance, i.e.

$$L_d \frac{di_1}{dt} = U_d - \left(R \cdot i_1 + \frac{d\psi_1}{dt} \right)$$

Dividing by the reference value of the voltage $U_n \sqrt{2}$ in order to transform it into the relative form, we get:

$$L_d^r \frac{di_1^r}{d\tau} = U_d^r - \left(R^r \cdot i_1^r + \frac{d\psi_1^r}{d\tau} \right)$$

where the per-unit value of the smoothing inductance is

$$L_d^r = \frac{\omega_n \cdot L_d}{R_n}$$

and the per-unit value of the applied d.c. voltage is

$$U_d^r = \frac{U_d}{U_n \sqrt{2}}$$

Introducing the time scaling mentioned in equation (75), we get:

$$L_d^r \frac{di_1^r}{dt_c} = 5 U_d^r - \left(5 R^r \cdot i_1^r + \frac{d\psi_1^r}{dt_c} \right)$$

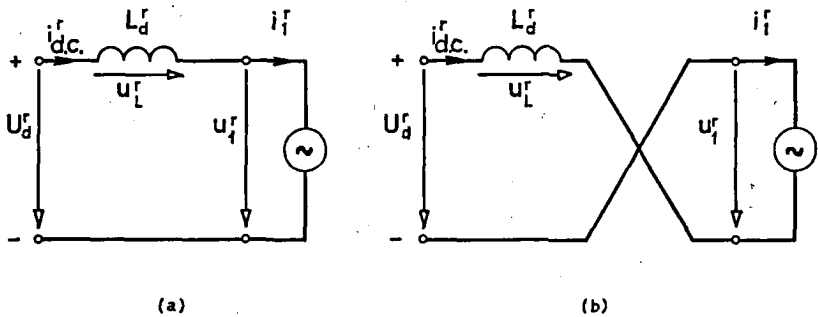


Fig. 15 Representation of the stator of the single-phase controlled synchronous machine

U_d^r = the per-unit value of the d.c. voltage driving the stator winding
 L_d^r = the per-unit value of the smoothing inductance
 u_L^r = the per-unit value of the voltage drop across the smoothing inductance
 u_1^r = the per-unit value of the phase voltage

$$= R^r \cdot i_1^r + \frac{d\psi_1^r}{d\tau}$$

i_1^r = the per-unit value of the stator current
 R^r = the per-unit value of the stator resistance
 ψ_1^r = the per-unit value of the total flux linking the stator winding
 τ = the per-unit value of the time t

(a) = case when current flows in the forward direction
 (b) = case when current flows in the reverse direction

$$\text{thus } i_1^r = -\frac{1}{L_d^r} \int \left(5 R^r \cdot i_1^r + \frac{d\psi_1^r}{dt_c} - 5 U_d^r \right) dt_c$$

The integrated function should be available at the input of the integrator for the period from α' to β' . It should be zero in the period from β' to $\pi + \alpha'$.

Now considering the case in the period where thyratrons 3 and 4 conduct. Here the direction of the current was assumed to be the same as that for the period from α' to $(\alpha' + \pi)$. This is illustrated in Fig. 15b.

Thus for the period $(\pi + \alpha')$ to $(\pi + \beta')$:

$$u_L = L_d \frac{di_{d.c.}}{dt} = U_d + \left(R \cdot i_1 + \frac{d\psi_1}{dt} \right)$$

since $i_{d.c.} = -i_1$, then:

$$L_d \frac{d i_1}{d t} = -U_d - \left(R \cdot i_1 + \frac{d \psi_1}{d t} \right)$$

Introducing the same amplitude and time scales given before, we get:

$$i_1^r = -\frac{1}{L_d^r} \int \left(5 R^r \cdot i_1^r + \frac{d \psi_1^r}{d t_c} + 5 U_d^r \right) dt_c$$

Thus if we form a voltage that equals U_d^r during the period from α' to $(\pi + \alpha')$ and equals $-U_d^r$ during the period from $(\pi + \alpha')$ to $(2\pi + \alpha')$, and if we denote this voltage by u_a^r , we obtain an equation valid for the current i_1^r , so long as the integrated function is available during the conduction periods and so long as that function is made zero during the nonconducting periods.

The equation of the stator current is thus:

$$i_1^r = -\frac{1}{L_d^r} \int \left(5 R^r \cdot i_1^r + \frac{d \psi_1^r}{d t_c} - 5 u_a^r \right) dt_c \quad (91)$$

The practical realization of the conditions made on this equation so that the thyatron effect may be fulfilled will be explained in section 6.2.

The following equations, together with equation (91) describe the phenomenon appearing in the single-phase controlled synchronous machine:

$$-0.5 \psi_f^r = -0.0215 \int (U_f^r - i_f^r) dt_c \quad (79)$$

$$-0.25 \psi_D^r = -0.0217 \int -i_D^r dt_c \quad (92)$$

$$-5 \psi_Q^r = -0.5112 \int -i_Q^r dt_c \quad (93)$$

$$0.5 i_D^r = -(-0.5 \psi_D^r + 0.4897 i_f^r + 0.2523 i_1^r \cdot \cos \gamma) \quad (94)$$

$$2 i_Q^r = -(-2 \psi_Q^r - 0.3851 i_1^r \cdot \sin \gamma) \quad (95)$$

$$0.5 i_f^r = -(-0.5 \psi_f^r + 0.2306 i_1^r \cdot \cos \gamma + 0.4475 i_D^r) \quad (96)$$

$$0.1 \psi_1^r = -\left[-(0.0424 + 0.0156 \cos 2 \gamma) \cdot i_1^r \right. \\ \left. - 0.1 (i_f^r + i_D^r) \cdot \cos \gamma + 0.1 i_Q^r \cdot \sin \gamma \right] \quad (97)$$

It is the general practice in the analog computing technique to avoid differentiation since it is a noise amplifying process. However, it is in some cases unavoidable as in our case where we have to form the function $d\psi_1^r/dt_c$ out of the quantity ψ_1^r , otherwise we need a much greater number of multipliers as will be given in details in chapter 9.

Satisfactory results can be obtained by approximate differentiation which can be made to approach arbitrarily close to the true derivative. Compromise has to be done so that the noise is not too high and at the same time the error in differentiation is not great. The circuit for differentiation is based on the solution of the implicit equation:

$$z = -x - \int z \cdot dt + k \cdot z$$

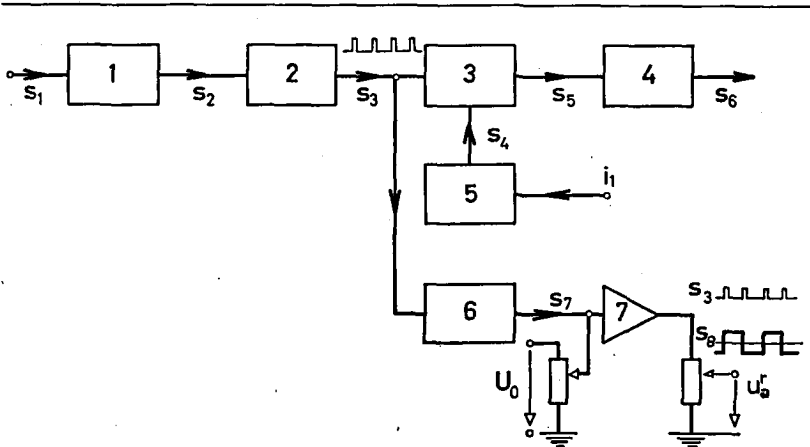


Fig. 16 Block diagram of the thyatron simulator for the single-phase controlled synchronous machine

- 1 = Schmitt trigger
- 2 = monostable multivibrator
- 3 = Schmitt trigger
- 4 = gate
- 5 = clipper and differentiator
- 6 = bistable multivibrator
- 7 = summing amplifier
- $s_1 = 50 \sin \gamma$
- $s_2 =$ reference pulses
- $s_3 =$ ignition pulses
- $s_4 =$ cut-off pulses
- $s_5 =$ square wave controlling the gate 4
- $s_6 =$ output of the gate
- $s_7 =$ square wave = output of the bistable multivibrator
- $U_0 =$ d.c. voltage to compensate the d.c. level of s_7

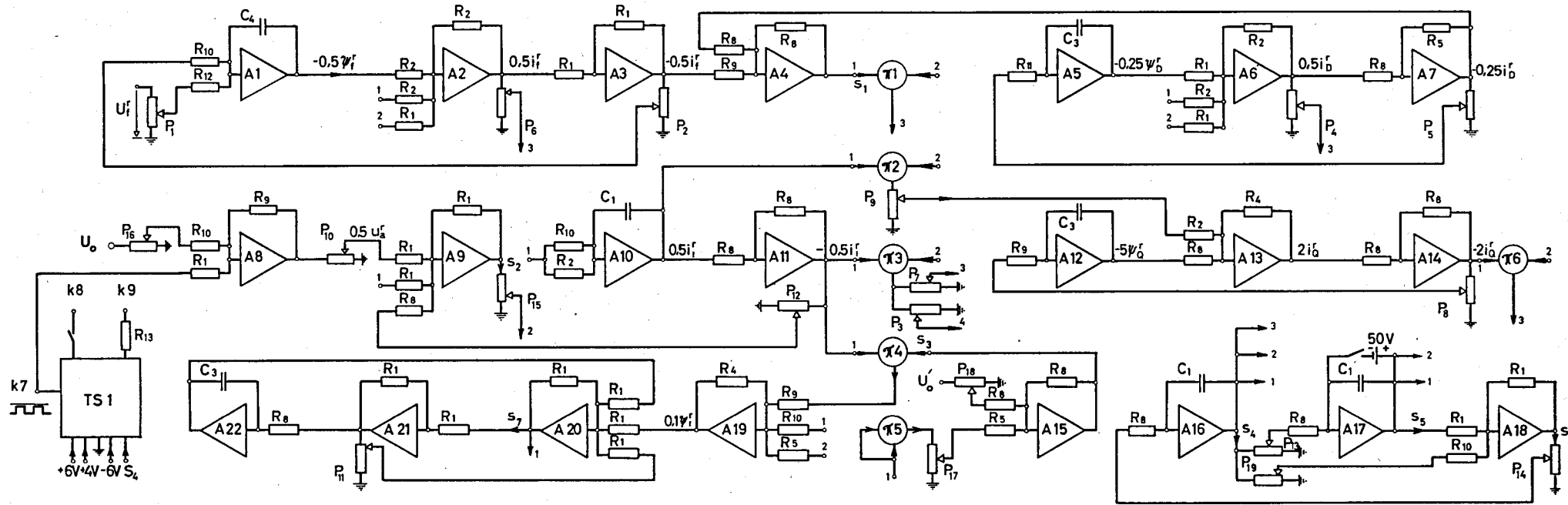


Fig. 17 Analog computer scheme simulating the single-phase controlled synchronous machine

$A2.1 = \pi 3.4$	$A2.2 = A6.3$	$A2.3 = A6.1$	$s_6 = -50 \cos \gamma$	$s_7 = -0.1 \frac{d\psi'_1}{dt_c}$
$A6.2 = \pi 3.3$	$A9.1 = A20.1$	$A9.2 = k8$	$U_0 = U'_0 = 100 \text{ V}$	$TS1 = \text{thyatron simulator}$
$A10.1 = k9$	$A16.1 = \pi 6.2$	$A16.2 = \pi 5.1$		
$A16.3 = \pi 2.2$	$A17.1 = \pi 3.2$	$A17.2 = \pi 1.2$		
$A19.1 = \pi 6.3$	$A19.2 = \pi 1.3$			
$P_1 = 0.4304$	$P_2 = 0.3443$	$P_3 = 0.9224$		
$P_4 = 0.4475$	$P_5 = 0.4431$	$P_6 = 0.9794$		
$P_7 = 0.5046$	$P_8 = 0.5112$	$P_9 = 0.7702$		
$P_{10} = \text{variable}$	$P_{11} = 0.9980$	$P_{12} = 0.5709$		
$P_{13} = 0.5 \omega_m^r = 0.5000$	$P_{16} = 0.8000$	$P_{14} = 0.5 \omega_m^r = 0.5000$		
$P_{15} = 0.1972$	$P_{19} = 0.0040$	$P_{17} = 0.6240$		
$P_{18} = 0.5804$				

$$s_1 = 0.25 (i'_f + i'_D) \quad s_2 = 0.1 L'_d \frac{di'_1}{dt_c}$$

$$s_3 = 100 (0.3120 \sin^2 \gamma - 0.5804)$$

$$s_4 = 50 \sin \gamma$$

$$s_5 = 50 \cos \gamma$$

Leer - Vide - Empty

which gives:

$$z = - \frac{p}{1 + (1 - k) \cdot p} x$$

so that

$$\lim_{k \rightarrow 1} z = - \frac{dx}{dt}$$

This is done by means of the 2 amplifiers $A20$ and $A21$ and the integrator $A22$ of the circuit shown in *Fig. 17*. The potentiometer-setting k is adjusted as near to unity as the noise level permits which achieved in our case the value of $k = 0.998$. Since the speed was assumed to be constant, the same method of building the $\sin \gamma$ and $\cos \gamma$ explained in section 5 was also used, namely by solving the differential equation (76).

6.2 Simulation of the inverter effect

A transistorized circuit was formerly built in a dissertation made in the Institute of General Electrical Engineering (Diss. No. 3060, ETH, BADR) to obtain a function similar to that required in this case. Benefit was made of a part of this apparatus after adding the necessary completions to fulfil the requirements asked for in our problem. A block diagram representing one phase of the mentioned circuit is given in *Fig. 16*.

In this diagram, the gate allows any function to exist during the conduction periods, otherwise this function will be intentionally made equal to zero. The pulses defining the ignition points are obtained by delaying the reference pulses by the angle α' . This is done by a monostable multivibrator. The cut-off pulses are obtained by means of a Schmitt trigger when the current i_1 crosses the zero axis.

In order to complete the circuit so that it may comply with the requirements of this problem, the voltage u_a' mentioned in section 6.1 should be generated. The series of pulses coming out of the monostable multivibrator were made to trigger a bistable multivibrator. The d.c. component contained in the output of that multivibrator was eliminated by adding a constant voltage U_0 to it. This takes place in the summing amplifier $A8$ of *Fig. 17*. The output thus obtained fulfils the requirements of u_a' [equation (91)].

In order to vary the amplitude of u_a' , the output of amplifier $A8$ is fed to a potentiometer. Thus u_a' will be positive during the period from α' to $(\alpha' + \pi)$, and it will be negative during the period from $(\pi + \alpha')$ to $(\alpha' + 2\pi)$.

6.3 Analog set-up

The equations (79) and (91)...(97) describing the phenomenon were simulated on the analog computer. Twenty-two amplifiers, six multipliers and nineteen potentiometers were necessary to carry out this simulation.

The transistorized circuit whose block diagram is shown in *Fig. 16* was used in conjunction with the analog computer (of the Donner type) to fulfil the ignition and extinction conditions required because of the thyatron effect.

The analog scheme is shown in *Fig. 17*. For the adjustment of the potentiometers on the required values, the null voltmeter was used to take into consideration the loading effect of the next stage.

6.4 Analog computer results

6.4.1 Oscillograms

Fig. 18 shows oscillograms representing the case of the single-phase controlled synchronous machine for a firing angle of $\alpha' = 140^\circ$ and for an applied voltage equal to 5% of the reference voltage. The angle α' was

Fig. 18 Oscillograms of the single-phase system

100 V \cong 100% of the reference value

$U_d^r = 30\%$ $U_f^r = 100\%$ $\omega_m^r = 1$ $\alpha' = 140^\circ$

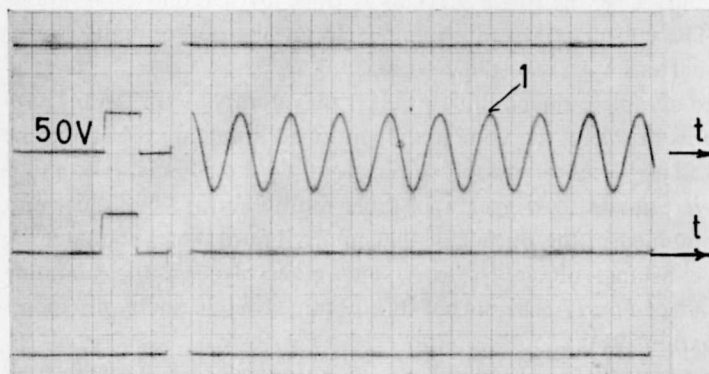


Fig. 18a The no load phase voltage u_1^r

$1 = 0.5 u_1^r$

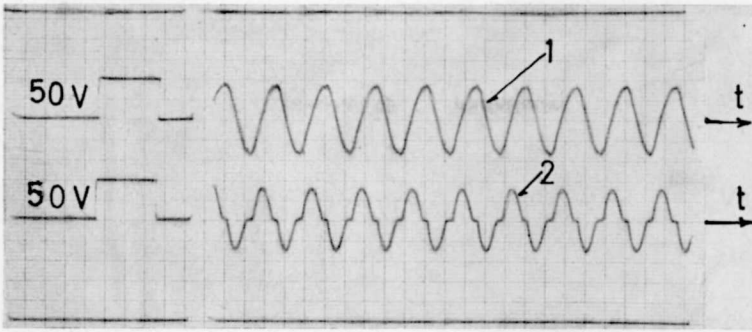


Fig. 18b The phase voltage u_1^r and the phase current i_1^r

$$1 = 0.5 u_1^r \quad 2 = 0.5 i_1^r$$

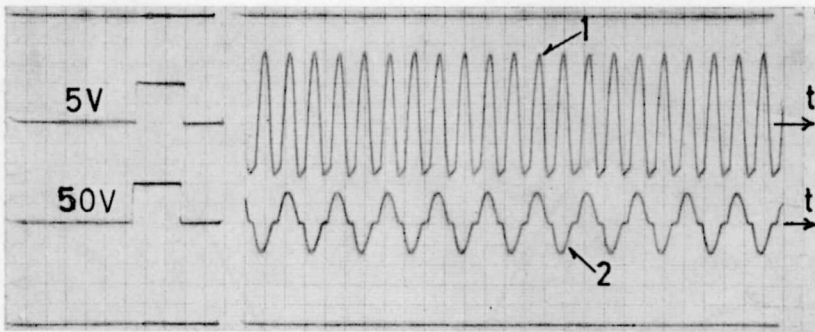


Fig. 18c The current in the damper winding in the direct axis direction i_d^r and the phase current i_1^r

$$1 = 0.25 i_d^r \quad 2 = 0.5 i_1^r$$

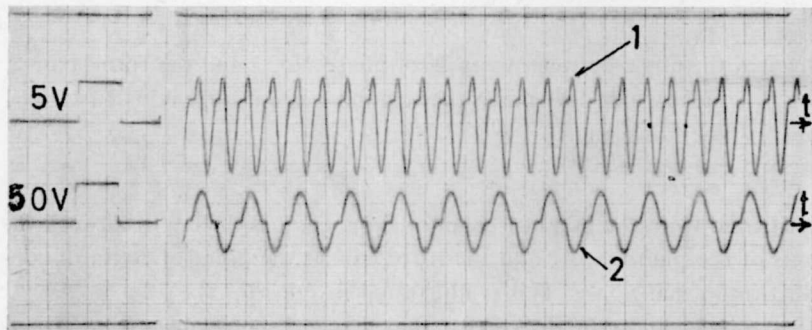


Fig. 18d The current in the damper winding in the quadrature axis direction i_q^r and the phase current i_1^r

$$1 = 2 i_q^r \quad 2 = 0.5 i_1^r$$

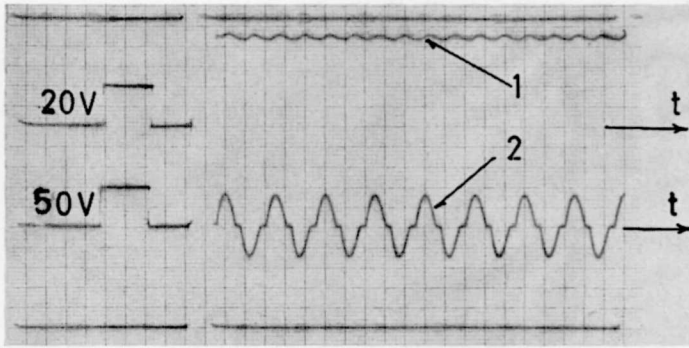


Fig. 18e The field current i_f' and the phase current i_1'
 $1 = 0.5 i_f'$ $2 = 0.5 i_1'$

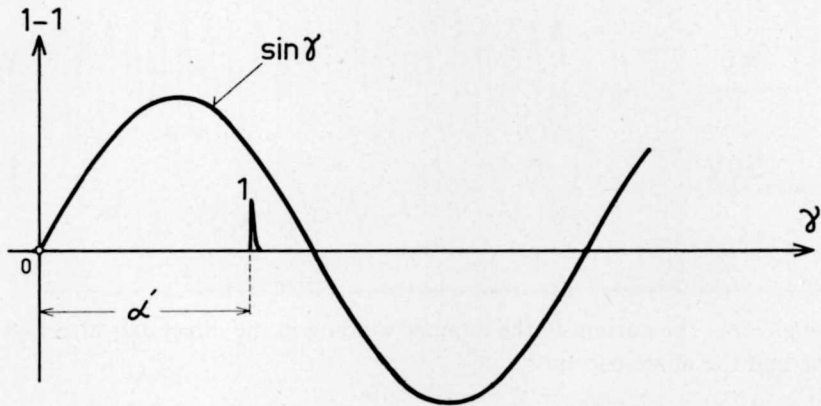


Fig. 19 Figure illustrating the definition of the firing angle

$1\gamma - 1$ = axis of the phase No. 1

1 = the angle between the axis of phase No. 1 and the rotor axis

1 = pulse which determines the beginning of the current in phase No. 1

α' = the firing angle

measured from the point of begin of $\sin \gamma$, i.e. it is the angle between the axis of the phase No. 1 and the rotor axis at the point of begin of conduction in that phase. This is illustrated in Fig. 19.

It is to be noted that the current that flows in the damper winding has a fundamental frequency equal to double that of the stator current. This is valid for both damper windings. The field current is also given and we note the effect of the stator current on it, formerly noted in Fig. 2.

6.4.2 External characteristics

The average value of the stator current i_1^r is to be determined according to the equation:

$$i_{d.c.}^r = \frac{2}{T_c} \int_0^{\frac{T_c}{2}} i_1^r dt_c$$

and since the period $T_c = 1.2566$ s, then

$$\begin{aligned} i_{d.c.}^r &= \frac{1}{0.6283} \int_0^{\frac{T_c}{2}} i_1^r dt_c \\ &= 1.5916 \int_0^{\frac{T_c}{2}} i_1^r dt_c \end{aligned}$$

Thus if the current i_1^r is integrated over half the period and then the output multiplied by the factor 1.5916, we get a voltage proportional to the d.c. current taken from the d.c. power supply. The definite integral is achieved with the help of a cyclic reset generator which resets the output of the integrator every $0.5 T_c$ s, i.e. after 0.6283 s. Since the cyclic reset

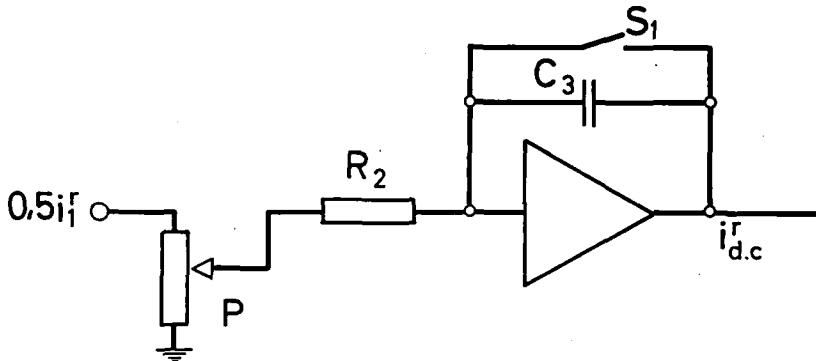


Fig. 20 Analog scheme to calculate the d.c. current $i_{d.c.}^r$ in the single-phase system

$$P = 0.6366$$

S_1 = a switch activated by the cyclic reset generator every $0.5 T_c$

generator possesses a reset time of 0.081 s, then its interval should be 0.7093 s. The finite reset time of the cyclic reset generator has no harmful effect on the results to be anticipated since the period of integration will always be $0.5 T_c$, but the moment at which it begins will be different. The circuit used to obtain the d.c. current is shown in *Fig. 20*. The output of the integrator used in this circuit was recorded with the help of a mingograph 230 recording instrument, being a 4-channel recorder driven by a synchronous motor.

The voltage u'_a was also recorded using the same recording instrument on another channel. For every firing angle α' , records were taken for $i'_{d.c.}$, where u'_a was varied from zero volts until the "tilting-limit" was achieved. The angle α' was measured with respect to $\sin \gamma$ using a time measuring instrument [20] (being of the digital type with an accuracy up to 0.1 ms). The measurements taken for $i'_{d.c.}$, u'_a with α' as parameter were plotted and shown in *Fig. 21*. For the sake of comparison between experimental and calculated results, one of the curves of the external characteristics of *Fig. 3* (the curve corresponding to the firing angle $\alpha' = 130^\circ$) was chosen and replotted on the same figure.

It is to be noted that in the calculated results no provision was made for the voltage drop across the thyatron tubes which ranges normally between 15...20 V. Since in our case two thyratrons conduct at the same time, then a voltage drop of 35 V was assumed as the sum of the voltage drop across these two thyratrons. Converting this to the per-unit value and shifting the curve by this value, we get the dotted curve which coincides with the calculated one at the region when ξ is near 180° . At values

Fig. 21 External characteristics of the single-phase controlled synchronous machine

U'_d = d.c. voltage (per unit)

$I'_{d.c.}$ = d.c. current (per unit)

1 = firing angle $\alpha' = 170^\circ$

2 = firing angle $\alpha' = 160^\circ$

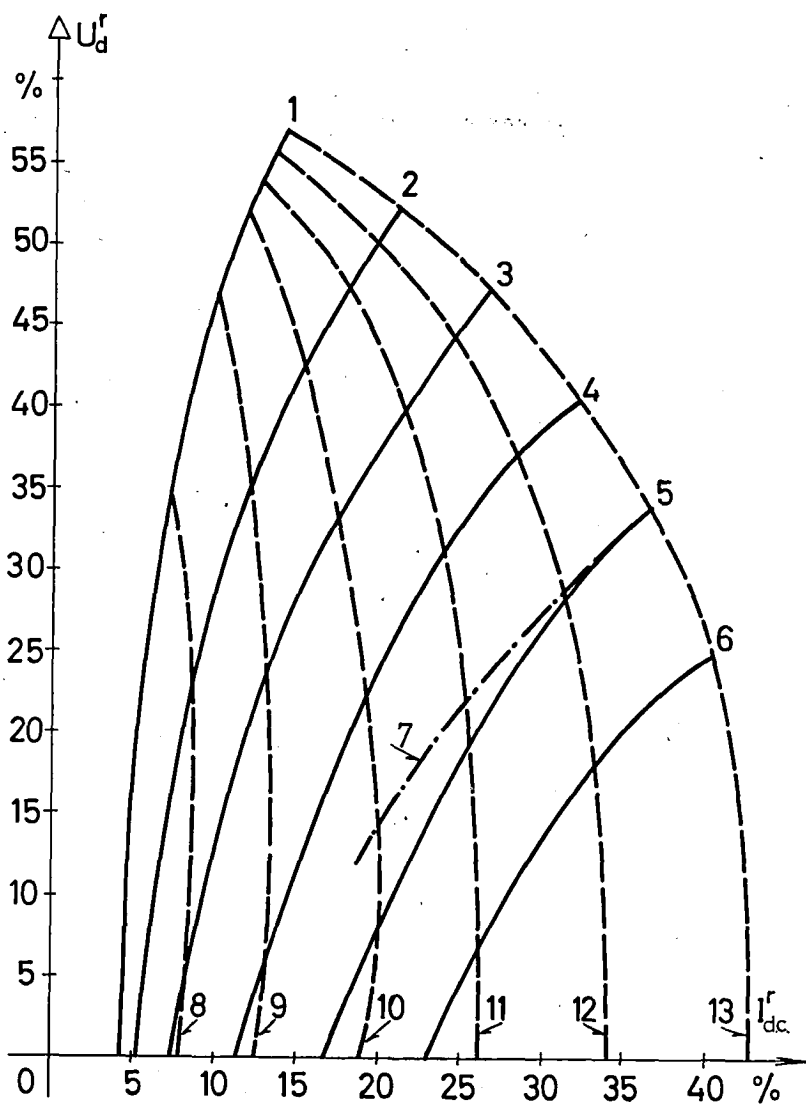
3 = firing angle $\alpha' = 150^\circ$

4 = firing angle $\alpha' = 140^\circ$

5 = firing angle $\alpha' = 130^\circ$

6 = firing angle $\alpha' = 120^\circ$

7 = the corresponding curve taken directly from the synchronous machine for $\alpha' = 130^\circ$



- 8 = conduction angle $\xi = 80^\circ$
- 9 = conduction angle $\xi = 100^\circ$
- 10 = conduction angle $\xi = 120^\circ$
- 11 = conduction angle $\xi = 140^\circ$
- 12 = conduction angle $\xi = 160^\circ$
- 13 = conduction angle $\xi = 180^\circ$

of ξ far from 180° electrical, there is a deviation between the calculated and experimental curves. This deviation is to be expected since the gate of Fig. 16 is not perfect in the sense that during the interval where the input to the integrator A 10 of Fig. 17 has to be zero, there is a small voltage drop across the diode of this gate. This voltage drop is integrated in the integrator A 10 resulting in an increase in the output d.c. current, and this increase is larger when the nonconducting period is larger. However, this effect was remedied on constructing the circuit simulating the thyatron effect in the three-phase case which will be given in section 7.3.7. Another method for improving this circuit was given by Dr. BADR in the "locomotive session" held in Zurich in Oktober 1961.

6.4.3 Current locus

It is to be noted that both the phase current and phase voltage contain harmonics. The current i_1^r can be put in the form:

$$i_1^r = I_{1c}^r \cdot \cos x + I_{5c}^r \cdot \cos 5x + I_{7c}^r \cdot \cos 7x + \dots \\ + I_{1s}^r \cdot \sin x + I_{5s}^r \cdot \sin 5x + I_{7s}^r \cdot \sin 7x + \dots \quad (98)$$

where $x = \gamma = 5 \omega_m^r t_c$,

and it is possible to put the voltage u_1^r in the form:

$$u_1^r = U_{1c}^r \cdot \cos x + U_{5c}^r \cdot \cos 5x + U_{7c}^r \cdot \cos 7x + \dots \\ + U_{1s}^r \cdot \sin x + U_{5s}^r \cdot \sin 5x + U_{7s}^r \cdot \sin 7x + \dots \quad (99)$$

In order to determine the behaviour of the fundamental component of the current, it is necessary to determine the value of I_{1c}^r , I_{1s}^r , U_{1c}^r , U_{1s}^r . These values were determined according to the following equations:

$$I_{1c}^r = \frac{2}{T_c} \int_0^{T_c} i_1^r \cdot \cos x \cdot dt_c = 1.5916 \int_0^{1.2566} i_1^r \cdot \cos x \cdot dt_c \quad (100)$$

$$I_{1s}^r = 1.5916 \int_0^{1.2566} i_1^r \cdot \sin x \cdot dt_c \quad (101)$$

$$U_{1c}^r = 1.5916 \int_0^{1.2566} u_1^r \cdot \cos x \cdot dt_c \quad (102)$$

$$U_{1s}^r = 1.5916 \int_0^{1.2566} u_1^r \cdot \sin x \cdot dt_c \quad (103)$$

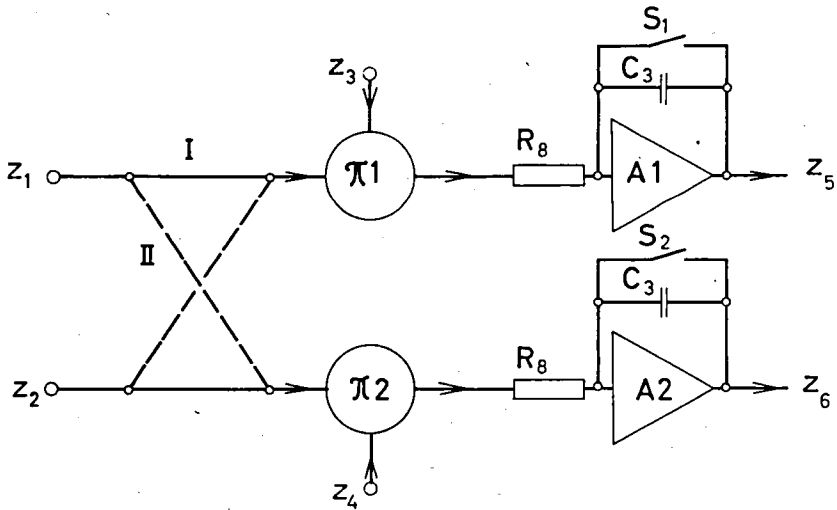


Fig. 22 Analog set-up for determining the current locus

$$z_1 = 50 \sin \gamma$$

$$z_2 = 50 \cos \gamma$$

$$z_3 = 0.5 i_1'$$

$$z_4 = 0.1 \frac{d\psi_1'}{dt_c}$$

$$z_5 = 0.6283 I_{1s}' \quad \text{switch in position I}$$

$$= 0.6283 I_{1c}' \quad \text{switch in position II}$$

$$z_6 = 0.6283 U_{1c}' \quad \text{switch in position I}$$

$$= 0.6283 U_{1s}' \quad \text{switch in position II}$$

The two switches S_1 and S_2 are activated by the cyclic reset generator having a period of 1.2566 s

The analog set-up of these equations is fulfilled by the scheme given in Fig. 22. The determination of the quantities I_{1c}' , I_{1s}' , U_{1c}' , U_{1s}' enables the calculation of the amplitude of the fundamental components of both the current and voltage and their phase angles with respect to the function $\sin x$. Hence it is possible to determine the amplitude and phase of the fundamental component of the current with respect to the fundamental component of the voltage. This was executed for different values of α' as parameter and the resulting family of curves is shown in Fig. 23.

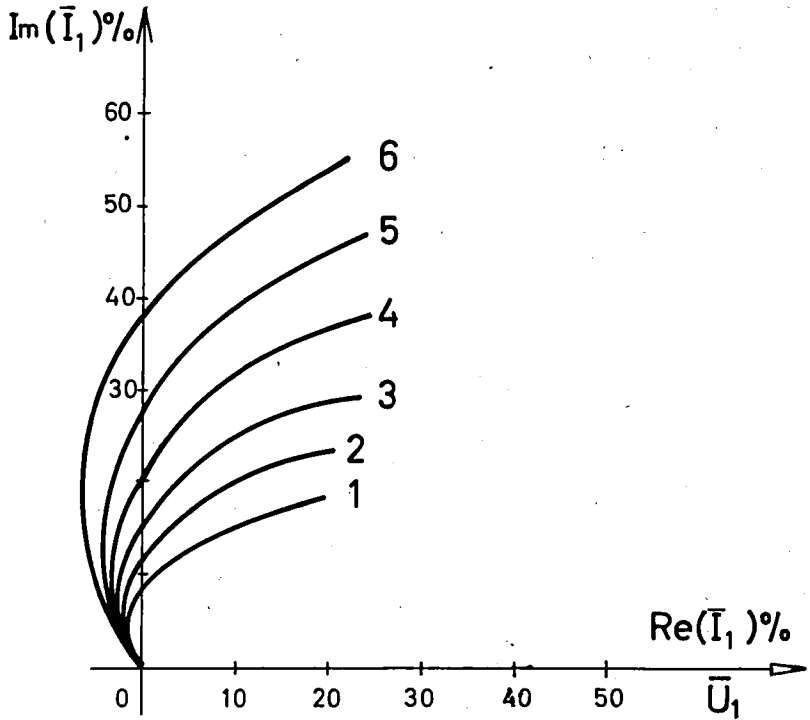


Fig. 23 Current loci for the single-phase operation

\bar{I}_1 = complex vector of the fundamental component of the phase current

$Re(\bar{I}_1)$ = the part of the fundamental component of the phase current which is in phase with the fundamental component of the voltage

$Im(\bar{I}_1)$ = the part of the fundamental component of the phase current which is in quadrature with the fundamental component of the voltage

1 : $\alpha' = 170^\circ$

3 : $\alpha' = 150^\circ$

5 : $\alpha' = 130^\circ$

2 : $\alpha' = 160^\circ$

4 : $\alpha' = 140^\circ$

6 : $\alpha' = 120^\circ$

The first quadrant, where the fundamental component of the current is in phase with that of the voltage represents the region where the machine works as a motor. The quadrant where this component is in antiphase is the region where the machine is a generator.

7. ANALOG COMPUTATION OF THE THREE-PHASE CONTROLLED SYNCHRO- NOUS MACHINE

7.1 The mathematical formulation

Feeding the stator of the three-phase synchronous machine from a d.c. power supply through 6 thyratrons, connected in a bridge circuit, results in stator currents represented in *Fig. 24*. The current in each phase suffers 6 switching intervals for every 180° electrical. In order to be able to simulate these currents on the analog computer, it is necessary to obtain a mathematical expression for the derivative of the current flowing in each phase. This expression should be valid during the interval at which that phase carries current and should be zero outside that interval. Considering the current flowing in phase No. 1, this expression should be valid during the intervals *AA'* and *BB'*, and should be intentionally made zero during the intervals *A'B* and *B'A*.

The fact that the phase current suffers 6 switching actions during each 180° electrical suggests dividing this period into 6 intervals, let us denote them by the letters *a, b, c, d, e, f* as shown in *Fig. 24*. The second half period (180°...360°) was also divided into 6 intervals, denoted by the letters *g, h, i, j, k, l*. During the overlapping interval *a* for example, the phases 1 and 3 are connected in parallel and their combination is in series with phase 2 and the smoothing inductance L_d . They form the load of the d.c. power supply U_d .

Applying KIRCHHOFF's law of circulating currents on this loop, and on the inner loop consisting of phases 1 and 3 in parallel, we get:

$$U_d = L_d \frac{d}{dt} (i_1 + i_3) + R(i_1 - i_2) + \frac{d}{dt} (\psi_1 - \psi_2)$$

$$R \cdot i_1 + \frac{d\psi_1}{dt} = R \cdot i_3 + \frac{d\psi_3}{dt}$$

$$\text{thus } L_d \frac{d i_1}{dt} = \frac{U_d}{2} + \frac{L_d}{2R} \cdot \frac{d^2}{dt^2} (\psi_3 - \psi_1)$$

$$+ \frac{R}{2} (i_2 - i_1) + \frac{1}{2} \cdot \frac{d}{dt} (\psi_2 - \psi_1) \quad (104)$$

Substituting the values of ψ_1, ψ_2, ψ_3 given in the equations (29)...(31) in

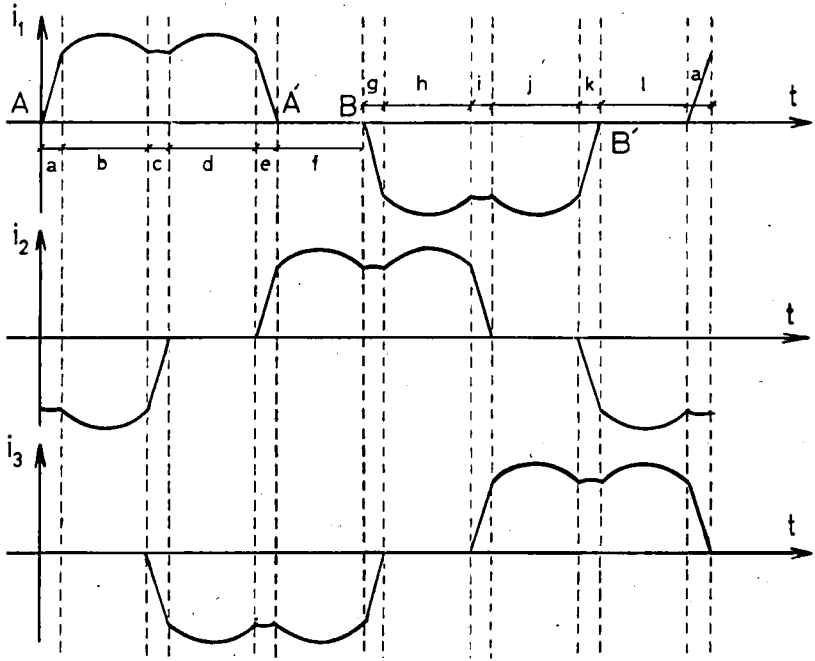


Fig. 24 Diagram representing the currents flowing in the stator of the three-phase controlled synchronous machine

a, c, e, g, i, k = overlapping intervals

b, d, f, h, j, l = nonoverlapping intervals

equation (104) and taking into consideration that $\psi_0 = 0$, we get:

$$L_d \frac{d i_1}{d t} = \frac{U_d}{2} - \frac{L_d}{2R} \cdot \frac{d^2}{d t^2} \left(\frac{3}{2} \psi_\alpha + \frac{\sqrt{3}}{2} \psi_\beta \right) + \frac{R}{2} (i_2 - i_1) + \frac{d}{d t} \left(-\frac{3}{4} \psi_\alpha + \frac{\sqrt{3}}{4} \psi_\beta \right) \quad (105)$$

During the nonoverlapping period b , the current flows from the positive pole of the d.c. power supply through the smoothing inductance L_d , phase 1 and phase 2. Applying KIRCHHOFF'S law, we get:

$$L_d \frac{d i_1}{d t} = U_d + R(i_2 - i_1) + \frac{d}{d t} (\psi_2 - \psi_1) = U_d + R \cdot (i_2 - i_1) + \frac{d}{d t} \left(-\frac{3}{2} \psi_\alpha + \frac{\sqrt{3}}{2} \psi_\beta \right) \quad (106)$$

If we continue applying this procedure on the rest of the intervals, and using the same amplitude and time scaling formerly given in chapter 5, we get an expression for $L'_d (di'_1/dt_c)$.

This was carried out, and the results are shown in table I.

Table I

Interval	$L'_d \frac{di'_1}{dt_c} =$
a	$\frac{5 U'_d}{2} - \frac{L'_d}{10 R^r} \cdot \frac{d^2}{dt_c^2} \left(\frac{3}{2} \psi'_\alpha + \frac{\sqrt{3}}{2} \psi'_\beta \right)$ $+ \frac{5 R^r}{2} (i'_2 - i'_1) + \frac{1}{2} \cdot \frac{d}{dt_c} \left(-\frac{3}{2} \psi'_\alpha + \frac{\sqrt{3}}{2} \psi'_\beta \right)$
b	$5 U'_d + 5 R^r (i'_2 - i'_1) + \frac{d}{dt_c} \left(-\frac{3}{2} \psi'_\alpha + \frac{\sqrt{3}}{2} \psi'_\beta \right)$
c	$5 U'_d + 5 R^r (i'_3 - i'_1) - \frac{d}{dt_c} \left(\frac{3}{2} \psi'_\alpha + \frac{\sqrt{3}}{2} \psi'_\beta \right)$
d	$5 U'_d + 5 R^r (i'_3 - i'_1) - \frac{d}{dt_c} \left(\frac{3}{2} \psi'_\alpha + \frac{\sqrt{3}}{2} \psi'_\beta \right)$
e	$\frac{5 U'_d}{2} + \frac{L'_d}{10 R^r} \cdot \frac{d^2}{dt_c^2} \left(-\frac{3}{2} \psi'_\alpha + \frac{\sqrt{3}}{2} \psi'_\beta \right)$ $+ \frac{5 R^r}{2} (i'_3 - i'_1) - \frac{1}{2} \cdot \frac{d}{dt_c} \left(\frac{3}{2} \psi'_\alpha + \frac{\sqrt{3}}{2} \psi'_\beta \right)$
f	0
g	$-\frac{5 U'_d}{2} - \frac{L'_d}{10 R^r} \cdot \frac{d^2}{dt_c^2} \left(\frac{3}{2} \psi'_\alpha + \frac{\sqrt{3}}{2} \psi'_\beta \right)$ $+ \frac{5 R^r}{2} (i'_2 - i'_1) + \frac{1}{2} \cdot \frac{d}{dt_c} \left(-\frac{3}{2} \psi'_\alpha + \frac{\sqrt{3}}{2} \psi'_\beta \right)$
h	$-5 U'_d + 5 R^r (i'_2 - i'_1) + \frac{d}{dt_c} \left(-\frac{3}{2} \psi'_\alpha + \frac{\sqrt{3}}{2} \psi'_\beta \right)$
i	$-5 U'_d + 5 R^r (i'_3 - i'_1) + \frac{d}{dt_c} \left(-\frac{3}{2} \psi'_\alpha - \frac{\sqrt{3}}{2} \psi'_\beta \right)$

Table I (cont.)

Interval	$L_d^r \frac{d i_1^r}{d t_c} =$
j	$-5 U_d^r + 5 R^r (i_3^r - i_1^r) + \frac{d}{d t_c} \left(-\frac{3}{2} \psi_\alpha^r - \frac{\sqrt{3}}{2} \psi_\beta^r \right)$
k	$-\frac{5 U_d^r}{2} + \frac{L_d^r}{10 R^r} \cdot \frac{d^2}{d t_c^2} \left(-\frac{3}{2} \psi_\alpha^r + \frac{\sqrt{3}}{2} \psi_\beta^r \right)$ $+ \frac{5 R^r}{2} (i_3^r - i_1^r) + \frac{1}{2} \cdot \frac{d}{d t_c} \left(-\frac{3}{2} \psi_\alpha^r - \frac{\sqrt{3}}{2} \psi_\beta^r \right)$
l	0

Carrying this procedure on the phases 2 and 3, with the aim of obtaining expressions for $L_d^r (d i_2^r / d t_c)$ and $L_d^r (d i_3^r / d t_c)$, we get the equations tabulated in table II and table III.

Table II

Interval	$L_d^r \frac{d i_2^r}{d t_c} =$
a	$-5 U_d^r + 5 R^r (i_1^r - i_2^r) + \frac{d}{d t_c} \left(\frac{3}{2} \psi_\alpha^r - \frac{\sqrt{3}}{2} \psi_\beta^r \right)$
b	$-5 U_d^r + 5 R^r (i_1^r - i_2^r) + \frac{d}{d t_c} \left(\frac{3}{2} \psi_\alpha^r - \frac{\sqrt{3}}{2} \psi_\beta^r \right)$
c	$-\frac{5 U_d^r}{2} + \frac{L_d^r}{10 R^r} \cdot \frac{d^2}{d t_c^2} (-\sqrt{3} \psi_\beta^r)$ $+ \frac{5 R^r}{2} (i_1^r - i_2^r) + \frac{1}{2} \cdot \frac{d}{d t_c} \left(\frac{3}{2} \psi_\alpha^r - \frac{\sqrt{3}}{2} \psi_\beta^r \right)$
d	0
e	$\frac{5 U_d^r}{2} + \frac{L_d^r}{10 R^r} \cdot \frac{d^2}{d t_c^2} \left(-\frac{\sqrt{3}}{2} \psi_\beta^r + \frac{3}{2} \psi_\alpha^r \right)$ $+ \frac{5 R^r}{2} (i_3^r - i_2^r) + \frac{1}{2} \cdot \frac{d}{d t_c} (-\sqrt{3} \psi_\beta^r)$

Table II (cont.)

Interval	$L'_d \frac{d i'_2}{d t_c} =$
f	$5 U'_d + 5 R' (i'_3 - i'_2) + \frac{d}{d t_c} (-\sqrt{3} \psi'_\beta)$
g	$5 U'_d + 5 R' (i'_1 - i'_2) + \frac{d}{d t_c} \left(\frac{3}{2} \psi'_\alpha - \frac{\sqrt{3}}{2} \psi'_\beta \right)$
h	$5 U'_d + 5 R' (i'_1 - i'_2) + \frac{d}{d t_c} \left(\frac{3}{2} \psi'_\alpha - \frac{\sqrt{3}}{2} \psi'_\beta \right)$
i	$\frac{5 U'_d}{2} + \frac{L'_d}{10 R'} \cdot \frac{d^2}{d t_c^2} (-\sqrt{3} \psi'_\beta)$ $+ \frac{5 R'}{2} (i'_1 - i'_2) + \frac{1}{2} \cdot \frac{d}{d t_c} \left(\frac{3}{2} \psi'_\alpha - \frac{\sqrt{3}}{2} \psi'_\beta \right)$
j	0
k	$-\frac{5 U'_d}{2} + \frac{L'_d}{10 R'} \cdot \frac{d^2}{d t_c^2} \left(\frac{3}{2} \psi'_\alpha - \frac{\sqrt{3}}{2} \psi'_\beta \right)$ $+ \frac{5 R'}{2} (i'_3 - i'_2) + \frac{1}{2} \cdot \frac{d}{d t_c} (-\sqrt{3} \psi'_\beta)$
l	$-5 U'_d + 5 R' (i'_3 - i'_2) + \frac{d}{d t_c} (-\sqrt{3} \psi'_\beta)$

Table III

Interval	$L'_d \frac{d i'_3}{d t_c} =$
a	$\frac{5 U'_d}{2} + \frac{L'_d}{10 R'} \cdot \frac{d^2}{d t_c^2} \left(\frac{3}{2} \psi'_\alpha + \frac{\sqrt{3}}{2} \psi'_\beta \right) + \frac{5 R'}{2} (i'_2 - i'_3)$ $+ \frac{1}{2} \cdot \frac{d}{d t_c} (\sqrt{3} \psi'_\beta)$

Table III (cont.)

Interval	$L_d^r \frac{d i_3^r}{d t_c} =$
b	0
c	$\frac{5 U_d^r}{2} + \frac{L_d^r}{10 R^r} \cdot \frac{d^2}{d t_c^2} (\sqrt{3} \psi_\beta^r) + \frac{5 R^r}{2} (i_1^r - i_3^r)$ $+ \frac{1}{2} \cdot \frac{d}{d t_c} \left(\frac{3}{2} \psi_\alpha^r + \frac{\sqrt{3}}{2} \psi_\beta^r \right)$
d	$-5 U_d^r + 5 R^r (i_1^r - i_3^r) + \frac{d}{d t_c} \left(\frac{3}{2} \psi_\alpha^r + \frac{\sqrt{3}}{2} \psi_\beta^r \right)$
e	$-5 U_d^r + 5 R^r (i_2^r - i_3^r) + \frac{d}{d t_c} (\sqrt{3} \psi_\beta^r)$
f	$-5 U_d^r + 5 R^r (i_2^r - i_3^r) + \frac{d}{d t_c} (\sqrt{3} \psi_\beta^r)$
g	$-\frac{5 U_d^r}{2} + \frac{L_d^r}{10 R^r} \cdot \frac{d^2}{d t_c^2} \left(\frac{3}{2} \psi_\alpha^r + \frac{\sqrt{3}}{2} \psi_\beta^r \right)$ $+ \frac{5 R^r}{2} (i_2^r - i_3^r) + \frac{1}{2} \cdot \frac{d}{d t_c} (\sqrt{3} \psi_\beta^r)$
h	0
i	$\frac{5 U_d^r}{2} + \frac{L_d^r}{10 R^r} \cdot \frac{d^2}{d t_c^2} (\sqrt{3} \psi_\beta^r)$ $+ \frac{5 R^r}{2} (i_1^r - i_3^r) + \frac{1}{2} \cdot \frac{d}{d t_c} \left(\frac{3}{2} \psi_\alpha^r + \frac{\sqrt{3}}{2} \psi_\beta^r \right)$
j	$5 U_d^r + 5 R^r (i_1^r - i_3^r) + \frac{d}{d t_c} \left(\frac{3}{2} \psi_\alpha^r + \frac{\sqrt{3}}{2} \psi_\beta^r \right)$
k	$5 U_d^r + 5 R^r (i_2^r - i_3^r) + \frac{d}{d t_c} (\sqrt{3} \psi_\beta^r)$
l	$5 U_d^r + 5 R^r (i_2^r - i_3^r) + \frac{d}{d t_c} (\sqrt{3} \psi_\beta^r)$

Table IV shows the different terms that constitute the derivative of each of the stator currents and the intervals during which each of these quantities should be present. Each quantity should be present during the corresponding interval, otherwise it should be made equal to zero. This is effectively done by means of a transistorized circuit which consists of a number of gates defining the right intervals specified in table IV. The transistorized circuit will be explained in detail in section 7.2.

If the right quantities constituting the derivative of each of the stator currents are given to three integrators, then the outputs will represent the three stator currents shown in *Fig. 24*.

Obtaining the three stator currents, it is possible to make the necessary transformations along the direct and quadrature axes. Equations (7), (8), (13) and (14) serve to obtain the currents i_{α}^r , i_{β}^r , i_d^r , and i_q^r .

Equations (19), (21), (5) and (6) allow the calculation of i_D^r , i_Q^r , ψ_D^r and ψ_Q^r respectively. ψ_d^r , ψ_q^r , ψ_{α}^r and ψ_{β}^r can be calculated using the equations (17), (20), (10) and (11). The derivative $d\psi_{\alpha}^r/dt_c$ and $d\psi_{\beta}^r/dt_c$ was done using the same principle mentioned in section 6.1, where the factor k could be adjusted to the value of 0.998.

Performing the differentiation another time is more difficult as the function becomes discontinuous. However, it was possible to obtain satisfactory results for this second differentiation with k adjusted to 0.9, but because of the shortage in the available number of amplifiers, the differentiation was performed using only one amplifier after shunting it with a condenser of 0.1 μF which is effectively the same as if k were 0.9.

Fig. 25 shows the complete analog scheme used to simulate the three-phase controlled synchronous machine.

Because of the lack of a two-channel multiplier at the beginning of the work, the system was solved for the case of constant speed. The $\sin \gamma$ and $\cos \gamma$ were calculated by solving equation (76). The electric torque was calculated according to the equation:

$$M_e^r = \psi_q^r \cdot i_d^r - \psi_d^r \cdot i_q^r \quad (107)$$

where M_e^r = the electric torque resulting from the machine in per unit.

Table IV

Current derivative	Constituents	Interval where each constituent exists
$-\frac{L'_d}{4} \cdot \frac{d i'_1}{d t_c}$	$(1) 50 z_1 = 50 \left[\frac{U'_d}{80} + \frac{3 L'_d}{4000 R^r} \cdot \frac{d^2 \psi'_\alpha}{d t_c^2} + \frac{\sqrt{3} L'_d}{4000 R^r} \cdot \frac{d^2 \psi'_\beta}{d t_c^2} + (i'_1 - i'_2) \cdot \frac{R^r}{80} + \frac{3}{800} \cdot \frac{d \psi'_\alpha}{d t_c} - \frac{\sqrt{3}}{800} \cdot \frac{d \psi'_\beta}{d t_c} \right]$	a, g
	$(2) 25 y_3 = 25 \left[(i'_1 - i'_2) \cdot \frac{R^r}{20} + \frac{3}{200} \cdot \frac{d \psi'_\alpha}{d t_c} - \frac{\sqrt{3}}{200} \cdot \frac{d \psi'_\beta}{d t_c} \right]$	b, h
	$(3) 25 y_1 = 25 \left[(i'_1 - i'_3) \cdot \frac{R^r}{20} + \frac{3}{200} \cdot \frac{d \psi'_\alpha}{d t_c} + \frac{\sqrt{3}}{200} \cdot \frac{d \psi'_\beta}{d t_c} \right]$	c, d, i, j
	$(4) 50 z_2 = 50 \left[-\frac{U'_d}{80} + \frac{3 L'_d}{4000 R^r} \cdot \frac{d^2 \psi'_\alpha}{d t_c^2} - \frac{\sqrt{3} L'_d}{4000 R^r} \cdot \frac{d^2 \psi'_\beta}{d t_c^2} + (i'_1 - i'_3) \cdot \frac{R^r}{80} + \frac{3}{800} \cdot \frac{d \psi'_\alpha}{d t_c} + \frac{\sqrt{3}}{800} \cdot \frac{d \psi'_\beta}{d t_c} \right]$	e, k
	(5) $1.25 U'_d$	h, i, j, k
	(6) $-1.25 U'_d$	a, b, c, d

Table IV (cont.)

Current derivative	Constituents	Interval where each constituent exists
$\frac{L'_d}{4} \frac{di'_2}{dt_c}$	(1) $50 z_4 = 50 \left[\frac{U'_d}{80} + \frac{3 L'_d}{4000 R'} \cdot \frac{d^2 \psi'_\alpha}{dt_c^2} - \frac{\sqrt{3} L'_d}{4000 R'} \cdot \frac{d^2 \psi'_\beta}{dt_c^2} + (i'_3 - i'_2) \cdot \frac{R'}{80} - \frac{\sqrt{3}}{400} \cdot \frac{d \psi'_\beta}{dt_c} \right]$	<i>e, k</i>
	(2) $25 y_5 = 25 \left[(i'_3 - i'_2) \cdot \frac{R'}{20} - \frac{\sqrt{3}}{100} \cdot \frac{d \psi'_\beta}{dt_c} \right]$	<i>f, l</i>
	(3) $25 y_3 = 25 \left[(i'_1 - i'_2) \cdot \frac{R'}{20} + \frac{3}{200} \cdot \frac{d \psi'_\alpha}{dt_c} - \frac{\sqrt{3}}{200} \cdot \frac{d \psi'_\beta}{dt_c} \right]$	<i>g, h, a, b</i>
	(4) $50 z_3 = 50 \left[-\frac{U'_d}{80} - \frac{\sqrt{3} L'_d}{2000 R'} \cdot \frac{d^2 \psi'_\beta}{dt_c^2} + (i'_1 - i'_2) \cdot \frac{R'}{80} + \frac{3}{800} \cdot \frac{d \psi'_\alpha}{dt_c} - \frac{\sqrt{3}}{800} \cdot \frac{d \psi'_\beta}{dt_c} \right]$	<i>i, c</i>
	(5) $1.25 U'_d$	<i>f, g, h, i</i>
	(6) $-1.25 U'_d$	<i>k, l, a, b</i>

Table IV. (cont.)

Current derivative	Constituents	Interval where each constituent exists
$\frac{L'_d}{4} \cdot \frac{d i'_3}{d t_c}$	(1) $50 z_5 = 50 \left[\frac{U'_d}{80} + \frac{\sqrt{3} L'_d}{2000 R'} \cdot \frac{d^2 \psi'_\beta}{d t_c^2} \right.$ $\left. + (i'_1 - i'_3) \cdot \frac{R'}{80} + \frac{3}{800} \cdot \frac{d \psi'_\alpha}{d t_c} \right.$ $\left. + \frac{\sqrt{3}}{800} \cdot \frac{d \psi'_\beta}{d t_c} \right]$	<i>i, c</i>
	(2) $25 y_1 = 25 \left[(i'_1 - i'_3) \cdot \frac{R'}{20} + \frac{3}{200} \cdot \frac{d \psi'_\alpha}{d t_c} \right.$ $\left. + \frac{\sqrt{3}}{200} \cdot \frac{d \psi'_\beta}{d t_c} \right]$	<i>d, j</i>
	(3) $25 y_6 = 25 \left[(i'_2 - i'_3) \cdot \frac{R'}{20} + \frac{\sqrt{3}}{100} \cdot \frac{d \psi'_\beta}{d t_c} \right]$	<i>e, f, k, l</i>
	(4) $50 z_6 = 50 \left[-\frac{U'_d}{80} + \frac{3 L'_d}{4000 R'} \cdot \frac{d^2 \psi'_\alpha}{d t_c^2} \right.$ $\left. + \frac{\sqrt{3} L'_d}{4000 R'} \cdot \frac{d^2 \psi'_\beta}{d t_c^2} + (i'_2 - i'_3) \cdot \frac{R'}{80} \right.$ $\left. + \frac{\sqrt{3}}{400} \cdot \frac{d \psi'_\beta}{d t_c} \right]$	<i>a, g</i>
	(5) $1.25 U'_d$	<i>j, k, l, a</i>
	(6) $-1.25 U'_d$	<i>c, d, e, f</i>

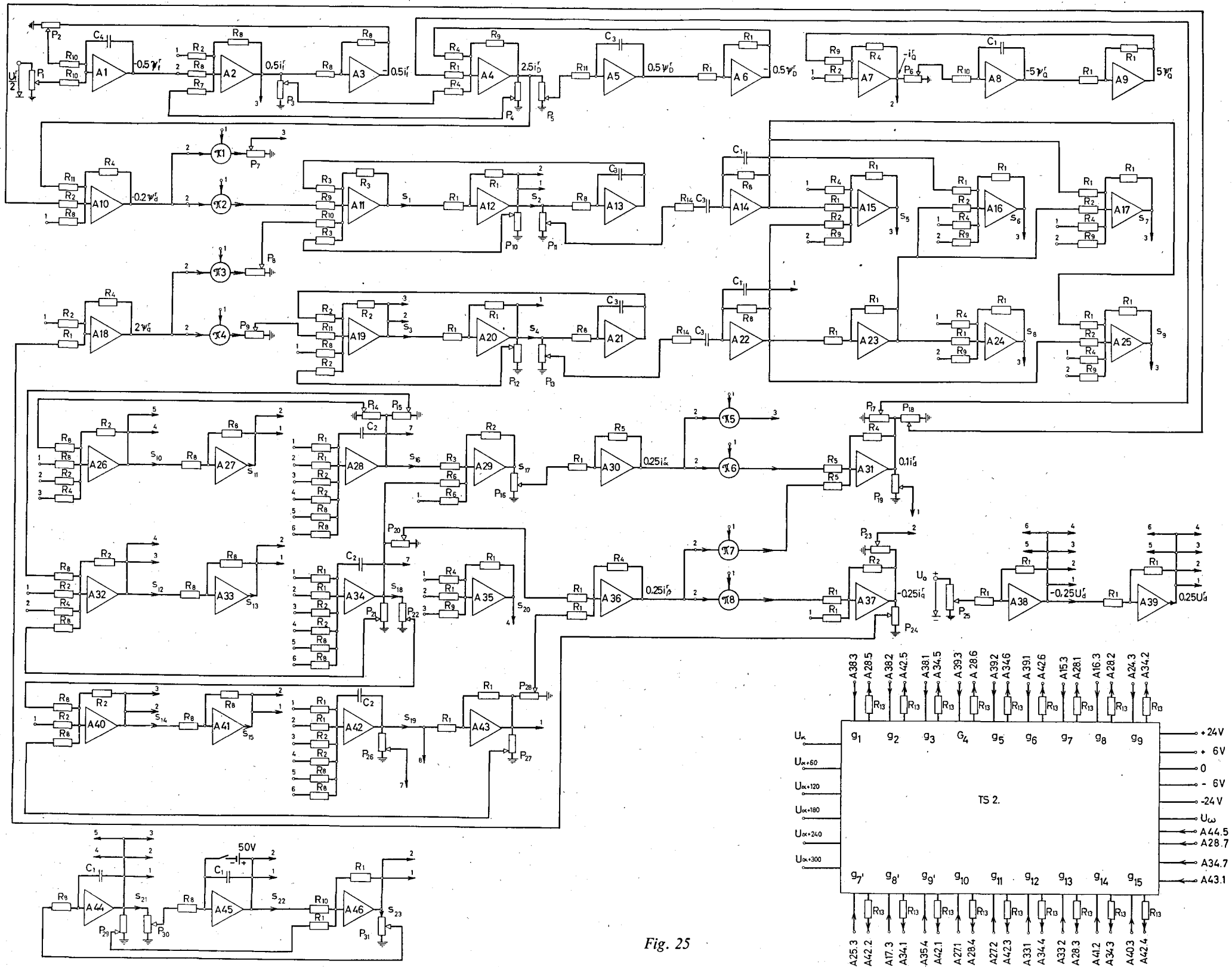


Fig. 25

Leer - Vide - Empty

Fig. 25 Analog computer scheme of the three-phase controlled synchronous machine

$A_{2.3} = A_{10.1}$	$A_{7.2} = A_{18.1}$	$A_{12.1} = A_{26.2}$
$A_{12.2} = A_{32.1}$	$A_{15.3} = A_{28.1}$	$A_{16.3} = A_{28.2}$
$A_{17.3} = A_{34.1}$	$A_{19.2} = A_{32.2}$	$A_{19.3} = A_{40.1}$
$A_{20.1} = A_{26.3}$	$A_{22.1} = A_{35.2}$	$A_{24.3} = A_{34.2}$
$A_{25.3} = A_{42.2}$	$A_{26.4} = A_{16.1}$	$A_{26.5} = A_{35.1}$
$A_{27.1} = A_{28.4}$	$A_{27.2} = A_{42.3}$	$A_{31.1} = A_{2.1}$
$A_{32.3} = A_{15.1}$	$A_{32.4} = A_{24.1}$	$A_{33.1} = A_{34.4}$
$A_{33.2} = A_{28.3}$	$A_{35.4} = A_{42.1}$	$A_{37.2} = A_{7.1}$
$A_{38.1} = A_{34.5}$	$A_{38.2} = A_{42.5}$	$A_{38.3} = A_{28.5}$
$A_{38.4} = A_{15.2}$	$A_{38.5} = A_{17.2}$	$A_{38.6} = A_{35.3}$
$A_{39.1} = A_{42.6}$	$A_{39.2} = A_{34.6}$	$A_{39.3} = A_{28.6}$
$A_{39.4} = A_{16.2}$	$A_{39.5} = A_{24.2}$	$A_{39.6} = A_{25.2}$
$A_{40.2} = A_{17.1}$	$A_{40.3} = A_{42.4}$	$A_{41.1} = A_{25.1}$
$A_{41.2} = A_{34.3}$	$A_{42.7} = A_{26.1}$	$A_{42.8} = A_{29.1}$
$A_{44.1} = \pi 5.1$	$A_{44.2} = \pi 3.1$	$A_{44.3} = \pi 1.1$
$A_{44.4} = \pi 7.1$	$A_{45.1} = \pi 6.1$	$A_{45.2} = \pi 2.1$
$A_{46.1} = \pi 8.1$	$A_{46.2} = \pi 4.1$	$\pi 1.3 = A_{19.1}$
$\pi 5.3 = A_{37.1}$		

$P_1 = 0.3443$	$P_2 = 0.3443$	$P_3 = 0.9794$
$P_4 = 0.1432$	$P_5 = 0.0886$	$P_6 = 0.2045$
$P_7 = 0.8660$	$P_8 = 0.2000$	$P_9 = 0.4330$
$P_{10} = 0.9980$	$P_{11} = 0.4451$	$P_{12} = 0.9980$
$P_{13} = 0.4451$	$P_{14} = 0.1123$	$P_{15} = 0.1123$
$P_{16} = 0.3936$	$P_{17} = 0.6307$	$P_{18} = 0.5805$
$P_{19} = 0.4611$	$P_{20} = 0.2840$	$P_{21} = 0.1123$
$P_{22} = 0.1123$	$P_{23} = 0.3851$	$P_{24} = 0.5368$
$P_{25} = \text{variable}$	$P_{26} = 0.1123$	$P_{27} = 0.1123$
$P_{28} = 0.2840$	$P_{29} = 0.0200$	$P_{30} = P_{31} = 0.5 \omega_m^r = 0.5000$

$$s_1 = -0.015 \frac{d\psi_\alpha^r}{dt_c}$$

$$s_2 = 0.015 \frac{d\psi_\alpha^r}{dt_c}$$

$$s_3 = -0.01732 \frac{d\psi_\beta^r}{dt_c}$$

$$s_4 = 0.01732 \frac{d\psi_\beta^r}{dt_c}$$

$$s_5 = z_1$$

$$s_6 = z_2$$

$$s_7 = z_4$$

$$s_8 = z_3$$

$$s_9 = z_6$$

$$s_{10} = y_2$$

$$s_{11} = y_1$$

$$s_{12} = y_4$$

$$s_{13} = y_3$$

$$s_{14} = y_6$$

$$s_{15} = y_5$$

$$s_{16} = \frac{L_d^r}{4} i_1^r$$

$$s_{17} = -\frac{L_d^r}{4} i_a^r$$

$$s_{18} = -\frac{L_d^r}{4} i_2^r$$

$$s_{19} = -\frac{L_d^r}{4} i_3^r$$

$$s_{20} = z_5$$

$$s_{21} = 50 \sin \gamma$$

$$s_{22} = 50 \cos \gamma$$

$$s_{23} = -50 \cos \gamma$$

($z_1 \dots z_6$ and $y_1 \dots y_6$ are given in table IV)

ST2 = thyatron simulator replacing the effect of the six thyratrons when they are connected in a bridge circuit

7.2 Machine with variable speed

The case of variable speed was calculated later on when the absent two-channel multiplier became available. The $\sin \gamma$ and $\cos \gamma$ were calculated by solving the following two simultaneous equations:

$$\frac{dz_1}{dt_c} = -\dot{\gamma} z_2 \quad (108)$$

$$\frac{dz_2}{dt_c} = \dot{\gamma} z_1 \quad (109)$$

giving the solution that:

$$z_1 = \cos \gamma$$

$$z_2 = \sin \gamma$$

Fig. 26 represents the analog scheme used to obtain the $\sin \gamma$ and $\cos \gamma$. Since the frequency is not constant in this case, two multipliers have to be used in order to form the functions ($\dot{\gamma} \cdot z_2$ and $\dot{\gamma} \cdot z_1$). The quantity $\dot{\gamma}$ was obtained from the mechanical equation of the synchronous machine, being:

$$J \cdot \frac{d\omega_m}{dt} + \rho \cdot \omega_m + M_e = M_a \quad (110)$$

where M_a is the torque required by the load from the shaft of the synchronous machine in $\text{kg} \cdot \text{m}$.

M_a is positive in the case of the synchronous generator.

M_a is negative in the case of the synchronous motor.

Dividing both sides of equation (110) by the reference torque in order to transform it into the per-unit form, we get:

$$\frac{\omega_n \cdot J \cdot \omega_s^2}{P_{sn}} \cdot \frac{d^2 \gamma}{d\tau^2} + \varrho \cdot \frac{\omega_s^2}{P_{sn}} \cdot \frac{d\gamma}{d\tau} + M_e^r = M_a^r$$

since,

$$M_e^r = \psi_q^r \cdot i_d^r - \psi_d^r \cdot i_q^r$$

substituting:

$$\frac{\omega_n \cdot J \cdot \omega_s^2}{P_{sn}} = T_m^r = \text{mechanical time constant,}$$

$$\varrho \cdot \frac{\omega_s^2}{P_{sn}} = \varrho^r, \text{ we get:}$$

$$T_m^r \cdot \frac{d^2 \gamma}{d\tau^2} + \varrho^r \cdot \frac{d\gamma}{d\tau} + \psi_q^r \cdot i_d^r - \psi_d^r \cdot i_q^r = M_a^r$$

For the machine under consideration, the mechanical time constant T_m^r was found to be 138.1, and

$$\varrho = 0.00585 \text{ J/rad/s} = 0.0006 \text{ kg*m/rad/s}$$

$$\varrho^r = 0.0416$$

Thus the mechanical equation becomes:

$$138.1 \frac{d^2 \gamma}{d\tau^2} + 0.0416 \frac{d\gamma}{d\tau} + \psi_q^r \cdot i_d^r - \psi_d^r \cdot i_q^r = M_a^r \quad (111)$$

Introducing the time scale given by equation (75), we get:

$$5.524 \frac{d^2 \gamma}{dt_c^2} + 0.0083 \frac{d\gamma}{dt_c} + \psi_q^r \cdot i_d^r - \psi_d^r \cdot i_q^r = M_a^r \quad (112)$$

This equation gives $d\gamma/dt_c$ as a function of M_a^r . This was solved and the analog set-up is also shown in Fig. 26.

7.3 The thyatron simulator

Inserting the thyratrons in the stator of the synchronous machine produces a current containing dead zones. The function of the thyatron simulator is to determine the ignition and extinction points of the currents

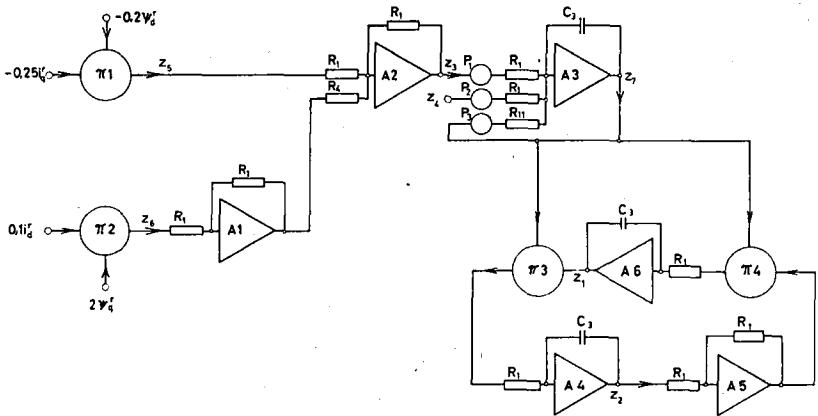


Fig. 26 Analog computer scheme to generate $\sin \gamma$ and $\cos \gamma$ where $\dot{\gamma}$ is not constant

$$z_1 = 50 \sin \gamma$$

$$z_2 = 50 \cos \gamma$$

$$z_3 = 0.005 (\psi_d^r i_q^r - \psi_q^r i_d^r)$$

$$z_4 = -18.1 \text{ V} = 100\% \text{ reference torque}$$

$$z_5 = -0.005 \psi_d^r i_q^r$$

$$z_6 = -0.02 \psi_q^r i_d^r$$

$$z_7 = -0.1 \frac{d\gamma}{dt_c}$$

$$P_1 = 0.3621$$

$$P_2 = \text{variable}$$

$$P_3 = 0.0075$$

Fig. 27 Block diagram of the thyatron simulator for the three-phase controlled synchronous machine

$S_1 \dots S_{17}$ = Schmitt triggers

$M_1 \dots M_{15}$ = bistable multivibrators

$G_1 \dots G_{15}$ = gates

$A54, A56$ = integrators

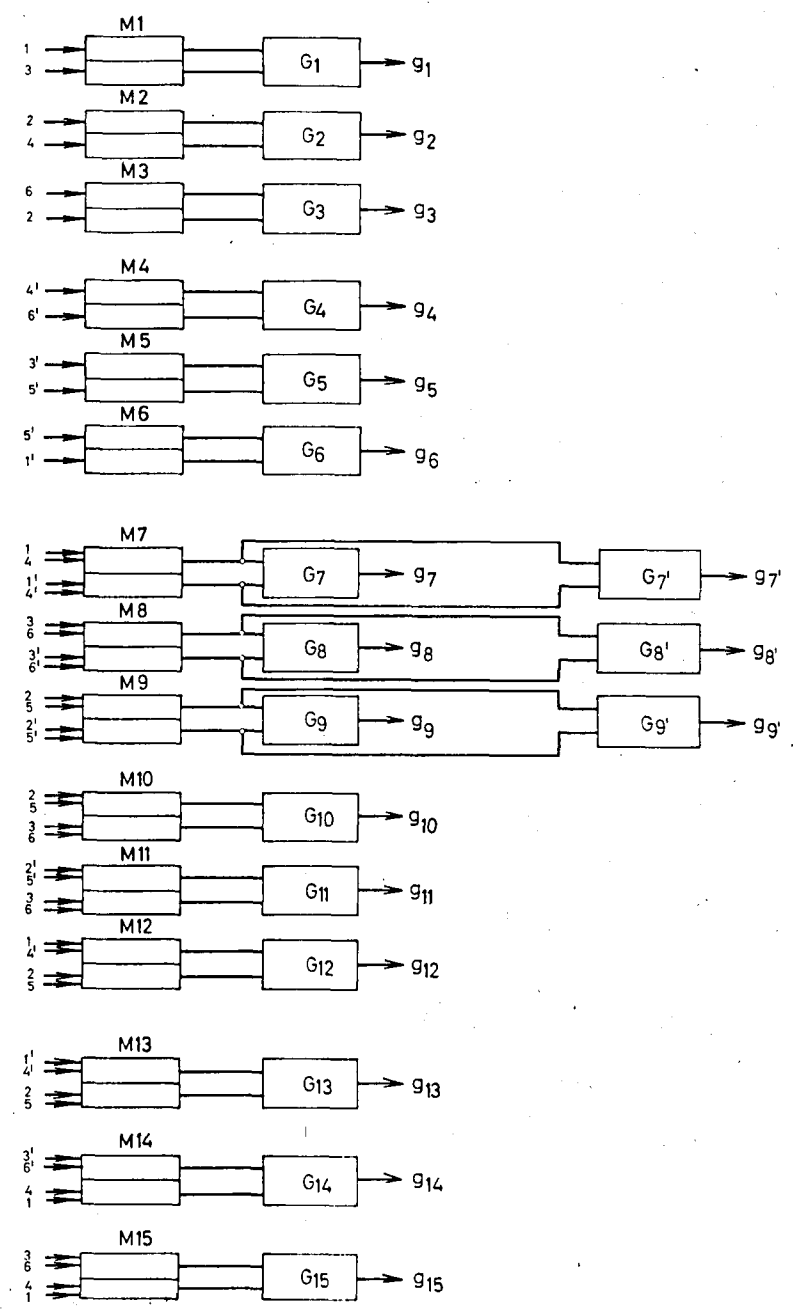
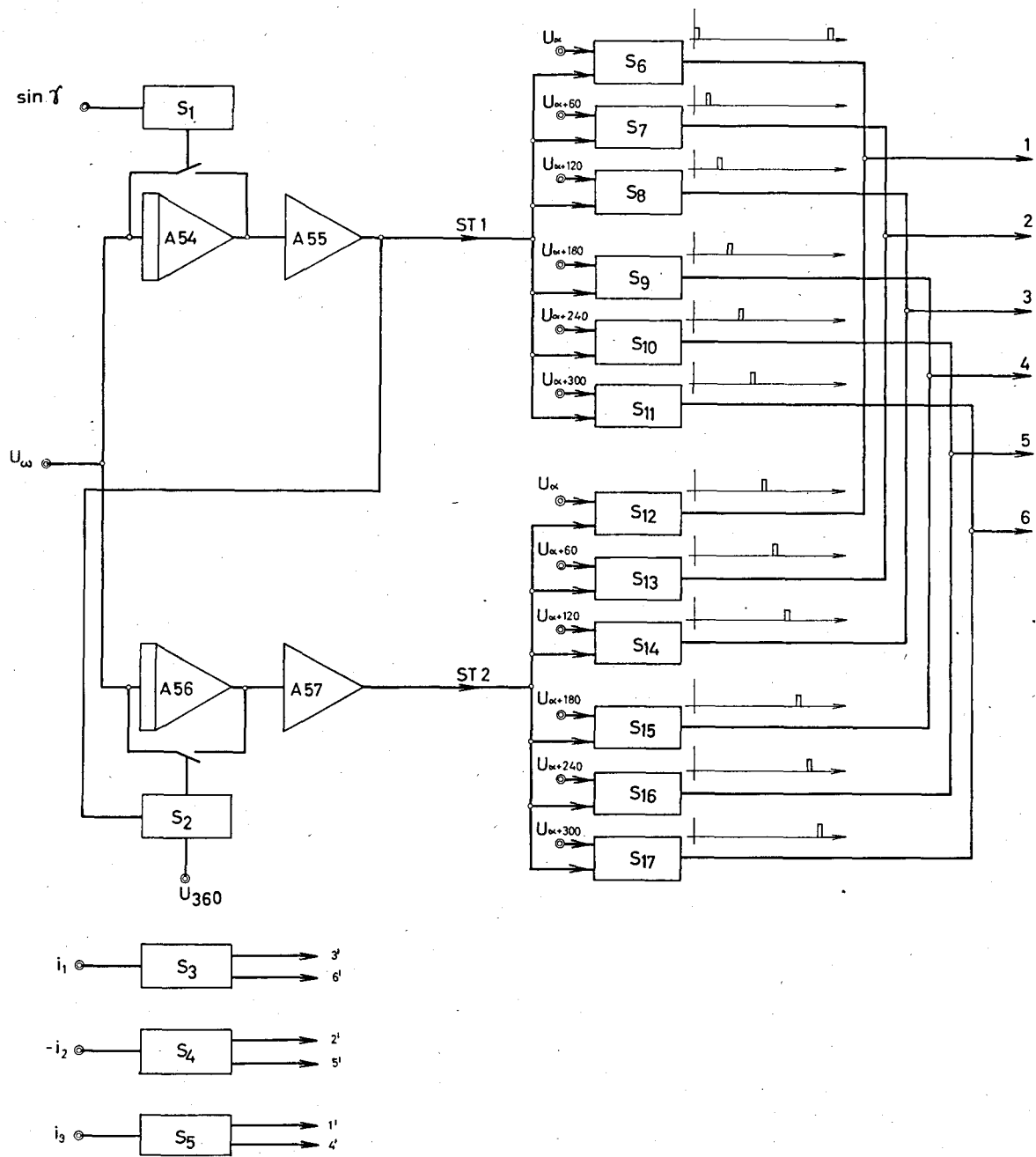
$A55, A57$ = inverters

U_ω = voltage proportional to the angular frequency ω_m^r

U_α = voltage proportional to the firing angle α

$ST1$ = saw-tooth whose period corresponds to $2T_c$ and whose amplitude is constant and independent of frequency

$ST2$ = saw-tooth having the same characteristics as $ST1$ but it is delayed by a time equals T_c s



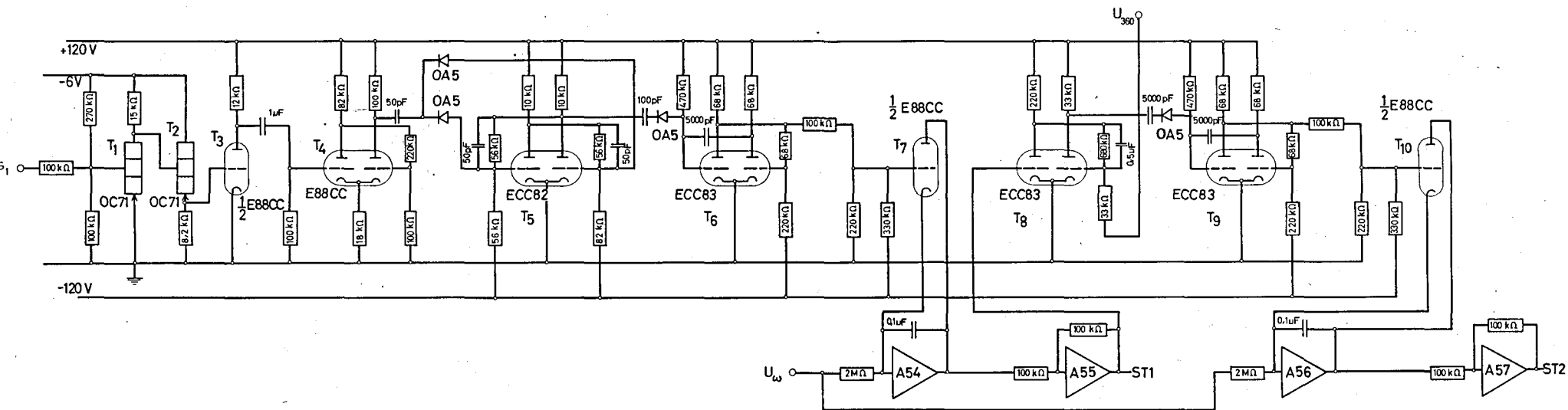


Fig. 28 Circuit generating a saw-tooth with a constant amplitude and variable frequency

$ST1$ = the first saw-tooth, having a period corresponding to 720°

$ST2$ = the second saw-tooth, with the same characteristics as $ST1$ except that it begins 360° after it

T_1, T_2 = transistors defining the points of intersection of $\sin \gamma$ with the zero axis

T_3 = amplifier

T_4 = a Schmitt trigger used as a pulse shaper

T_5 = bistable multivibrator

T_6 = monostable multivibrator

T_7 = a triode used as a switch which ends $ST1$

T_8 = amplitude comparator which gives a sudden change when $ST1 = U_{360}$

T_9 = monostable multivibrator

T_{10} = a triode used as a switch which ends $ST2$

U_ω = a voltage proportional to the circular frequency ω'_m

U_{360} = a voltage, which equals half the amplitude of any of $ST1$ or $ST2$ and which corresponds to the angle 360°

flowing in each phase and to build the necessary gates required to drive the inputs of the integrators A_{28} , A_{34} and A_{42} of *Fig. 25*. The following describes the apparatus built to simulate the thyatron effect in our problem.

7.3.1 Block diagram

Fig. 27 shows a block diagram for the thyatron simulator. It comprises two "saw-tooth generators", each of which is disposed 360° from the other and each is synchronized with $\sin \gamma$. As will be given, the amplitude of this saw-tooth is constant and independent of the frequency. For each frequency, its period should correspond to 720° electrical.

The six ignition points which determine the begin of the positive and negative parts of each of the three stator currents were obtained by comparing each saw-tooth with six voltages displaced 60° electrical ($U_{\alpha'}$, $U_{\alpha'+60} \dots U_{\alpha'+300}$). The firing angle α' between the pulse No.1—which defines the beginning of the stator current in phase No. 1—and the function $\sin \gamma$ could be varied by adding a d.c. voltage (proportional to the angle α') to each of the six voltages. The six points defining the ends of the positive and negative parts of each of the three stator currents were also obtained by comparing them with the zero axis.

For every gate, it was required to build a bistable multivibrator, a cathode follower and the gating transistors. The pulses defining each gate were made to trigger the corresponding bistable multivibrator.

According to table IV, we need 18 gates, and since the timing of 12 of these gates are different from one another, but as for the remaining 6 every 2 are similar in their timing, then we need in fact only 15 bistable multivibrators. In *Fig. 27* are given the 15 bistable multivibrators and the 18 gates.

7.3.2 The "saw-tooth" generators

The solution of the mechanical equation (112) leads to the achievement of a voltage proportional to the quantity $\dot{\gamma}$. Benefit was made of this fact in order to generate a saw-tooth that is synchronized with the function $\sin \gamma$, and that has a fixed amplitude irrespective of the circular frequency $\dot{\gamma}$. This quantity $\dot{\gamma}$ was given into the input of an integrator. Supposing that the integrator is stopped from integrating after a period of T_c seconds,

the integrating condenser is discharged, and the saw-tooth is allowed to begin another period, then the maximum value achieved by the saw-tooth is

$$\text{equal to } \int_0^{T_c} \dot{\gamma} dt_c = 2\pi$$

Therefore we have to expect that the maximum value is constant and independent of the frequency. The maximum value will in this case correspond to the angle 360° electrical, we shall denote it by U_{360} . Since we are going to compare this saw-tooth with voltages corresponding to the ignition points, i.e. with $U_{\alpha'}$, $U_{\alpha'+60}$... $U_{\alpha'+300}$, then we cannot change the firing angle α' outside the range 0° ... 60° . In order to extend the range of α' , the saw tooth was allowed to exist for a period of $2T_c$ instead of T_c and the maximum value in this case will correspond to the angle 720° electrical. So it was possible to change the firing angle α' in the range between 0° ... 360° . But we had to generate another saw-tooth that begins after 360° electrical from the beginning of the first one. Then, again by comparing this saw-tooth with the six voltages, we got the six ignition pulses which appear 360° later than the first group of pulses. Thus we obtained the train of ignition pulses from the first saw-tooth for the first 360° , and from the second saw-tooth for the second 360° and so on. These two trains of pulses were then added by and-circuits.

Integrator A54 of Fig. 27 allows the voltage corresponding to $\dot{\gamma}$ to be integrated, and after 720° we get a pulse that discharges the integrating condenser.

Considering the Fig. 28, tube T_7 acts as a switch discharging the condenser in a time of $500 \mu\text{s}$ which can be neglected when compared with the saw tooth period that equals 2.5132 s at the reted frequency. Transistors T_1 , T_2 determine the points of intersection of the sine wave with the zero axis. Then the bistable multivibrator consisting of the double triode T_3 yields pulses every 720° . These pulses were widened in the monostable multivibrator composed of the double triode T_6 . The thus produced pulse was made to control the triode T_7 used to discharge the integrating condenser. The second "saw-tooth generator" functions on the same principle, but instead of the extinction pulse being obtained by comparing the sine wave with the zero axis, it was obtained by comparing the first saw-tooth with the voltage U_{360} . This was done by the comparator consisting of the double triode T_8 .

The rest of the circuit functions exactly as the corresponding part that controls the first saw-tooth generator.

7.3.3 The coinciding voltages

The six voltages which—when compared with the saw tooth in comparators—produce the six ignition pulses were formed by the scheme shown in Fig. 29. It consists of six d.c. amplifiers, the output of the first is a d.c. voltage corresponding to the angle α' ($U_{\alpha'}$), the output of the second corresponds to the angle $60 + \alpha'$ ($U_{60 + \alpha'}$) and so on. Thus we see that, for any angle α' , the difference between each two successive voltages corresponds to the angle 60° . The angle α' was varied simply by shifting these voltages in the vertical direction which took place by varying $U_{\alpha'}$, that is common to the input of the six amplifiers.

The sudden variation of the voltage $U_{\alpha'}$ results in a sudden shift of the six coinciding voltages. Thus the apparatus is effective not only for slow variations of α' , but also for sudden variations. It responds also quickly to any sudden change in the value of $\dot{\gamma}$.

7.3.4 The Schmitt trigger

The Schmitt trigger used to produce the ignition pulses is shown in Fig. 30. It has two inputs, namely the saw-tooth and the coinciding voltage. When the first saw-tooth $ST1$ equals the coinciding voltage, the Schmitt trigger changes its condition, and we obtain a sudden change in the output voltage which, when differentiated, yields a negative pulse.

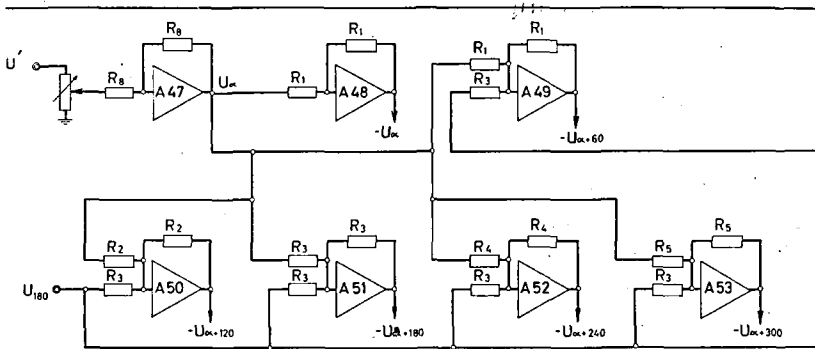


Fig. 29 Scheme producing the six coinciding voltages

$-U_{\alpha'}$, $-U_{\alpha'+60}$, $-U_{\alpha'+120}$, $-U_{\alpha'+180}$, $-U_{\alpha'+240}$, $-U_{\alpha'+300}$ are voltages proportional to the angles α'° , $(\alpha'+60)^\circ$, $(\alpha'+120)^\circ$, $(\alpha'+180)^\circ$, $(\alpha'+240)^\circ$, $(\alpha'+300)^\circ$ respectively

U_{180} = voltage proportional to the angle 180°

$U' = -100$ V

The second saw-tooth *ST2* comes 360° after the beginning of *ST1*. This *ST2* in addition to the coinciding voltage were given to the input of another Schmitt trigger, and when they coincided, we got a negative pulse. These two negative pulses were added together by the and-circuit consisting of the two diodes OA5 and the transistor OC71. *Fig. 30* shows the two Schmitt triggers and the and-circuit.

7.3.5 The pulses determining the end-points of the currents

The circuit shown in *Fig. 31* serves to determine the end points of each of the positive and negative parts of the stator currents. Effectively, it consists of two Schmitt triggers, one of which is sensitive to the positive part of the current, and the other to the negative part.

Two p-n-p transistors form the Schmitt trigger that selects the positive portion of the current with the zero axis, and three n-p-n transistors form the other Schmitt trigger.

7.3.6 The bistable multivibrator

This bistable multivibrator was fed from two voltage sources, +24 V and -24 V, and was used to obtain a rectangular wave that varies between -22 V and +22 V. The cause for choosing such high voltages for the bistable multivibrator will be given in the next section.

The pulses—determining the begin and end of each gate as given in table IV—were made to trigger the bistable multivibrator. *Fig. 32* shows the bistable multivibrator triggered by the pulses 1, 1', 4, 4'.

7.3.7 The gate

The function to be anticipated from the gating circuit is to allow the voltage given to it (constituting the derivative of the stator current) to be integrated during a pre-determined period of time, and to earth that input outside that period. Ideally, the impedance of that gate should be infinite during the integrating period, and zero during the nonintegrating period. We have seen that in the single phase investigation, an error has arisen from the fact that the impedance of the gate was not zero during the non-integrating period, and there was a voltage drop across the gate during that period. This voltage drop was of the order of 0.3 V, which was integrated during the nonintegrating period.

In case that the integrator multiplies by a factor more than unity and if the ratio of the nonintegrating period to the integrating one is big, the error can be troublesome.

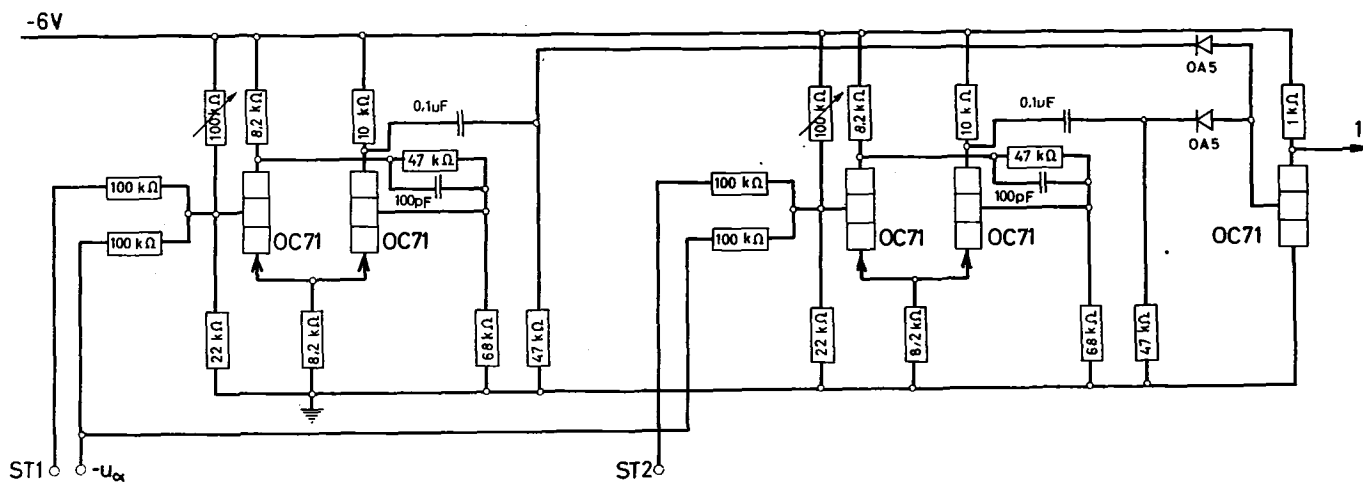


Fig. 30 Schmitt trigger producing one of the ignition pulses (pulse No. 1)

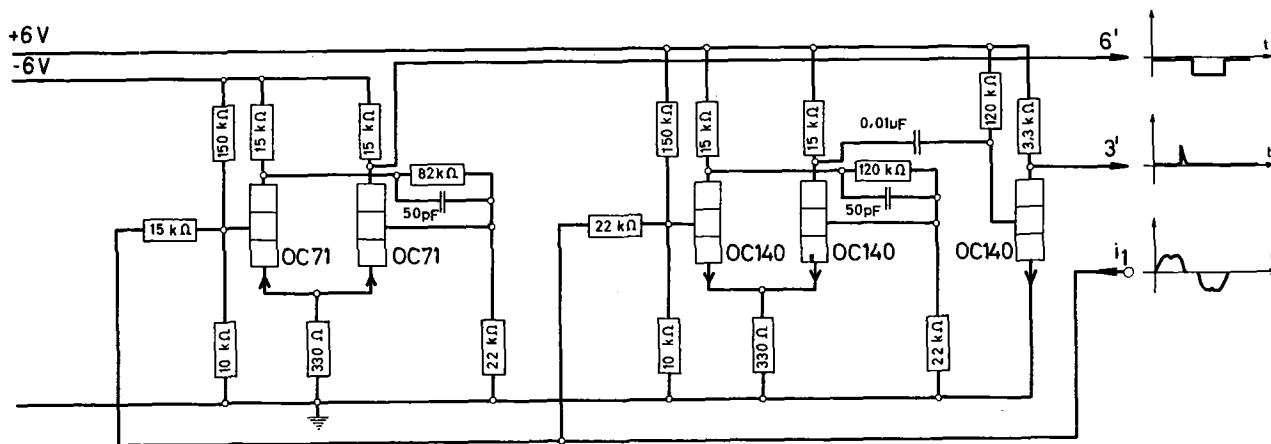


Fig. 31 Schmitt trigger determining the end points of the current i_1

i_1 = current in the stator winding No. 1 of the synchronous machine

3 = pulse produced at the end of the positive part of the current i_1

6 = a rectangular wave defining the end point of the negative part of the current i_1

Leer - Vide - Empty

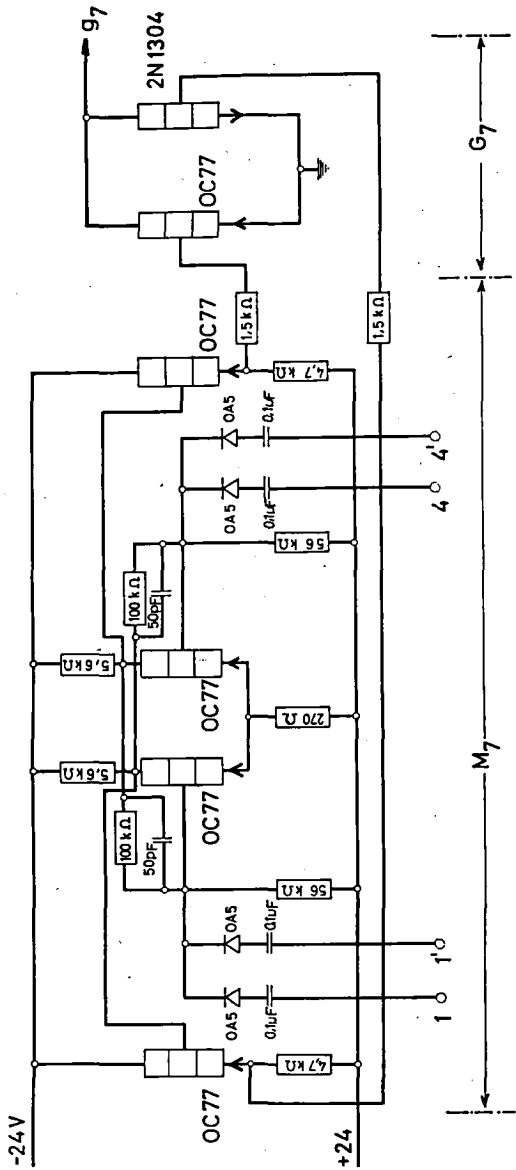


Fig. 32 One of the gates driving the integrators A 28, A 34, A 42 of Fig. 25 and the bistable multivibrator that controls this gate

This is indeed the case in our problem where this ratio may be equal to two or more, and where the integrators A_{28} , A_{34} and A_{42} of *Fig. 25* multiply the integrated input by factors which may reach 50.

It has been found that in the above mentioned gate (which consists of two parallel branches, each composed of a transistor in series with a diode), only a voltage drop of 0.02 V was across the transistor, and that the rest was across the diode. The diodes were necessary to isolate the positive and negative voltages from the collectors of the p-n-p and the n-p-n transistor respectively. This isolation was necessary in that case, since the voltage of the preceding multivibrator which steers the gate ranged between +3 and -3 V, and when the voltage at the collector of the p-n-p reached a value more positive than +3 V, the diode consisting of the collector and the base would conduct.

Hence the collector voltage would have been clipped at the voltage of +3 V, if the diodes were absent. The same is also valid for negative voltages, and the voltage across the gate would have ranged only between +3 and -3 V.

If, however, the voltage of the preceding multivibrator was made to range between +22 and -22 V, it would have been possible for the voltage across the gate to take any value between +20 and -20 V without the need of the isolating diodes, and without any danger that that voltage would be clipped. But we should search for n-p-n and p-n-p transistors whose base-emitter junction can withstand voltages of -20 and +20 V respectively. The transistor OC77 (Philips) is a good example for the first type and the transistor 2N 1304 (Texas Instruments) for the second type. The last part of *Fig. 32* represents the gate thus formed.

7.3.8 Advantages of the thyatron simulator

- (a) It works for variable frequencies, the angle between every two successive ignition pulses being always 60° for every frequency.
- (b) The firing angle α' can be varied between 0° and 360° .
- (c) The voltage drop across the gate is 0.02 V when it is closed, for input voltages not exceeding ± 20 V.
- (d) It is effective when the variation of the firing angle is slowly or suddenly executed. Also when the circular frequency γ is slowly or suddenly varied.

8. ANALOG INVESTIGATION

The current $i_{d.c.}^r$ flowing from the positive pole of the d.c. power supply through the smoothing inductance is equal to the sum of the currents in the three thyratrons I, III, IV of Fig. 4. It equals also the sum of the positive portions of the currents i_1^r, i_2^r, i_3^r .

The positive parts of these currents are selected and added by means of the circuit shown in Fig. 33 where the diodes perform the job of selection. An oscillogram for the current $i_{d.c.}^r$ is shown in Fig. 34, which consists as is to be expected of a d.c. component and a pulsating part with a fundamental frequency equals to six times the fundamental frequency of the stator current. In this figure are also given oscillograms for the stator current and phase voltage.

The noises encountered in the differentiation of the fluxes to obtain the phase voltages are noted in the voltage wave. These noises are to be found only in the voltage wave, but the currents are free from these noises since they are obtained from integrators. This differentiation was avoided when the system was simulated on the PACE analog computer as will be given in chapter 9.

An oscillogram for the instantaneous wave of the torque is also given. Again as in the case of the current $i_{d.c.}^r$, the torque wave consists of a d.c.

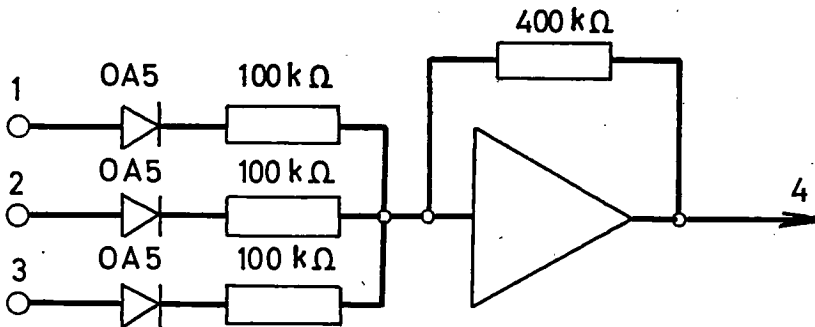


Fig. 33 Analog scheme to obtain the instantaneous current $i_{d.c.}^r$.

$$\begin{aligned}
 1 &= 0.25 i_1^r & 3 &= 0.25 i_3^r \\
 2 &= 0.25 i_2^r & 4 &= i_{d.c.}^r
 \end{aligned}$$

component plus a pulsating one with a fundamental frequency equals six times that of the stator current.

The same is also valid for the fluxes ψ_d^r and ψ_q^r which are also given in the same figure.

The currents flowing in the damper windings i_D^r and i_Q^r and also the currents i_d^r and i_q^r are shown in the same figure.

Fig. 34 Oscillograms of the three-phase system

$$U_d^r = 16\% \quad U_f^r = 100\% \quad \omega_m^r = 1 \quad \alpha' = 115^\circ$$

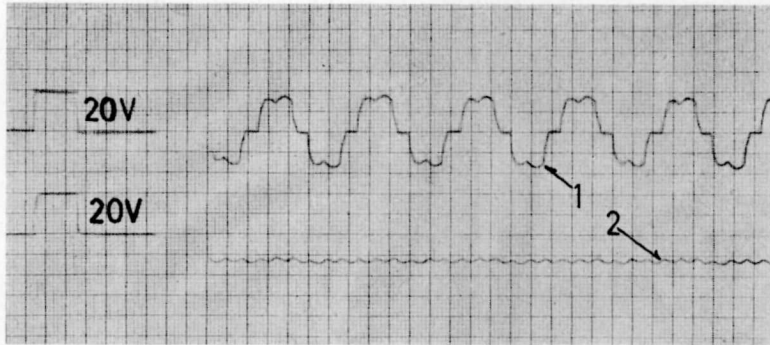


Fig. 34a Phase current i_1^r and the current i_d^r

$$1 = 0.25 L_d^r i_1^r \quad 2 = 0.1 i_d^r$$

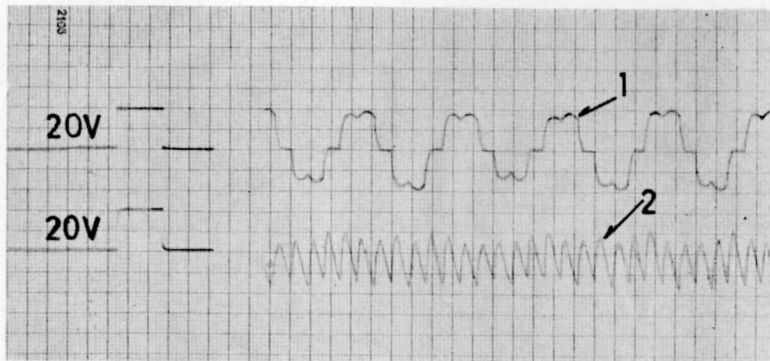


Fig. 34b Phase current i_1^r and the current i_q^r

$$1 = 0.25 L_d^r i_1^r \quad 2 = -0.25 i_q^r$$

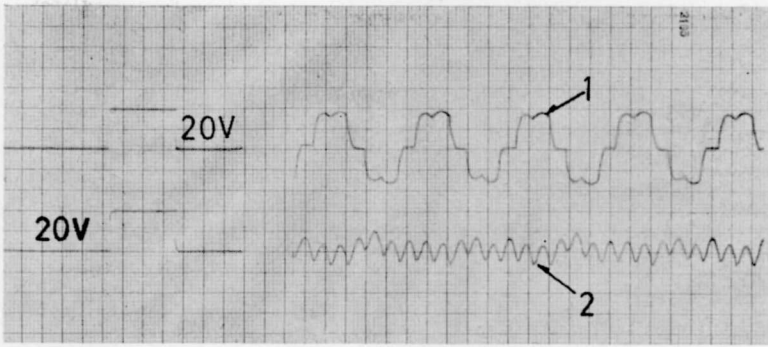


Fig. 34c Phase current i_1^r and the current in the damper winding i_D^r
 $1 = 0.25 L_d^r i_1^r$ $2 = i_D^r$

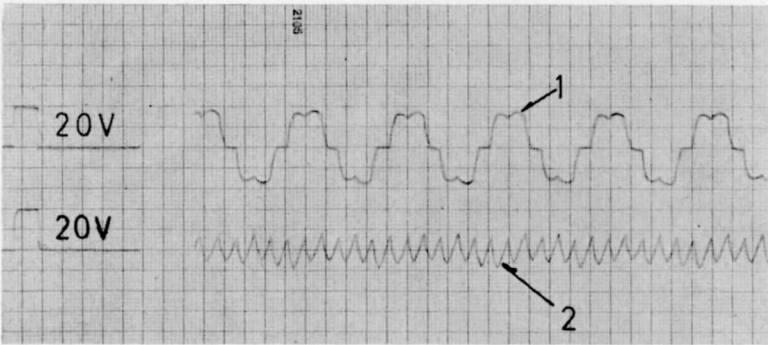


Fig. 34d Phase current i_1^r and the current in the damper winding i_Q^r
 $1 = 0.25 L_d^r i_1^r$ $2 = -i_Q^r$



Fig. 34e Phase current i_1^r and the field current i_f^r
 $1 = 0.25 L_d^r i_1^r$ $2 = 0.2 i_f^r$

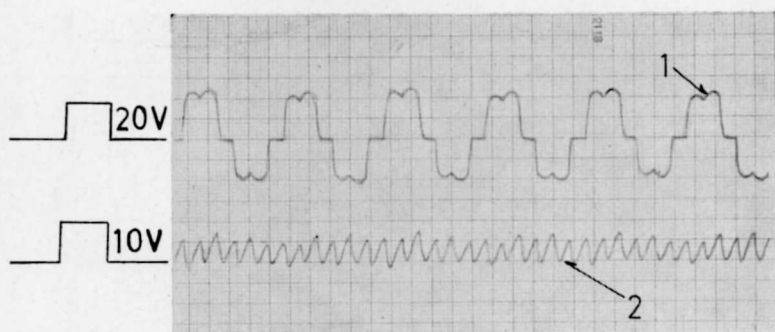


Fig. 34f Phase current i_1^r and the electromagnetic torque M_e^r

$$1 = 0.25 L_d^r i_1^r \quad 2 = -0.05 M_e^r$$



Fig. 34g Phase current and the d.c. current $i_{d,c}^r$.

$$1 = 0.25 L_d^r i_1^r \quad 2 = 0.25 L_d^r i_{d,c}^r$$

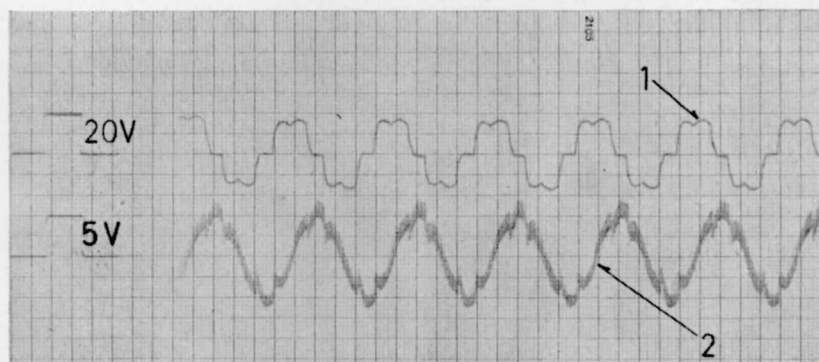


Fig. 34h Phase current i_1^r and the phase voltage u_1^r

$$1 = 0.25 L_d^r i_1^r \quad 2 = 0.075 u_1^r$$

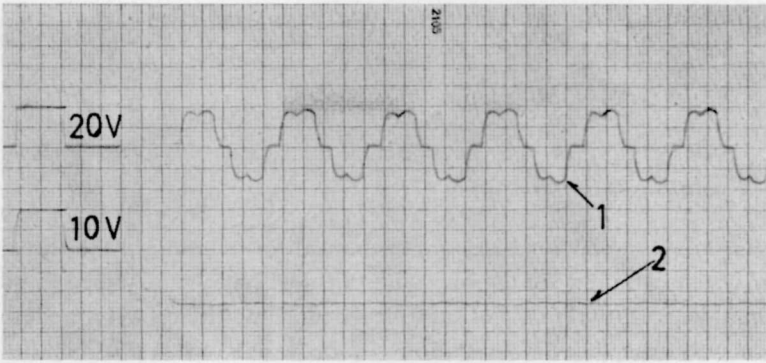


Fig. 34i Phase current i_1^r and the flux ψ_d^r linking the coil d

$$1 = 0.25 L_d^r i_1^r \quad 2 = -0.2 \psi_d^r$$

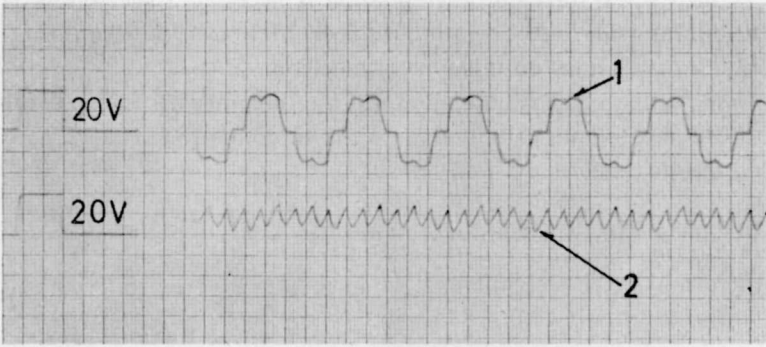


Fig. 34j Phase current i_1^r and the flux ψ_q^r linking the coil q

$$1 = 0.25 L_d^r i_1^r \quad 2 = 2 \psi_q^r$$

9. SIMULATION OF THE SYSTEM ON THE PACE ANALOG COMPUTER

9.1 The mathematical formulation

As was shown in chapter 8, the mathematical formulation of the three-phase system required the use of 8 multipliers when $\dot{\gamma}$ was assumed to be constant, whereas in the case of variable speed, 12 multipliers were needed. As generally accepted, differentiation is to be avoided when possible. Because of the limited number of available multipliers, we were obliged to carry it on. A larger computer was then established in the institute, and thus it became possible to formulate the three-phase system mathematically in such a way that no differentiation is necessary. The following simulation was made in co-operation with Mr. M. MANSOUR, who is making other investigations on this type of machine.

Fig. 35 shows the connection diagram of the three-phase system, where each of the d.c. supply voltage U_d and the smoothing inductance L_d is divided into two halves.

Now for phase No. 1, when

$$\left. \begin{array}{l} \text{(i) thyatron No. 1 is conducting, we have } u_1^r = \frac{U_d^r}{2} - \frac{u_L^r}{2} \\ \text{(ii) thyatron No. 4 is conducting, we have } u_1^r = -\left(\frac{U_d^r}{2} - \frac{u_L^r}{2}\right) \\ \text{(iii) both thyatrons No. 1 and No. 4 are nonconducting, we have} \\ \qquad \qquad \qquad u_1^r = \frac{d\psi_1^r}{d\tau} + u_0^r \end{array} \right\} \quad (113)$$

For phase No. 2, when

$$\left. \begin{array}{l} \text{(i) thyatron No. 3 is conducting, we have } u_2^r = \frac{U_d^r}{2} - \frac{u_L^r}{2} \\ \text{(ii) thyatron No. 6 is conducting, we have } u_2^r = -\left(\frac{U_d^r}{2} - \frac{u_L^r}{2}\right) \\ \text{(iii) both thyatrons No. 3 and No. 6 are nonconducting, we have} \\ \qquad \qquad \qquad u_2^r = \frac{d\psi_2^r}{d\tau} + u_0^r \end{array} \right\} \quad (114)$$

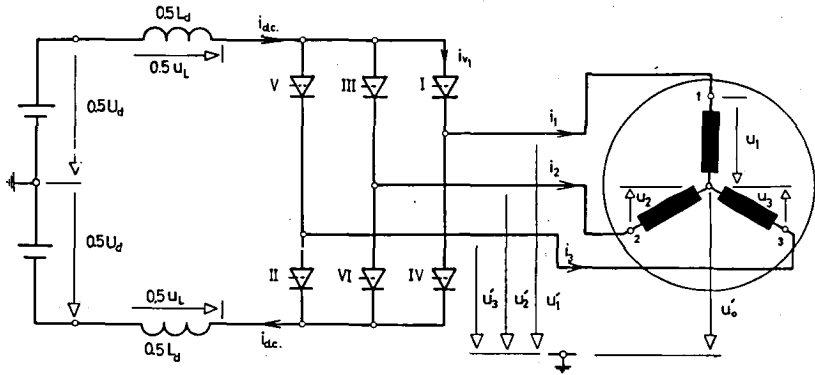


Fig. 35 Connection diagram of the stator of the three-phase controlled synchronous machine

For phase No. 3, when

- (i) thyatron No. 5 is conducting, we have $u_3^{r'} = \frac{U_d^r}{2} - \frac{u_L^r}{2}$
- (ii) thyatron No. 2 is conducting, we have $u_3^{r'} = -\left(\frac{U_d^r}{2} - \frac{u_L^r}{2}\right)$
- (iii) both thyratrons No. 5 and No. 2 are nonconducting, we have $u_3^{r'} = \frac{d\psi_3^r}{d\tau} + u_0^r$

$u_0^r = 0$. Since the machine is star connected.

$$u_0^r = \frac{1}{3}(u_1^r + u_2^r + u_3^r) \tag{116}$$

$$i_{d.c.}^r = i_{v1}^r + i_{v3}^r + i_{v5}^r = i_{1+}^r + i_{2+}^r + i_{3+}^r$$

$$u_L^r = L_d^r \left(\frac{d i_{d.c.}^r}{d\tau} \right) \tag{117}$$

The voltage equations of the synchronous machine are

$$\begin{aligned} u_d^r &= R^r \cdot i_d^r + \frac{d\psi_d^r}{d\tau} - \dot{\gamma} \cdot \psi_q^r \\ &= R^r \cdot i_d^r + x_d \cdot \frac{d i_d^r}{d\tau} + \frac{d i_D^r}{d\tau} + \frac{d i_f^r}{d\tau} - \dot{\gamma} (x_q \cdot i_q^r + i_Q^r) \end{aligned}$$

$$0 = i_D^r + T_D^r \frac{d\psi_D^r}{d\tau} = i_D^r + T_D^r \cdot x_a(1 - \sigma_{ad}) \frac{di_a^r}{d\tau} + T_D^r(1 - \mu_D) \frac{di_f^r}{d\tau} + T_D^r \frac{di_D^r}{d\tau}$$

$$U_f^r = i_f^r + T_f^r \frac{d\psi_f^r}{d\tau} = i_f^r + T_f^r \cdot x_a(1 - \sigma_{af}) \frac{di_a^r}{d\tau} + T_f^r(1 - \mu_f) \frac{di_D^r}{d\tau} + T_f^r \frac{di_f^r}{d\tau}$$

$$u_q^r = R^r \cdot i_q^r + \frac{d\psi_q^r}{d\tau} + \dot{\gamma} \cdot \psi_q^r$$

$$= R^r \cdot i_q^r + x_q \frac{di_q^r}{d\tau} + \frac{di_Q^r}{d\tau} + \dot{\gamma}(x_a \cdot i_a^r + i_D^r + i_f^r)$$

$$0 = i_Q^r + T_Q^r \frac{d\psi_Q^r}{d\tau} = i_Q^r + T_Q^r \cdot x_q(1 - \sigma_q) \frac{di_q^r}{d\tau} + T_Q^r \cdot \frac{di_Q^r}{d\tau}$$

$$[u^r] = [R^r] \cdot [i^r] + [L^r] \frac{d}{d\tau} [i^r] + \dot{\gamma} [L^r] \cdot [i^r]$$

$$\frac{d}{d\tau} [i^r] = [L^r]^{-1} [u^r] - [L^r]^{-1} \cdot [R^r] \cdot [i^r] - \dot{\gamma} [L^r]^{-1} [L^r] \cdot [i^r] \quad (118)$$

$[L^r]^{-1}$ was calculated and the numerical values representing the different constants of the machine were substituted in the matrix equation (118) resulting in the following set of equations:

$$\frac{di_a^r}{d\tau} = 13.45 \frac{d\psi_a^r}{d\tau} - 0.01934 (U_f^r - i_f^r) + 0.2028 i_D^r$$

$$\frac{di_D^r}{d\tau} = -5.772 \frac{d\psi_a^r}{d\tau} - 0.06005 (U_f^r - i_f^r) - 0.2307 i_D^r$$

$$\frac{di_f^r}{d\tau} = -1.037 \frac{d\psi_a^r}{d\tau} + 0.07128 (U_f^r - i_f^r) + 0.1130 i_D^r$$

$$\frac{di_q^r}{d\tau} = 13.19 \frac{d\psi_q^r}{d\tau} + 0.2710 i_Q^r$$

$$\frac{di_Q^r}{d\tau} = -2.540 \frac{d\psi_q^r}{d\tau} - 0.07273 i_Q^r$$

where,

$$\frac{d\psi_a^r}{d\tau} = u_a^r + \dot{\gamma} (0.2684 i_q^r + i_Q^r) - 0.0571 i_a^r \quad (119)$$

$$\text{and } \frac{d\psi_q^r}{d\tau} = u_q^r - \dot{\gamma} (0.5805 i_a^r + i_D^r + i_f^r) - 0.0571 i_q^r \quad (120)$$

The transformation from the

$$\frac{d i_d^r}{d \tau}, \frac{d i_q^r}{d \tau} \text{ to } \frac{d i_\alpha^r}{d \tau}, \frac{d i_\beta^r}{d \tau}$$

is done according to the equations:

$$\frac{d i_\alpha^r}{d \tau} = \frac{d i_d^r}{d \tau} \cdot \cos \gamma - \frac{d i_q^r}{d \tau} \cdot \sin \gamma - \dot{\gamma} \cdot i_\beta^r \quad (121)$$

$$\frac{d i_\beta^r}{d \tau} = \frac{d i_d^r}{d \tau} \cdot \sin \gamma + \frac{d i_q^r}{d \tau} \cdot \cos \gamma + \dot{\gamma} \cdot i_\alpha^r \quad (122)$$

Out of these it is possible to obtain the derivatives of the currents i_1^r , i_2^r , i_3^r .

$$\frac{d i_1^r}{d \tau} = \frac{d i_\alpha^r}{d \tau}$$

$$\frac{d i_2^r}{d \tau} = -0.5 \frac{d i_\alpha^r}{d \tau} + \frac{\sqrt{3}}{2} \frac{d i_\beta^r}{d \tau}$$

$$\frac{d i_3^r}{d \tau} = -0.5 \frac{d i_\alpha^r}{d \tau} - \frac{\sqrt{3}}{2} \frac{d i_\beta^r}{d \tau}$$

Thus after introducing the conditions of the thyatron action, we obtain the stator currents i_1^r , i_2^r , i_3^r .

But we need to build $\frac{d \psi_d^r}{d \tau}$ and $\frac{d \psi_q^r}{d \tau}$. The simulation of these quantities

are made according to the equations (119), (120) and thus no differentiation is needed. In order to obtain the quantities u_d^r , u_q^r , we need the quantities u_1^r , u_2^r , u_3^r whose constituents are

$$U_d^r, u_L^r, \frac{d \psi_1^r}{d \tau}, \frac{d \psi_2^r}{d \tau}, \frac{d \psi_3^r}{d \tau}, u_0^r$$

u_L^r was simulated according to the equation (117), where

$\frac{d i_{v1}^r}{d \tau}$ is equal to the part of $\frac{d i_1^r}{d \tau}$ during the period in which thyatron No. 1

is conducting.

$\frac{d \psi_\alpha^r}{d \tau}$, $\frac{d \psi_\beta^r}{d \tau}$ are related to $\frac{d \psi_d^r}{d \tau}$, $\frac{d \psi_q^r}{d \tau}$ by the following equations

$$\frac{d \psi_\alpha^r}{d \tau} = \frac{d \psi_d^r}{d \tau} \cdot \cos \gamma - \frac{d \psi_q^r}{d \tau} \cdot \sin \gamma - \dot{\gamma} \cdot \psi_\beta^r$$

$$\frac{d\psi_\beta^r}{d\tau} = \frac{d\psi_\alpha^r}{d\tau} \sin \gamma + \frac{d\psi_q^r}{d\tau} \cdot \cos \gamma + \dot{\gamma} \cdot \psi_\alpha^r$$

This simulation is, however, to be avoided as it results in an algebraic loop with a total gain equal to unity. The reason why an algebraic loop has to be avoided is that it tends to amplify any noise present in the system. This algebraic loop was avoided by carrying on the following substitution:

$$\psi_\alpha^r = \psi_D^r + x_d \cdot \sigma_{dD} i_\alpha^r + \mu_D \cdot i_f^r$$

$$\frac{d\psi_\alpha^r}{d\tau} = \frac{d\psi_D^r}{d\tau} + x_d \cdot \sigma_{dD} \frac{d i_\alpha^r}{d\tau} + \mu_D \cdot \frac{d i_f^r}{d\tau} = -\frac{i_D^r}{T_D^r} + x_d \cdot \sigma_{dD} \frac{d i_\alpha^r}{d\tau} + \mu_D \cdot \frac{d i_f^r}{d\tau}$$

$$\psi_q^r = \psi_Q^r + x_q \sigma_q \cdot i_q^r$$

$$\frac{d\psi_q^r}{d\tau} = \frac{d\psi_Q^r}{d\tau} + x_q \sigma_q \cdot \frac{d i_q^r}{d\tau} = -\frac{i_Q^r}{T_Q^r} + x_q \sigma_q \cdot \frac{d i_q^r}{d\tau}$$

$$\begin{aligned} \text{Thus } \frac{d\psi_\alpha^r}{d\tau} &= \sin \gamma \left[(x_d \sigma_{dD} - x_q \sigma_q) \frac{d i_q^r}{d\tau} + \frac{i_Q^r}{T_Q^r} \right] + \cos \gamma \left(\mu_D \frac{d i_f^r}{d\tau} - \frac{i_D^r}{T_D^r} \right) \\ &\quad + x_d \sigma_{dD} \frac{d i_\alpha^r}{d\tau} - \dot{\gamma} (\psi_\beta^r - x_d \sigma_{dD} i_\beta^r) \end{aligned} \quad (123)$$

$$\begin{aligned} \frac{d\psi_\beta^r}{d\tau} &= -\cos \gamma \left[(x_d \sigma_{dD} - x_q \sigma_q) \frac{d i_q^r}{d\tau} + \frac{i_Q^r}{T_Q^r} \right] + \sin \gamma \left(\mu_D \frac{d i_f^r}{d\tau} - \frac{i_D^r}{T_D^r} \right) \\ &\quad + x_d \sigma_{dD} \frac{d i_\beta^r}{d\tau} + \dot{\gamma} (\psi_\alpha^r - x_d \sigma_{dD} i_\alpha^r) \end{aligned} \quad (124)$$

Substituting the numerical values of the machine constants in equations (123), (124), we get:

$$\begin{aligned} \frac{d\psi_\alpha^r}{d\tau} &= \sin \gamma \left(0.0001 \frac{d i_q^r}{d\tau} + 0.0205 i_Q^r \right) + \cos \gamma \left(0.0206 \frac{d i_f^r}{d\tau} - 0.0177 i_D^r \right) \\ &\quad + 0.0759 \frac{d i_\alpha^r}{d\tau} - \dot{\gamma} (\psi_\beta^r - 0.0759 i_\beta^r) \end{aligned}$$

$$\begin{aligned} \frac{d\psi_\beta^r}{d\tau} &= -\cos \gamma \left(0.0001 \frac{d i_q^r}{d\tau} + 0.0205 i_Q^r \right) \\ &\quad + \sin \gamma \left(0.0206 \frac{d i_f^r}{d\tau} - 0.0177 i_D^r \right) \\ &\quad + 0.0759 \frac{d i_\beta^r}{d\tau} + \dot{\gamma} (\psi_\alpha^r - 0.0759 i_\alpha^r) \end{aligned}$$

Thus, the gain of the algebraic loop is effectively reduced to 0.0206 instead of unity.

The derivatives $\frac{d\psi_1^r}{d\tau}$, $\frac{d\psi_2^r}{d\tau}$, $\frac{d\psi_3^r}{d\tau}$ were formed according to

$$\begin{aligned}\frac{d\psi_1^r}{d\tau} &= \frac{d\psi_\alpha^r}{d\tau} \\ \frac{d\psi_2^r}{d\tau} &= -0.5 \frac{d\psi_\alpha^r}{d\tau} + \frac{\sqrt{3}}{2} \cdot \frac{d\psi_\beta^r}{d\tau} \\ \frac{d\psi_3^r}{d\tau} &= -0.5 \frac{d\psi_\alpha^r}{d\tau} - \frac{\sqrt{3}}{2} \cdot \frac{d\psi_\beta^r}{d\tau}\end{aligned}$$

The quantity u_0^r was simulated according to equation (116).

The thyatron effect has to be taken into consideration in the simulation of the voltages u_1^r , u_2^r , u_3^r and we have to follow equations (113)...(115). Ideally, these conditions put on these voltages should be enough to give the dead zones in the stator currents, i.e. the derivative of each of the stator current will be zero during the intervals where the currents themselves have to be zero.

But any minute error in the derivative causes a small current to flow during that period, thus activating the comparators so that the voltages u_1^r , u_2^r , u_3^r are not right any more. In order to avoid this difficulty, we have to prevent the derivative from being integrated during the interval where no current has to flow.

Since all the calculations are made at first in the fixed axes co-ordinates (α , β), and then transformed into the (1, 2, 3) directions, then the mentioned condition of isolating the derivatives was made on the derivatives of the currents i_α^r , i_β^r , accordingly

$$\text{when } i_1^r = 0, \text{ then } i_\alpha^r = 0, \quad \text{i.e. } \frac{di_\alpha^r}{d\tau} = 0$$

$$\text{when } i_2^r = 0, \text{ then } i_\beta^r = \frac{i_\alpha^r}{\sqrt{3}}, \quad \text{i.e. } \frac{di_\beta^r}{d\tau} = \frac{1}{\sqrt{3}} \cdot \frac{di_\alpha^r}{d\tau}$$

$$\text{when } i_3^r = 0, \text{ then } i_\beta^r = \frac{-i_\alpha^r}{\sqrt{3}}, \quad \text{i.e. } \frac{di_\beta^r}{d\tau} = -\frac{1}{\sqrt{3}} \cdot \frac{di_\alpha^r}{d\tau}$$

Thus $\frac{di_\alpha^r}{d\tau}$ has to be isolated from being integrated during the intervals

$$\text{when } i_1^r = 0.$$

$\frac{d i_{\beta}^r}{d \tau}$ is to be taken from $\frac{1}{\sqrt{3}} \cdot \frac{d i_a^r}{d \tau}$ when $i_2^r = 0$

$\frac{d i_{\beta}^r}{d \tau}$ is to be taken from $\left(-\frac{1}{\sqrt{3}} \cdot \frac{d i_a^r}{d \tau}\right)$ when $i_3^r = 0$

$\frac{d i_{\beta}^r}{d \tau}$ is to be taken from equation (122) when both $i_2^r \neq 0$, and $i_3^r \neq 0$.

As for the time scaling, the relation between the per-unit time τ and the time on the computer t_c was taken to be unity, i.e. $\tau = t_c$ which means that the relation between t and t_c is

$$t_c = 2 \pi f_n \cdot t$$

The following gives the scaled equations:

for phase No. 1

(i) thyatron No. 1 conducts

$$0.25 u_1^r = \frac{U_d^r}{8} - \frac{u_L^r}{8}$$

(ii) thyatron No. 4 conducts

$$0.25 u_1^r = -\left(\frac{U_d^r}{8} - \frac{u_L^r}{8}\right)$$

(iii) thyatrons No. 1 and 4 not conducting

$$0.25 u_1^r = \frac{d}{d t_c} (0.25 \psi_1^r) + 0.25 u_0^r$$

for phase No. 2

(i) thyatron No. 3 conducts

$$0.25 u_2^r = \frac{U_d^r}{8} - \frac{u_L^r}{8}$$

(ii) thyatron No. 6 conducts

$$0.25 u_2^r = -\left(\frac{U_d^r}{8} - \frac{u_L^r}{8}\right)$$

(iii) thyatrons No. 3 and 6 not conducting

$$0.25 u_2^r = \frac{d}{d t_c} (0.25 \psi_2^r) + 0.25 u_0^r$$

for phase No. 3

(i) thyatron No. 5 conducts

$$0.25 u_3^r = \frac{U_d^r}{8} - \frac{u_L^r}{8}$$

(ii) thyatron No. 2 conducts

$$0.25 u_3^r = - \left(\frac{U_d^r}{8} - \frac{u_L^r}{8} \right)$$

(iii) thyatrons No. 5 and 2 not conducting

$$0.25 u_3^r = \frac{d}{dt_c} (0.25 \psi_3^r) + 0.25 u_0^r$$

and $0.25 u_0^r = \frac{1}{3} (0.25 u_1^r + 0.25 u_2^r + 0.25 u_3^r)$

$$0.25 u_L^r = 5 L_d^r \left[\frac{d}{dt_c} (0.05 i_{v1}^r) + \frac{d}{dt_c} (0.05 i_{v3}^r) + \frac{d}{dt_c} (0.05 i_{v5}^r) \right]$$

$$\begin{aligned} \frac{d}{dt_c} (0.05 i_d^r) &= 2.69 \frac{d}{dt_c} (0.25 \psi_d^r) - 0.0097 (0.1 U_f^r) + 0.0039 (0.25 i_f^r) \\ &\quad + 0.0507 (0.2 i_b^r) \end{aligned}$$

$$\begin{aligned} \frac{d}{dt_c} (0.2 i_b^r) &= -4.618 \frac{d}{dt_c} (0.25 \psi_d^r) - 0.1201 (0.1 U_f^r) \\ &\quad + 0.0480 (0.25 i_f^r) - 0.2307 (0.2 i_b^r) \end{aligned}$$

$$\begin{aligned} \frac{d}{dt_c} (0.25 i_f^r) &= -1.037 \frac{d}{dt_c} (0.25 \psi_d^r) + 0.1782 (0.1 U_f^r) \\ &\quad - 0.0713 (0.25 i_f^r) + 0.1413 (0.2 i_b^r) \end{aligned}$$

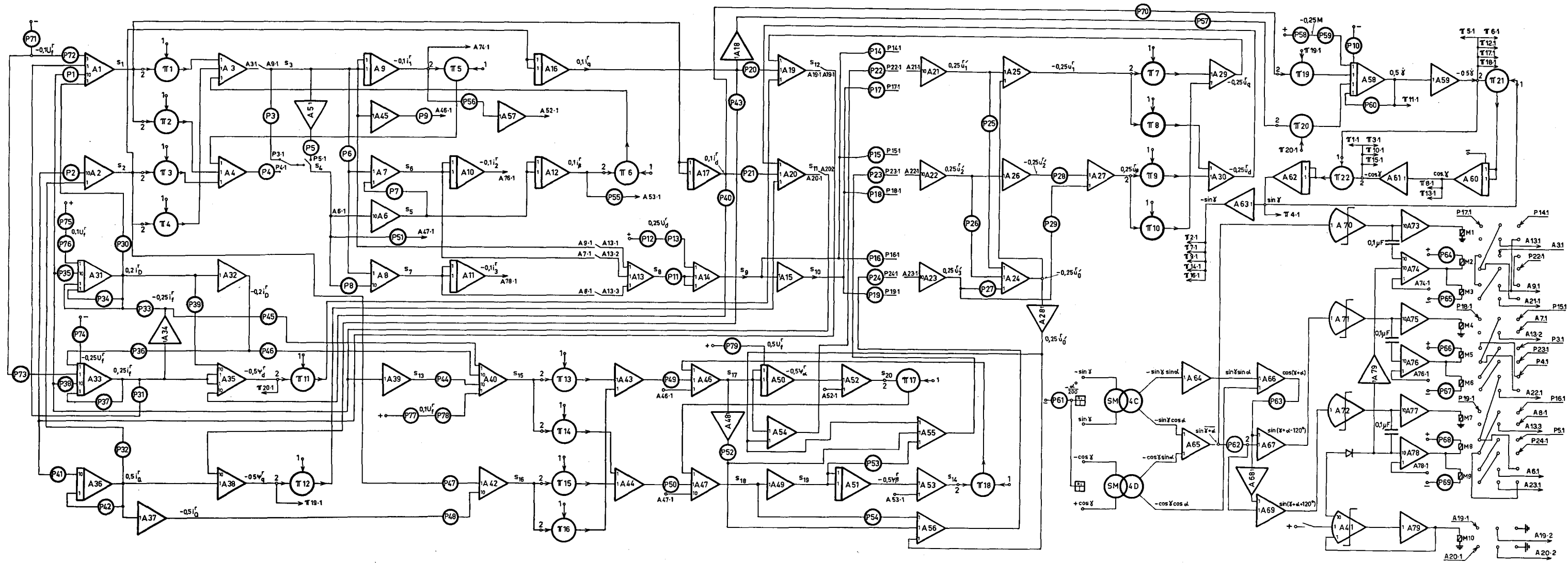
$$\frac{d}{dt_c} (0.05 i_q^r) = 2.638 \frac{d}{dt_c} (0.25 \psi_q^r) + 0.0271 (0.5 i_Q^r)$$

$$\frac{d}{dt_c} (0.5 i_Q^r) = -5.080 \frac{d}{dt_c} (0.25 \psi_q^r) - 0.0727 (0.5 i_Q^r)$$

$$\frac{d}{dt_c} (0.25 \psi_d^r) = (0.25 u_d^r) + 0.5 \dot{\gamma} (0.5 \psi_q^r) - 0.1428 (0.1 i_d^r)$$

Fig. 36 Analog scheme for the simulation of the three-phase controlled synchronous machine

$$\begin{aligned}
 s_1 &= -0.05 \frac{d i_a^r}{d t_c} & s_2 &= -0.05 \frac{d i_a^r}{d t_c} & s_3 &= 0.05 \frac{d i_a^r}{d t_c} \\
 s_4 &= 0.005 \frac{d i_\beta^r}{d t_c} & s_5 &= -0.05 \frac{d i_\beta^r}{d t_c} & s_6 &= 0.05 \frac{d i_2^r}{d t_c} \\
 s_7 &= 0.05 \frac{d i_3^r}{d t_c} & s_8 &= -0.05 \frac{d i_{a.c.}^r}{d t_c} & s_9 &= -\frac{1}{8}(U_d^r - u_L^r) \\
 s_{10} &= \frac{(U_d^r - u_L^r)}{8} & s_{11} &= 0.25 \frac{d \psi_d^r}{d t_c} & s_{12} &= 0.25 \frac{d \psi_q^r}{d t_c} \\
 s_{13} &= -0.25 \frac{d \psi_d^r}{d t_c} & s_{14} &= (0.5 \psi_\beta^r - 0.038 i_\beta^r) \\
 s_{15} &= 25 \left(-0.0206 \frac{d i_f^r}{d t_c} + 0.0177 i_D^r \right) \\
 s_{16} &= 25 \left(0.0001 \frac{d i_q^r}{d t_c} + 0.0205 i_Q^r \right) \\
 s_{17} &= 0.25 \frac{d \psi_\alpha^r}{d t_c} & s_{18} &= -0.25 \frac{d \psi_\beta^r}{d t_c} & s_{19} &= 0.25 \frac{d \psi_\beta^r}{d t_c} \\
 s_{20} &= (0.5 \psi_\alpha^r - 0.038 i_\alpha^r) \\
 P1 &= 0.2690 & P2 &= 0.2638 & P3 &= 0.0577 \\
 P4 &= 0.1000 & P5 &= 0.0577 & P6 &= 0.5000 \\
 P7 &= 0.8660 & P8 &= 0.8660 & P9 &= 0.3795 \\
 P10 &= 0.5 \dot{\gamma}_0 & P11 &= 1.25 L_d^r & P12 &= 0.25 U_d^r \\
 P13 &= 0.5000 & P14 &= 0.1000 & P15 &= 0.1000 \\
 P16 &= 0.1000 & P17 &= 0.1000 & P18 &= 0.1000 \\
 P19 &= 0.1000 & P20 &= 0.1428 & P21 &= 0.1428 \\
 P22 &= 0.1000 & P23 &= 0.1000 & P24 &= 0.1000 \\
 P25 &= 0.3253 & P26 &= 0.3325 & P27 &= 0.3325 \\
 P28 &= 0.3577 & P29 &= 0.5773 & P30 &= 0.0507 \\
 P31 &= 0.0039 & P32 &= 0.0271 & P33 &= 0.0480 \\
 P34 &= 0.2307 & P35 &= 0.4618 & P36 &= 0.1413 \\
 P37 &= 0.0713 & P38 &= 0.1037 & P39 &= 0.2500
 \end{aligned}$$



$P40 = 0.2903$	$P41 = 0.5080$	$P42 = 0.0727$	$P61 = 0.005 \alpha'^0$	$P62 = 0.5000$	$P63 = 0.8660$
$P43 = 0.1342$	$P44 = 0.2136$	$P45 = 0.1468$	$P64 = 0.0020$	$P65 = 0.0019$	$P66 = 0.0007$
$P46 = 0.1922$	$P47 = 0.0550$	$P48 = 0.1025$	$P67 = 0.0011$	$P68 = 0.0009$	$P69 = 0.0008$
$P49 = 0.0100$	$P50 = 0.0100$	$P51 = 0.3795$	$P70 = 0.0724$	$P71 = 0.1 U_f'$	$P72 = 0.0097$
$P52 = 0.5000$	$P53 = 0.8660$	$P54 = 0.8660$	$P73 = 0.1782$	$P74 = 0.25 U_f'$	$P75 = 0.1 U_f'$
$P55 = 0.3795$	$P56 = 0.3795$	$P57 = 0.0724$	$P76 = 0.1201$	$P77 = 0.1 U_f'$	$P78 = 0.3671$
$P58 = 0.25 M_d'$	$P59 = 0.0145$	$P60 = 0.0003$			

Leer - Vide - Empty

$$\frac{d}{dt_c}(0.25 \psi'_a) = (0.25 u'_a) - 0.5 \dot{\gamma} (0.5 \psi'_a) - 0.1428 (0.1 i'_q)$$

$$\frac{d}{dt_c}(0.05 i'_a) = \cos \gamma \cdot \frac{d}{dt_c}(0.05 i'_a) - \sin \gamma \cdot \frac{d}{dt_c}(0.05 i'_q) - 0.5 \dot{\gamma} (0.1 i'_\beta)$$

$$\frac{d}{dt_c}(0.05 i'_\beta) = \sin \gamma \cdot \frac{d}{dt_c}(0.05 i'_a) + \cos \gamma \cdot \frac{d}{dt_c}(0.05 i'_q) + 0.5 \dot{\gamma} (0.1 i'_a)$$

$$\frac{d}{dt_c}(0.05 i'_1) = \frac{d}{dt_c}(0.05 i'_a)$$

$$\frac{d}{dt_c}(0.05 i'_2) = -0.5 \frac{d}{dt_c}(0.05 i'_a) + \frac{\sqrt{3}}{2} \cdot \frac{d}{dt_c}(0.05 i'_\beta)$$

$$\frac{d}{dt_c}(0.05 i'_3) = -0.5 \frac{d}{dt_c}(0.05 i'_a) - \frac{\sqrt{3}}{2} \cdot \frac{d}{dt_c}(0.05 i'_\beta)$$

$$\begin{aligned} \frac{d}{dt_c}(0.25 \psi'_a) &= (0.01) \cdot \sin \gamma \left[0.055 \frac{d}{dt_c}(0.05 i'_q) + 1.025 (0.5 i'_Q) \right] \\ &+ (0.01) \cdot \cos \gamma \left[-2.136 \frac{d}{dt_c}(0.25 \psi'_a) + 0.3671 (0.1 U'_f) \right. \\ &\left. - 0.1468 (0.25 i'_f) - 1.922 (0.2 i'_D) \right] \\ &+ 0.3795 \frac{d}{dt_c}(0.05 i'_a) - 0.5 \dot{\gamma} [0.5 \psi'_\beta - 0.3795 (0.1 i'_\beta)] \end{aligned}$$

$$\begin{aligned} \frac{d}{dt_c}(0.25 \psi'_\beta) &= -(0.01) \cdot \cos \gamma \left[0.055 \frac{d}{dt_c}(0.05 i'_q) + 1.025 (0.5 i'_Q) \right] \\ &+ (0.01) \cdot \sin \gamma \left[-2.136 \frac{d}{dt_c}(0.25 \psi'_a) + 0.3671 (0.1 U'_f) \right. \\ &\left. - 0.1468 (0.25 i'_f) - 1.922 (0.2 i'_D) \right] \\ &+ 0.3795 \frac{d}{dt_c}(0.05 i'_\beta) + 0.5 \dot{\gamma} [0.5 \psi'_a - 0.3795 (0.1 i'_a)] \end{aligned}$$

$$\frac{d}{dt_c}(0.25 \psi'_1) = \frac{d}{dt_c}(0.25 \psi'_a)$$

$$\frac{d}{dt_c}(0.25 \psi_2^r) = -0.5 \frac{d}{dt_c}(0.25 \psi_a^r) + 0.8660 \frac{d}{dt_c}(0.25 \psi_\beta^r)$$

$$\frac{d}{dt_c}(0.25 \psi_3^r) = -0.5 \frac{d}{dt_c}(0.25 \psi_a^r) - 0.8660 \frac{d}{dt_c}(0.25 \psi_\beta^r)$$

$$\begin{aligned} \frac{d}{dt_c}(0.5 \dot{\gamma}) &= \int [0.0145(0.25 M_a^r) + 0.0724(0.5 \psi_a^r)(0.1 i_a^r) \\ &\quad - 0.0724(0.5 \psi_\beta^r)(0.1 i_\beta^r) - 0.0003(0.5 \dot{\gamma})] dt_c \end{aligned}$$

Fig. 36 shows the complete analog scheme, where the comparators $M_1 \dots M_9$ take the job of replacing the switching action of the thyratrons. In addition, 22 multipliers, one servo resolver, 79 amplifiers as integrators, summaters, inverters and high gain amplifiers (14 of them are integrators) and 79 potentiometers were needed for this simulation.

In order to begin the inverter action, the pulses No. 2 and 5 were added to the pulses No. 3 and 6 so that when either pulse No. 2 or No. 5 appears tending to make the current i_3^r ready to begin, it causes also the current i_2^r to begin at the same time. Thus, the problem of finding a closed path for the current as the first pulse appears was solved.

It is also necessary that the system should represent the no load case from the moment of begin of computation until the first pulse appears. In order to make sure that this condition is also realized, the values $d/dt_c(0.25 \psi_a^r)$ and $d/dt_c(0.25 \psi_\beta^r)$ were made open and exactly at the point when the first pulse appears, they are switched on. This is done by means of the comparator M_{10} . It is controlled by means of a step function which is normally positive and only at the moment of the first pulse it suddenly becomes negative. This is done by means of the amplifiers (A_{41}, A_{79}) of Fig. 36.

9.2 Oscillograms

Oscillograms for the quantities of interest were taken for the case when $\alpha' = 170^\circ$, $U_d^r = 1.3$, $U_f^r = 1$, $M_a^r = 0.4$, $\dot{\gamma}_0 = 1$, $\gamma_0 = 0$. These are given in Fig. 37i...37iv.

Fig. 37i shows the 3 stator currents (i_1^r, i_2^r, i_3^r), the phase voltage u_1^r , the voltage of the star point with respect to the middle point of the d.c. source (u_0^r), the currents in the damper windings and the field current. The transient behaviour as well as the steady state are to be seen on that figure. The current in the damper winding possesses a d.c. component

which dies out in the steady state. Also the field current shows a similar behaviour. *Fig. 37ii* shows the currents i_a^r , i_b^r , i_d^r , i_q^r , the derivatives

$$\frac{d i_d^r}{d t_c}, \frac{d i_q^r}{d t_c}, \frac{d i_1^r}{d t_c} \text{ and the voltage across the inductance.}$$

Fig. 37iii shows the transformed stator voltages in the fixed axes co-ordinates (u_α^r , u_β^r), those in the moving axes co-ordinates (u_d^r , u_q^r), the voltage across the thyatron No. 1 (u_{o1}^r), the voltage of the star point with respect to the cathodes of the thyatrons 2, 4, 6 (u_{ok}^r), and the de-

rivatives $\frac{d \psi_d^r}{d t_c}, \frac{d \psi_q^r}{d t_c}$. *Fig. 37iv* shows the produced electric torque M_e^r , the

fluxes ψ_d^r , ψ_q^r linking the windings d , q , the fluxes (ψ_α^r , ψ_β^r), the deriva-

tives $\frac{d \psi_\alpha^r}{d t_c}, \frac{d \psi_\beta^r}{d t_c}$, and the speed $\dot{\gamma}$.

In all the oscillograms the behaviour of the transient component as well as the steady state component from the moment of switching on of the voltage U_d^r are to be shown.

Fig. 38i...38iv show exactly the same oscillograms given in the *Fig. 37i...37iv* in the steady state. They are extended in the time axis and their amplitudes are amplified as high as the recorder allows. Thus all the details of the oscillograms can be easily seen.

Fig. 37 Oscillograms for the different quantities corresponding to the three-phase controlled synchronous machine as taken from the PACE analog computer

$$\begin{array}{lll} U_d^r = 1.3 & U_f^r = 1 & \alpha' = 170^\circ \\ M_a^r = 0.4 & \dot{\gamma}_0 = 1 & \gamma_0 = 0 \end{array}$$

Fig. 37i

$$\begin{array}{lll} (a) = 0.1 i_1^r & (d) = 0.25 u_1^r & (g) = 5 i_Q^r \\ (b) = 0.1 i_2^r & (e) = 0.75 u_0^r & (h) = 0.25 i_f^r \\ (c) = 0.1 i_3^r & (f) = 2 i_D^r & \end{array}$$

Fig. 37ii

$$U_d^r = 1.3$$

$$M_a^r = 0.4$$

$$(a) = 0.1 i_\alpha^r$$

$$(b) = 0.1 i_\beta^r$$

$$(c) = 0.5 i_d^r$$

$$U_f^r = 1$$

$$\dot{\gamma}_0 = 1$$

$$(d) = 0.5 i_q^r$$

$$(e) = 0.05 \frac{d i_d^r}{d t_c}$$

$$(f) = 0.05 \frac{d i_q^r}{d t_c}$$

$$\alpha' = 170^\circ$$

$$\dot{\gamma}_0 = 0$$

$$(g) = 0.05 \frac{d i_1^r}{d t_c}$$

$$(h) = \frac{1}{2 L_d^r} \cdot u_L^r$$

Fig. 37iii

$$U_d^r = 1.3$$

$$M_a^r = 0.4$$

$$(a) = 0.25 u_\alpha^r$$

$$(b) = 0.25 u_\beta^r$$

$$(c) = 0.25 u_d^r$$

$$U_f^r = 1$$

$$\dot{\gamma}_0 = 1$$

$$(d) = 0.25 u_q^r$$

$$(e) = 0.25 u_{v1}^r$$

$$(f) = 0.25 u_{0k}^r$$

$$\alpha' = 170^\circ$$

$$\dot{\gamma}_0 = 0$$

$$(g) = 0.25 \frac{d \psi_d^r}{d t_c}$$

$$(h) = 0.25 \frac{d \psi_q^r}{d t_c}$$

Fig. 37iv

$$U_d^r = 1.3$$

$$M_a^r = 0.4$$

$$(a) = 0.25 M_\alpha^r$$

$$(b) = 0.5 \psi_d^r$$

$$(c) = 0.5 \psi_q^r$$

$$U_f^r = 1$$

$$\dot{\gamma}_0 = 1$$

$$(d) = 0.5 \psi_\alpha^r$$

$$(e) = 0.5 \psi_\beta^r$$

$$(f) = 0.25 \frac{d \psi_\alpha^r}{d t_c}$$

$$\alpha' = 170^\circ$$

$$\dot{\gamma}_0 = 0$$

$$(g) = 0.25 \frac{d \psi_\beta^r}{d t_c}$$

$$(h) = 0.5 \dot{\gamma}$$

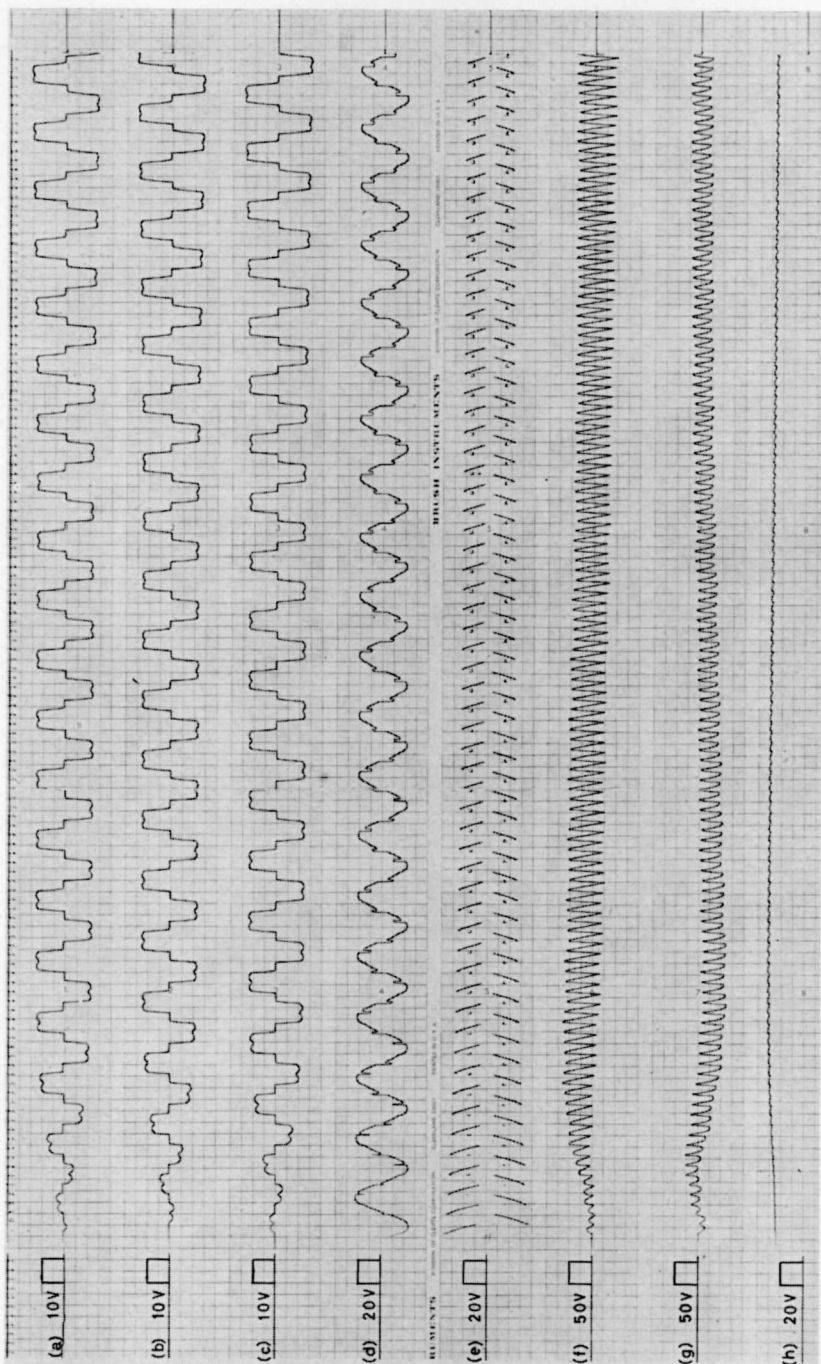


Fig. 37i

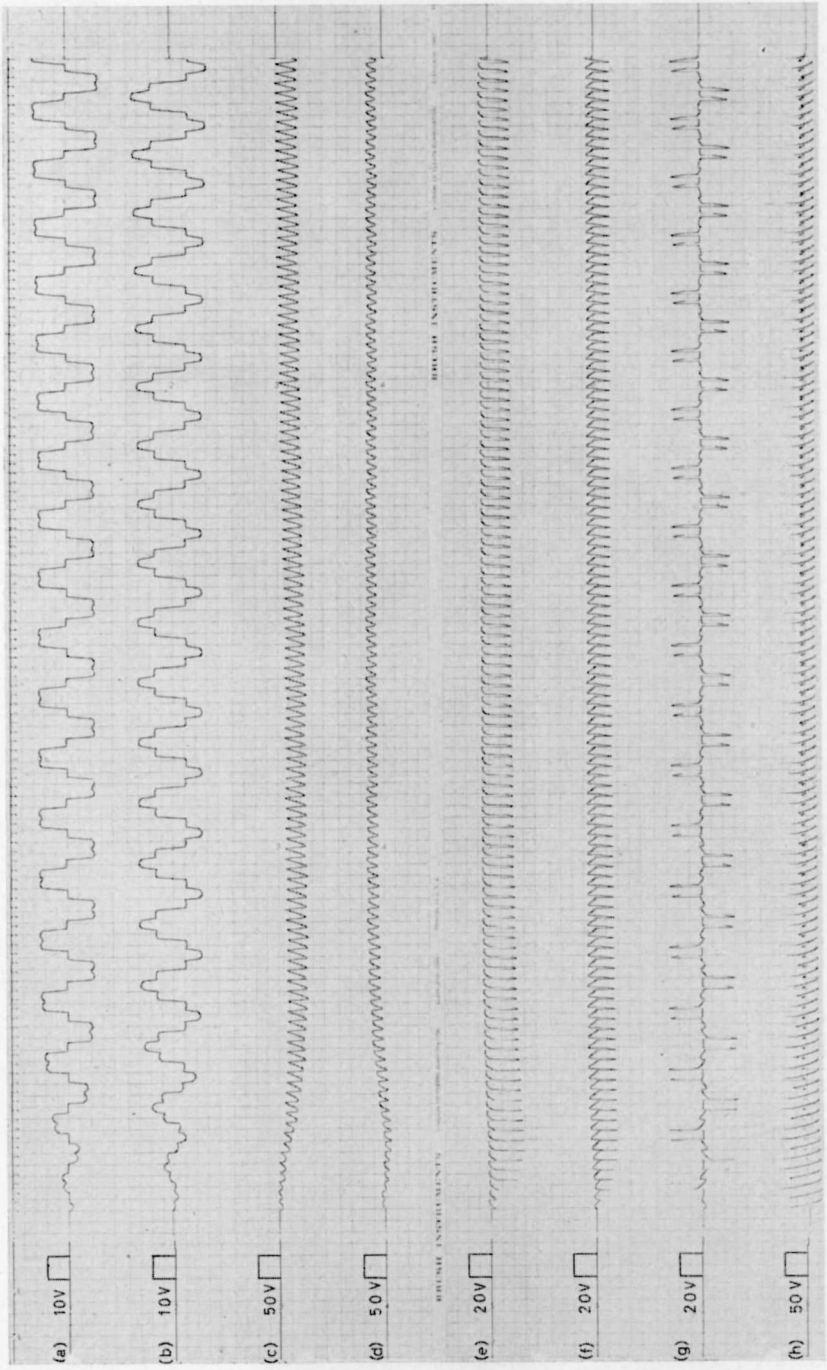


Fig. 37 ii

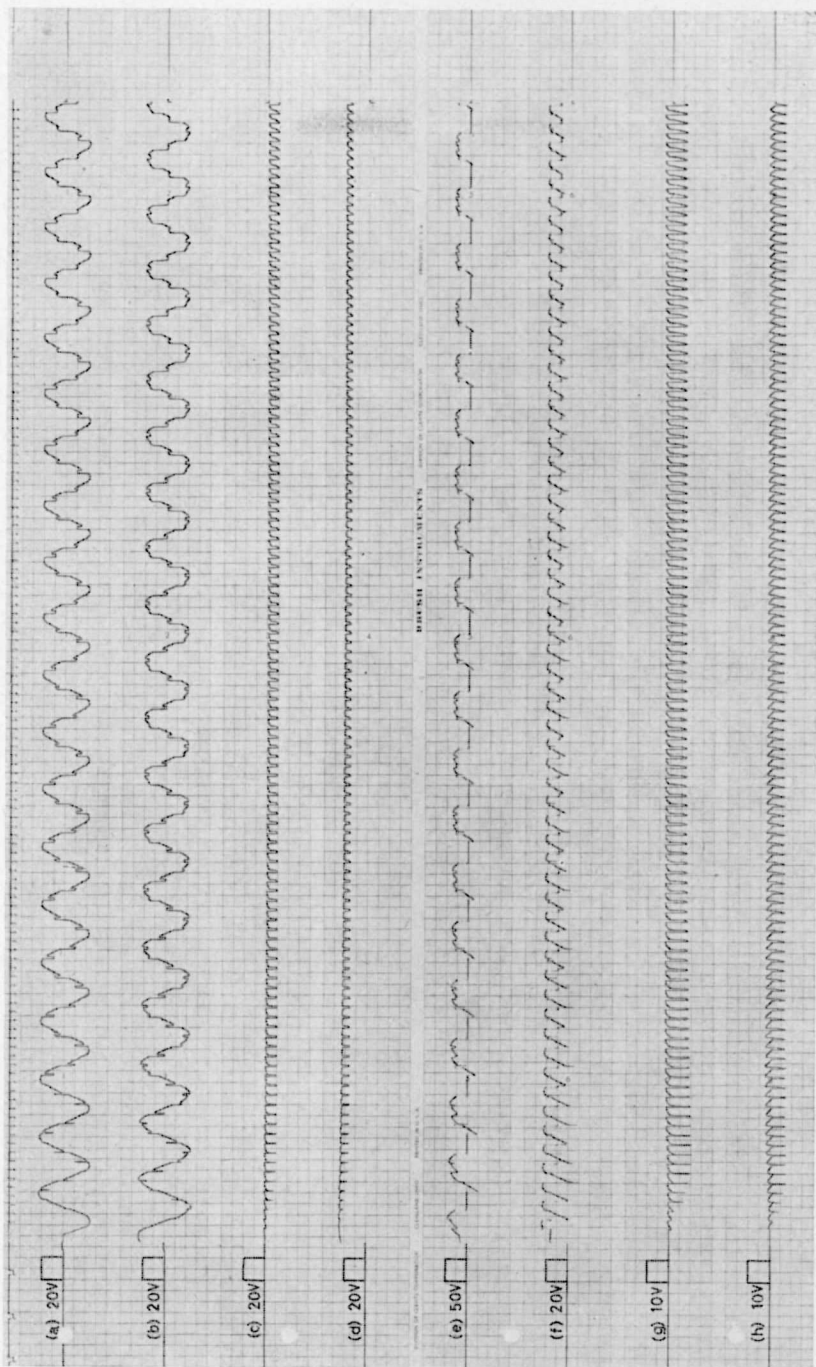


Fig. 37 iii

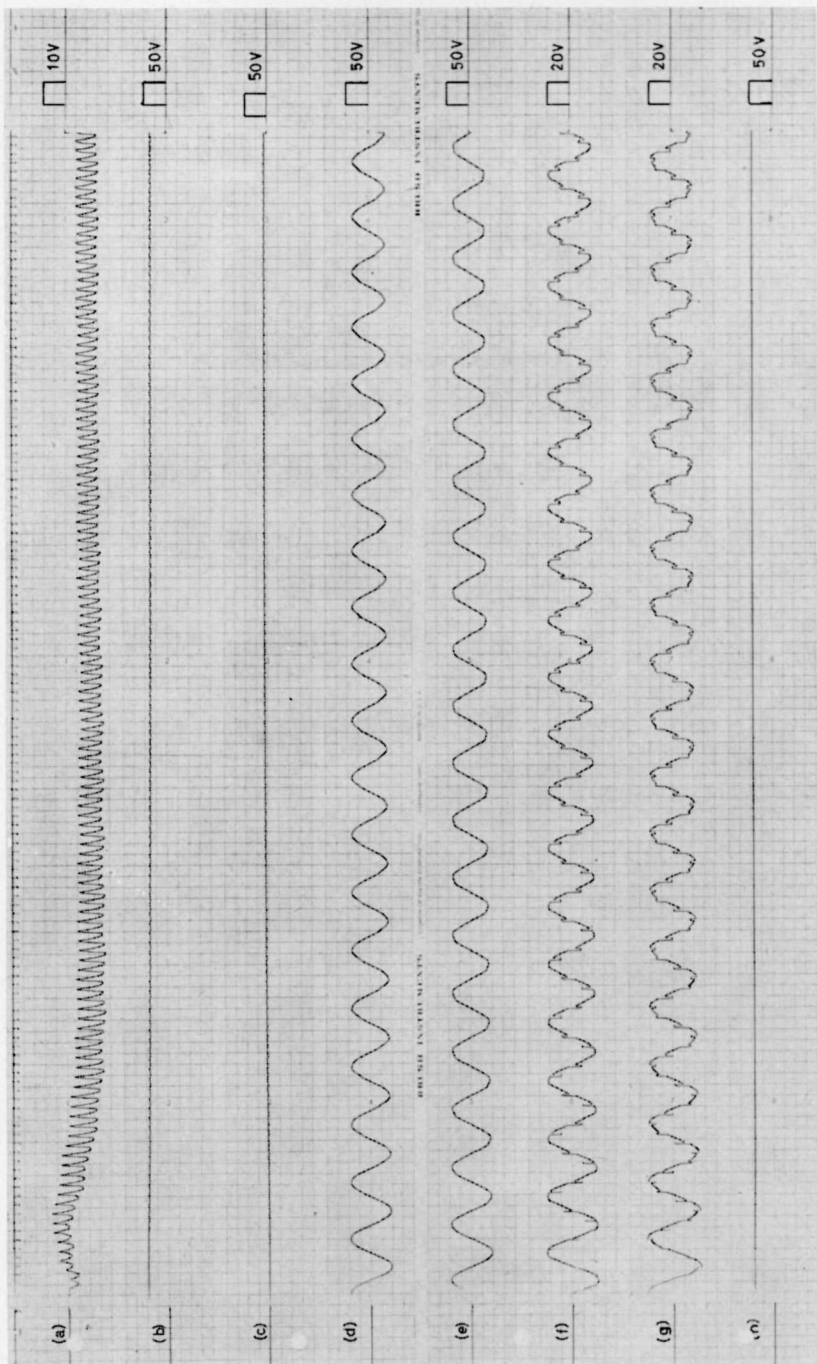


Fig. 37 iv

Fig. 38 The same oscillograms of Fig. 37 taken with enlarged scale.

$$\begin{array}{lll}
 U_d^r = 1.3 & U_f^r = 1 & \alpha' = 170^\circ \\
 M_a^r = 0.4 & \dot{\gamma}_0 = 1 & \gamma_0 = 0
 \end{array}$$

Fig. 38i

$$\begin{array}{lll}
 (a) = 0.1 i_1^r & (d) = 0.25 u_1^r & (g) = 5 i_Q^r \\
 (b) = 0.1 i_2^r & (e) = 0.75 u_0^r & (h) = 0.25 i_f^r \\
 (c) = 0.1 i_3^r & (f) = 2 i_D^r &
 \end{array}$$

Fig. 38ii

$$\begin{array}{lll}
 U_d^r = 1.3 & U_f^r = 1 & \alpha' = 170^\circ \\
 M_a^r = 0.4 & \dot{\gamma}_0 = 1 & \gamma_0 = 0 \\
 (a) = 0.1 i_\alpha^r & (d) = 0.5 i_q^r & (g) = 0.05 \frac{d i_1^r}{d t_c} \\
 (b) = 0.1 i_\beta^r & (e) = 0.05 \frac{d i_d^r}{d t_c} & (h) = \frac{0.5 u_L^r}{L_d^r} \\
 (c) = 0.5 i_d^r & (f) = 0.05 \frac{d i_q^r}{d t_c} &
 \end{array}$$

Fig. 38iii

$$\begin{array}{lll}
 U_d^r = 1.3 & U_f^r = 1 & \alpha' = 170^\circ \\
 M_a^r = 0.4 & \dot{\gamma}_0 = 1 & \gamma_0 = 0 \\
 (a) = 0.25 u_\alpha^r & (d) = 0.25 u_q^r & (g) = 0.25 \frac{d \psi_d^r}{d t_c} \\
 (b) = 0.25 u_\beta^r & (e) = 0.25 u_{v1}^r & (h) = 0.25 \frac{d \psi_q^r}{d t_c} \\
 (c) = 0.25 u_d^r & (f) = 0.25 u_{0k}^r &
 \end{array}$$

Fig. 38iv

$$\begin{array}{lll}
 U_d^r = 1.3 & U_f^r = 1 & \alpha' = 170^\circ \\
 M_a^r = 0.4 & \dot{\gamma}_0 = 1 & \gamma_0 = 0 \\
 (a) = 0.25 M_c^r & (d) = 0.5 \psi_\alpha^r & (g) = 0.25 \frac{d \psi_\beta^r}{d t_c} \\
 (b) = 0.5 \psi_d^r & (e) = 0.5 \psi_\beta^r & (h) = 0.5 \dot{\gamma} \\
 (c) = 0.5 \psi_q^r & (f) = 0.25 \frac{d \psi_\alpha^r}{d t_c} &
 \end{array}$$

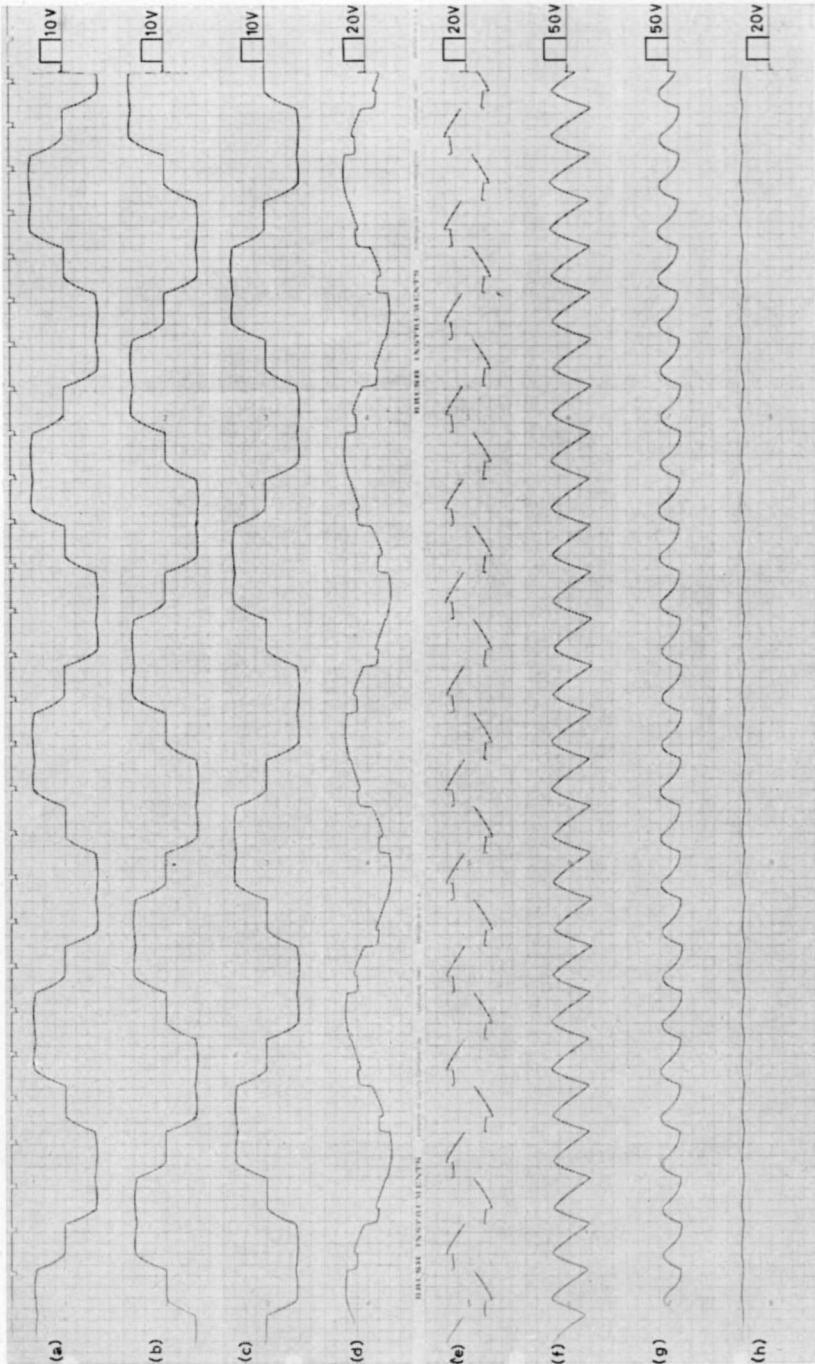


Fig. 381

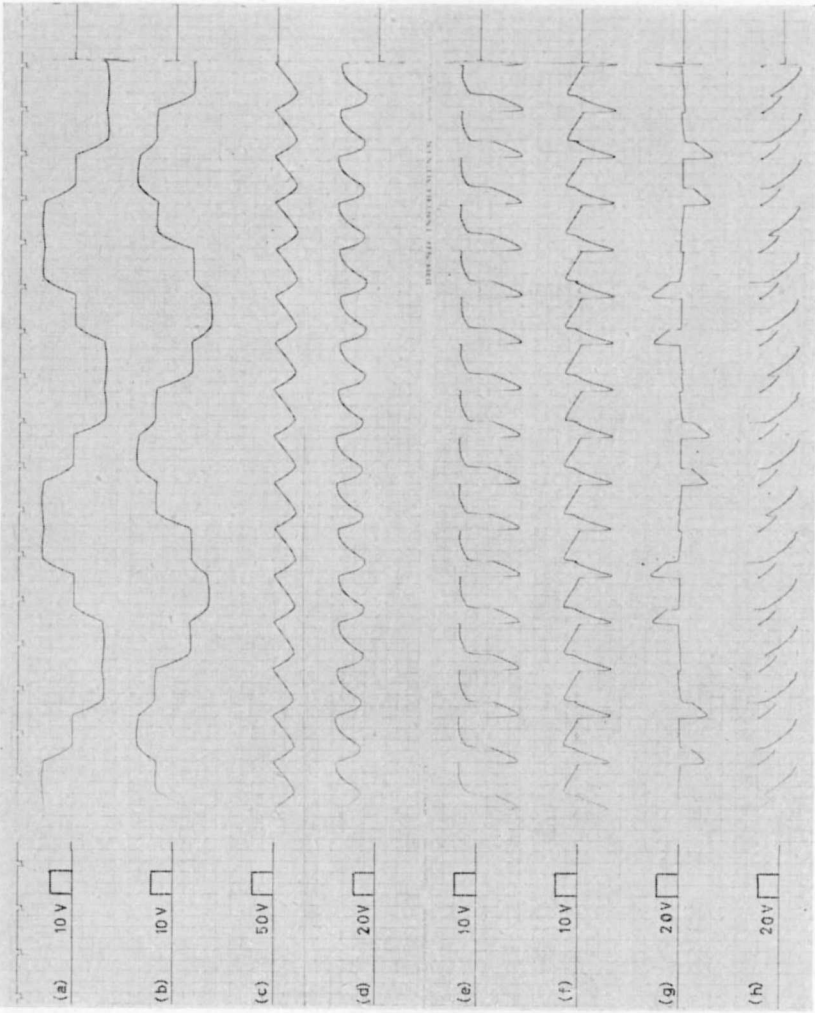


Fig. 38 ii

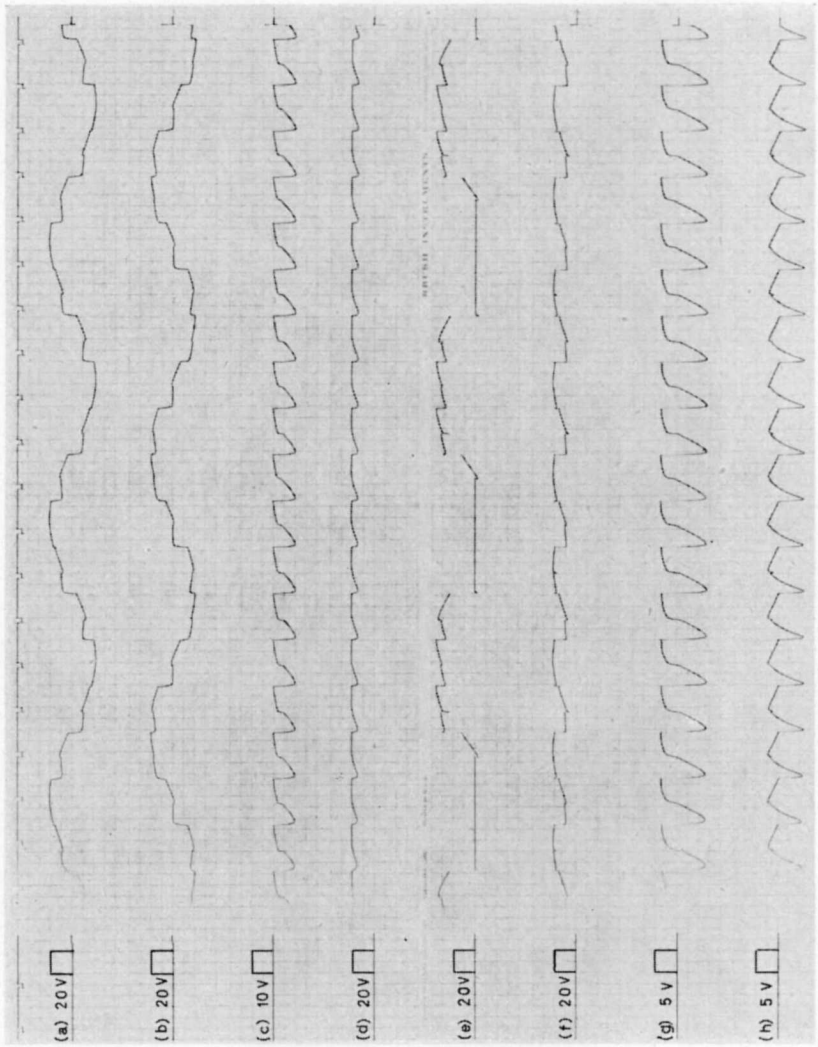


Fig. 38 iii

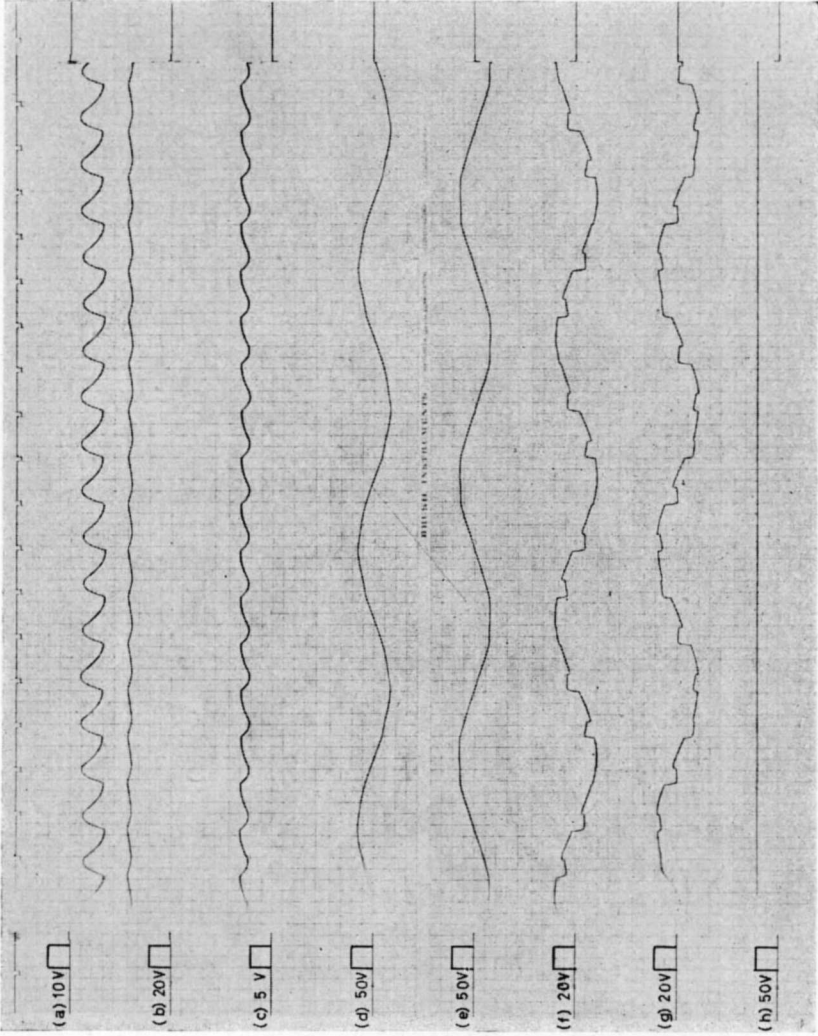


Fig. 38 iv

9.3 Characteristic curves

9.3.1 External characteristics

This shows the behaviour of the average value of the d.c. current $I_{d.c.}^r$ with respect to the applied voltage U_d^r and with α' as parameter. The current $I_{d.c.}^r$ is given by

$$I_{d.c.}^r = \frac{1}{2\pi} \int_0^{2\pi} (i_{1+}^r + i_{2+}^r + i_{3+}^r) dt_c$$

This was carried on for the case when $\gamma = 1$ and $U_f^r = 1$.

Fig. 39 shows the $U_d^r - I_{d.c.}^r$ curves for different values of α' as parameter.

9.3.2 Current locus

The same procedure given in section 6.4.3 to obtain the locus of the fundamental component of the current in the single-phase case was again applied in the case of the three-phase machine. Thus it was taken into consideration the fact that the phase voltage is not a pure sine wave. The fundamental component of the current was drawn with the fundamental component of the voltage as reference. This was carried on for the case when $\gamma = 1$ and $U_f^r = 1$ and with α' as parameter. It is noted that the machine works with a better power factor when it is operated with higher α' , than with lower α' which is nearer to the region where the machine works as a generator.

Fig. 40 shows the family of curves where the machine works as a motor.

9.4 Behaviour of the air gap flux vector

The aim of this section is to show the behaviour of the resultant air gap flux vector and the vector corresponding to the armature reaction in the case of the three-phase controlled synchronous machine.

The flux ψ_d^r linking the d -winding was recorded with the time axis extended in order to increase the accuracy of the measurement. In order to obtain the air gap flux corresponding to that winding, the leakage flux was subtracted from ψ_d^r , then it was drawn on polar co-ordinates. Because this oscillogram was taken for the case of constant speed, the time is a direct measure for the angle γ , which the rotor has moved.

The same was also made on the flux ψ_q^r after subtracting the leakage flux and taking into consideration the position effect of the q -winding with respect to the d -winding, namely 90° in advance.

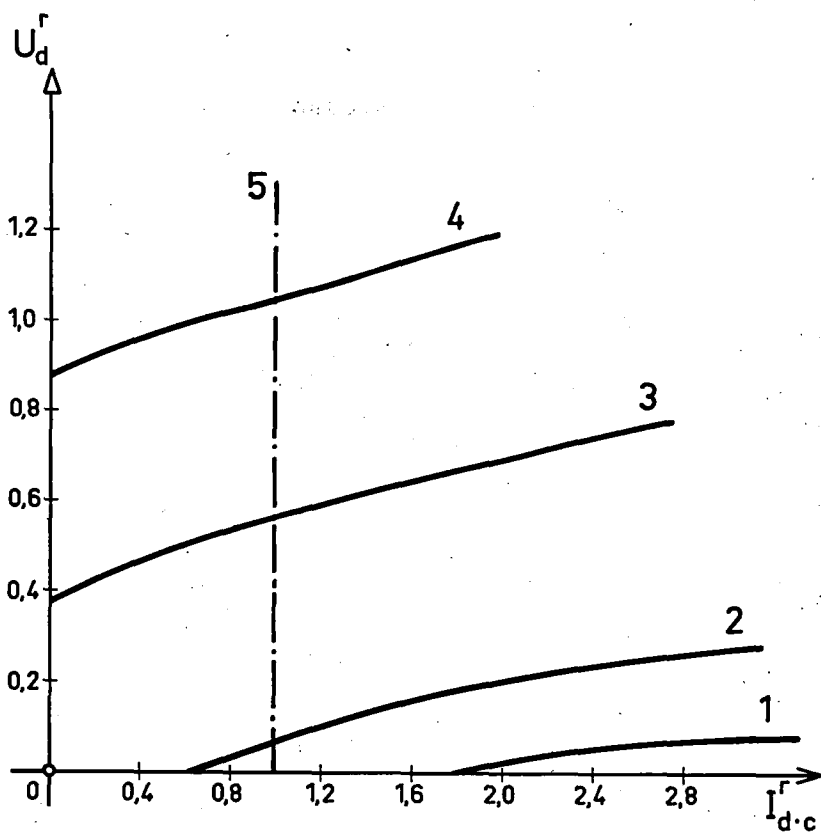


Fig. 39 External characteristics of the three-phase controlled synchronous machine

$\dot{\gamma} = 1$	$U_f^r = 1$
1 $\alpha' = 110^\circ$	4 $\alpha' = 160^\circ$
2 $\alpha' = 120^\circ$	5 $I_{d.c.}^r = 1$
3 $\alpha' = 140^\circ$	

The resultant of these two curves multiplied by the factor 1.5 was plotted and shown in Fig. 41 (curve No. 3).

The factor 1.5 is a direct consequence of the mathematical definition of ψ_d^r and ψ_q^r as a function of $\psi_1^r, \psi_2^r, \psi_3^r$. Curve No. 1 of Fig. 41 represents the direct axis flux vector with respect to the fixed axes co-ordinates. Also curve No. 2 represents the quadrature axis flux.

In order to obtain the vector of the flux originated by the armature

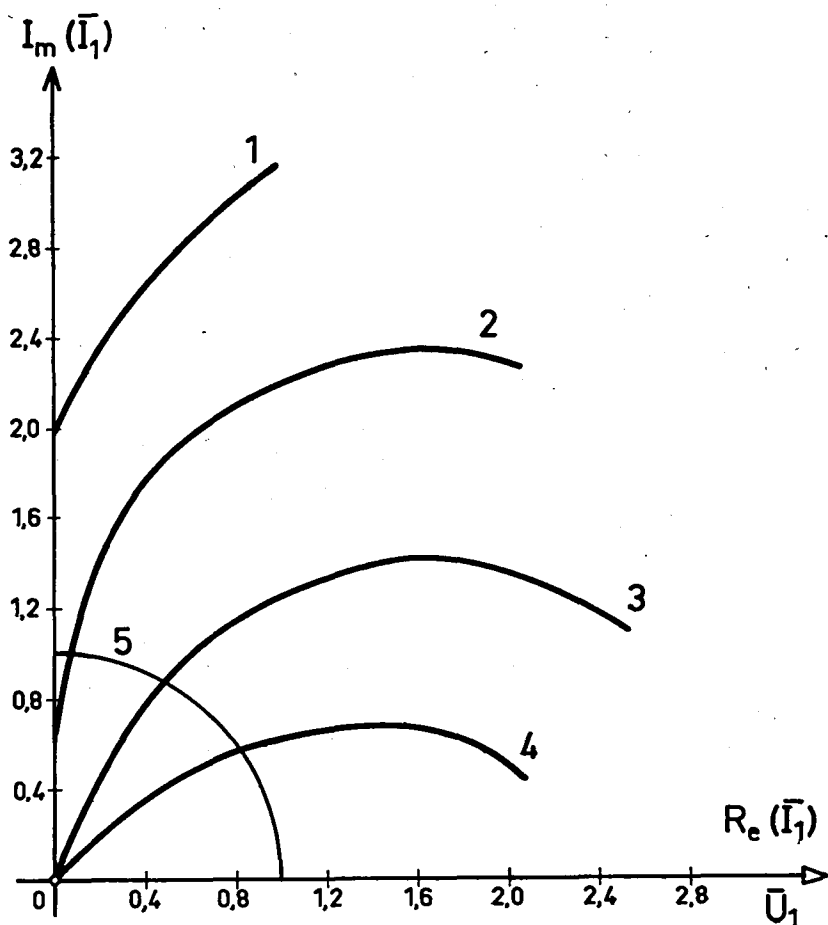


Fig. 40 Current locus for the three-phase controlled synchronous machine

$$\dot{\varphi} = 1$$

$$U_f' = 1$$

$$1 \quad \alpha' = 110^\circ$$

$$4 \quad \alpha' = 160^\circ$$

$$2 \quad \alpha' = 120^\circ$$

$$5 \quad \bar{I}_1 = 1$$

$$3 \quad \alpha' = 140^\circ$$

reaction, we had to draw the flux linking the winding d when the armature reaction is not present, which equals the total flux of the field winding minus the leakage flux. Thus we obtained curve No. 4 of Fig. 41.

The point A on curve No. 3 corresponds to the point B on curve No. 4. Thus the armature reaction at this instant is represented by the vector \vec{BA} .

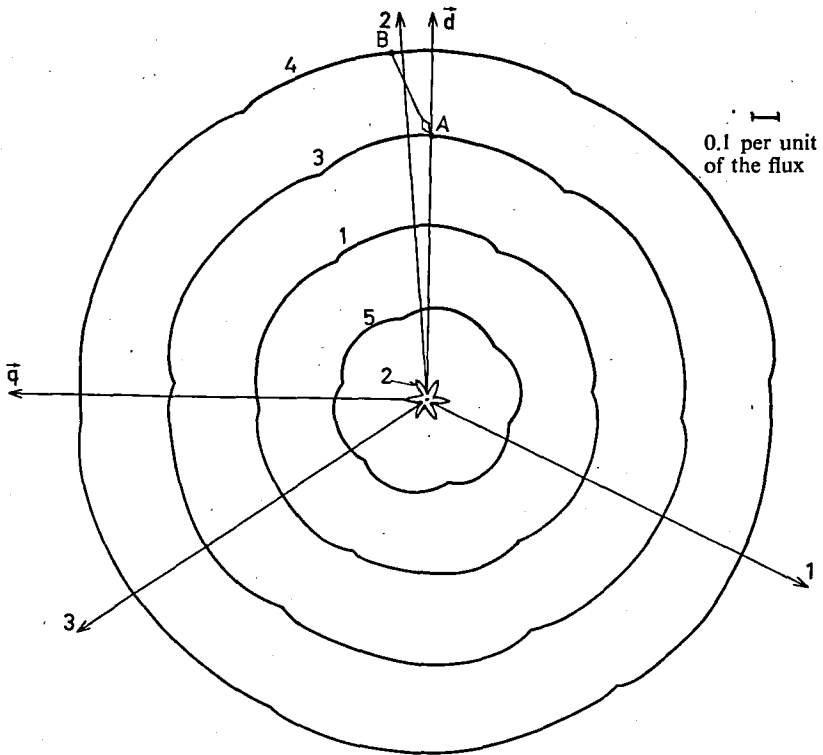


Fig. 41 The flux vector linking the different coils of the three-phase controlled synchronous machine and the armature reaction flux vector drawn with respect to the fixed axes

$$U_d' = 0.16$$

$$U_f' = 1.5$$

$$\dot{\gamma} = 1$$

$$\alpha' = 115^\circ$$

1 = the flux vector linking the d -coil

2 = the flux vector linking the q -coil

3 = the total air gap flux vector

4 = the total air gap flux vector without the armature reaction

5 = the armature reaction flux vector

This was repeated on different points on curve No. 4, determining the corresponding points on curve No. 3 and deducing the vector of the armature reaction. Hence vectors were then drawn from the origin O, and the curve No. 5 was obtained representing the armature reaction flux vector with respect to the fixed axes.

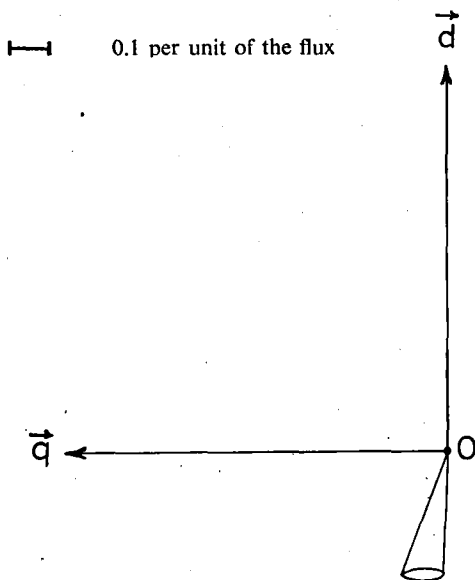


Fig. 42 The armature reaction flux vector drawn with respect to the moving axes d, q

$$\begin{array}{ll}
 U_d^r = 0.16 & U_f^r = 1.5 \\
 \dot{\gamma} = 1 & \alpha' = 115^\circ
 \end{array}$$

It is also of interest to draw that vector with respect to the movable axes d and q . This was again deduced from curve No. 5 of Fig. 41, where every vector was moved backwards by the angle that the rotor has moved. Thus the curve shown in Fig. 42 was obtained.

9.5 Transient behaviour

The effect of sudden change of the applied voltage U_d^r and the mechanical torque M_a^r on the different oscillograms of the machine were carried on. Fig. 43 i...43 iv gives the effect of suddenly decreasing the voltage U_d^r from 1.3 to 1.1. The oscillograms of the waves in the quadrature axis direction are much greatly affected than those on the direct axis because the field time constant tries to keep the flux in the direct axis constant.

The effect of the sudden increase of the mechanical torque M_a^r from 0.4 to 0.7 is to be seen in Fig. 44 i...44 iv.

Fig. 43 The effect of sudden decrease of the applied voltage U_d^r on the oscillograms of the three-phase controlled synchronous machine

$$U_f^r = 1 \qquad \alpha' = 170^\circ \qquad M_a^r = 0.4$$

U_d^r is suddenly reduced from 1.3 to 1.1

Fig. 43 i

$$\begin{aligned} (a) &= 0.1 i_1^r & (d) &= 0.25 u_1^r & (g) &= 5 i_Q^r \\ (b) &= 0.1 i_2^r & (e) &= 0.25 i_f^r & (h) &= 0.125 U_d^r \\ (c) &= 0.1 i_3^r & (f) &= 2 i_D^r \end{aligned}$$

Fig. 43 ii

$$\begin{aligned} (a) &= 0.1 i_a^r & (d) &= 0.5 i_q^r & (g) &= 0.05 \frac{d i_1^r}{d t_c} \\ (b) &= 0.1 i_\beta^r & (e) &= 0.05 \frac{d i_d^r}{d t_c} & (h) &= 0.125 U_d^r \\ (c) &= 0.5 i_d^r & (f) &= 0.05 \frac{d i_q^r}{d t_c} \end{aligned}$$

Fig. 43 iii

$$\begin{aligned} (a) &= 0.25 u_\alpha^r & (d) &= 0.25 u_q^r & (g) &= 0.25 \frac{d \psi_q^r}{d t_c} \\ (b) &= 0.25 u_\beta^r & (e) &= 0.25 u_{v1}^r & (h) &= 0.125 U_d^r \\ (c) &= 0.25 u_d^r & (f) &= 0.25 \frac{d \psi_d^r}{d t_c} \end{aligned}$$

Fig. 43 iv

$$\begin{aligned} (a) &= 0.25 M_e^r & (d) &= 0.5 \psi_\alpha^r & (g) &= 0.25 \frac{d \psi_\beta^r}{d t_c} \\ (b) &= 0.5 \psi_d^r & (e) &= 0.5 \psi_\beta^r & (h) &= 0.125 U_d^r \\ (c) &= 0.5 \psi_q^r & (f) &= 0.25 \frac{d \psi_\alpha^r}{d t_c} \end{aligned}$$

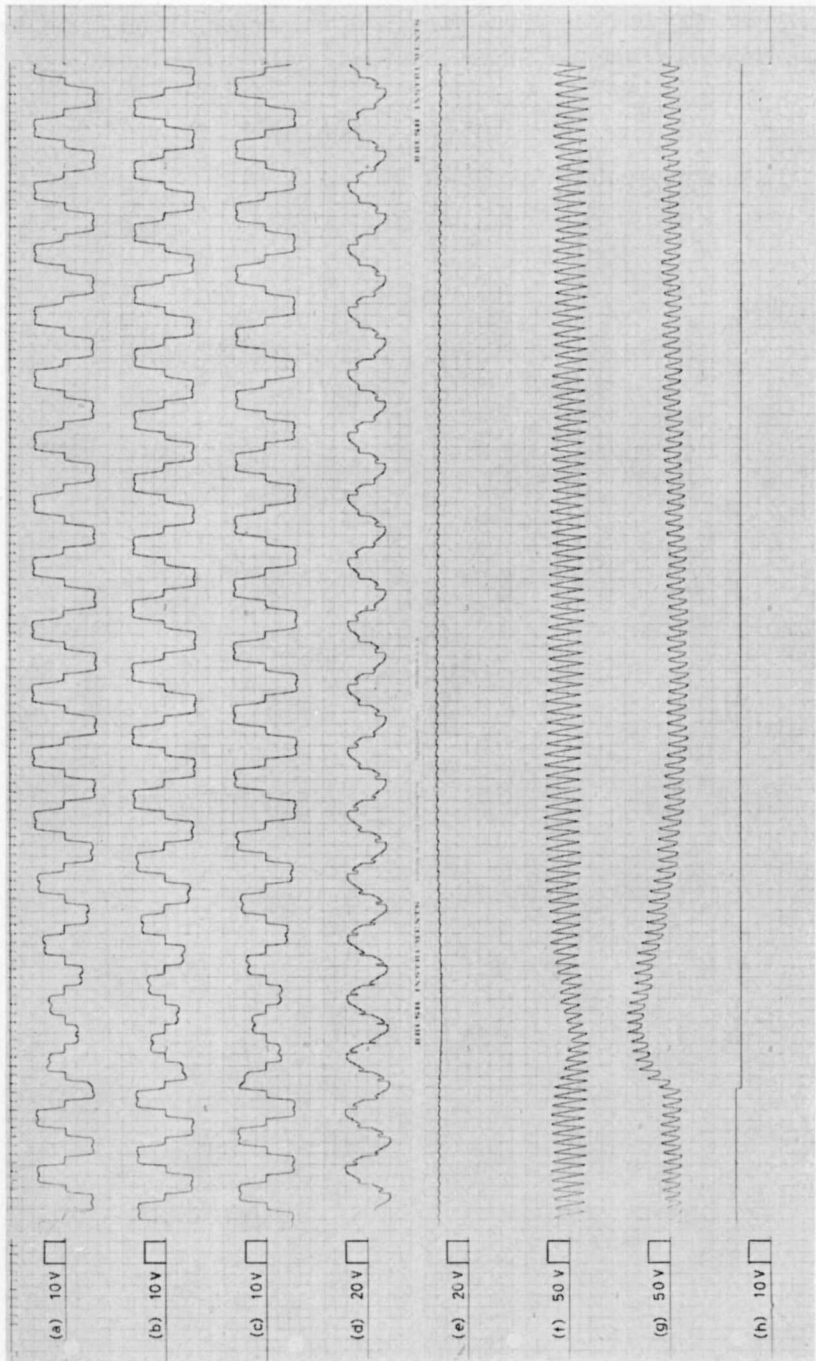


Fig. 43 i

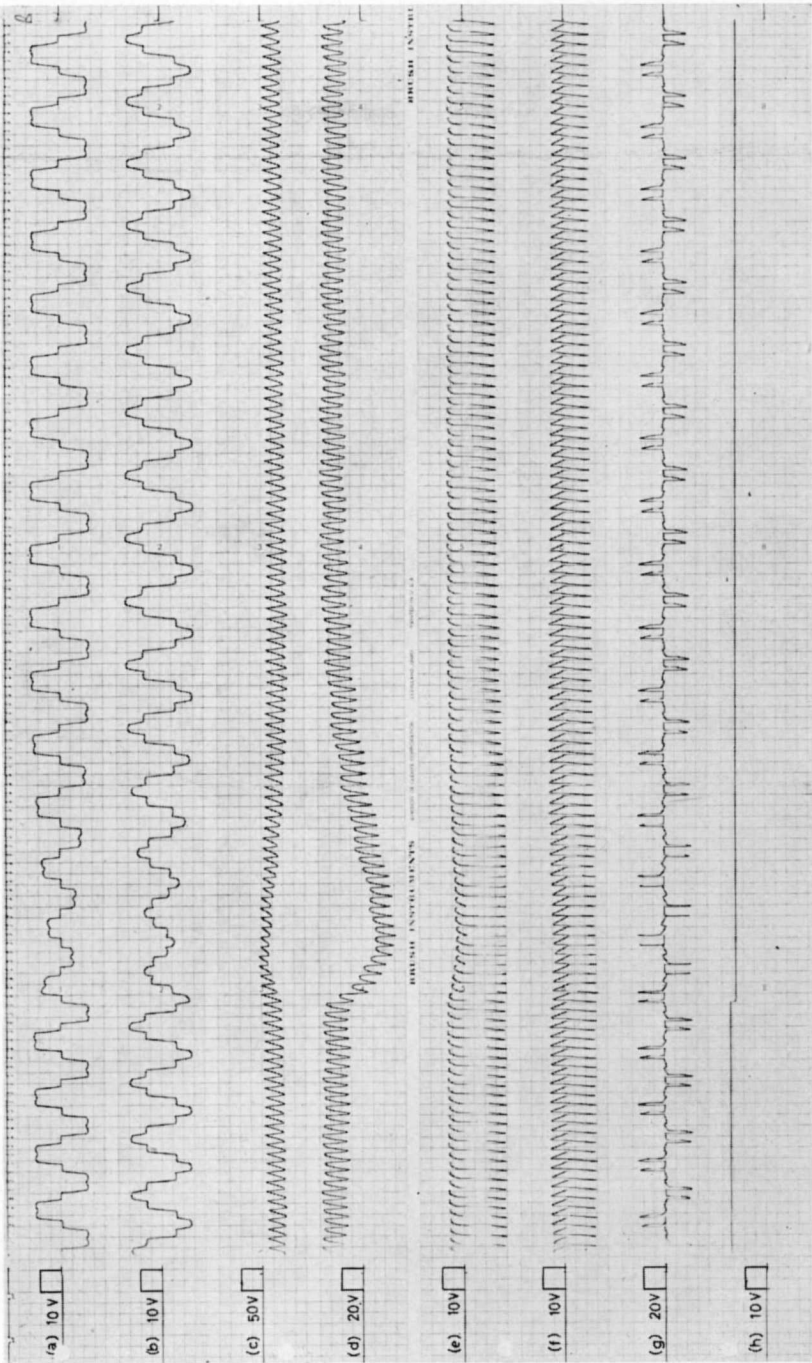


Fig. 43 ii

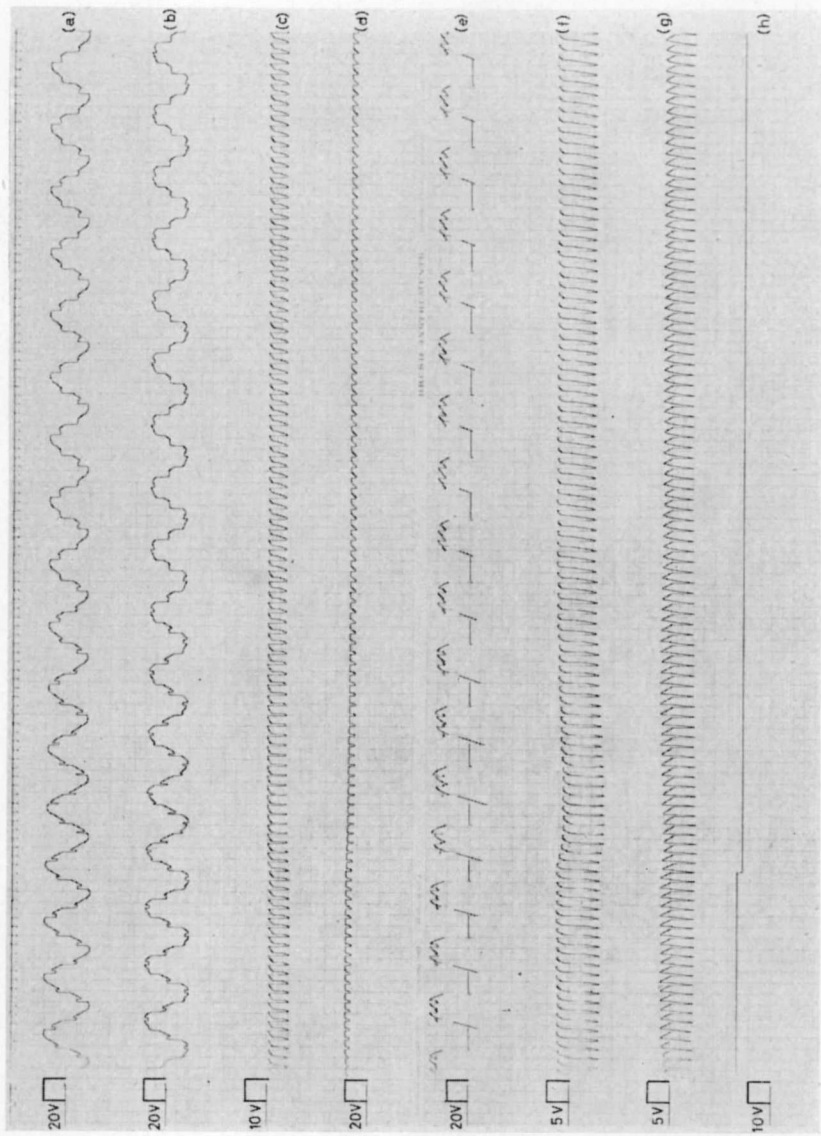


Fig. 43 iii

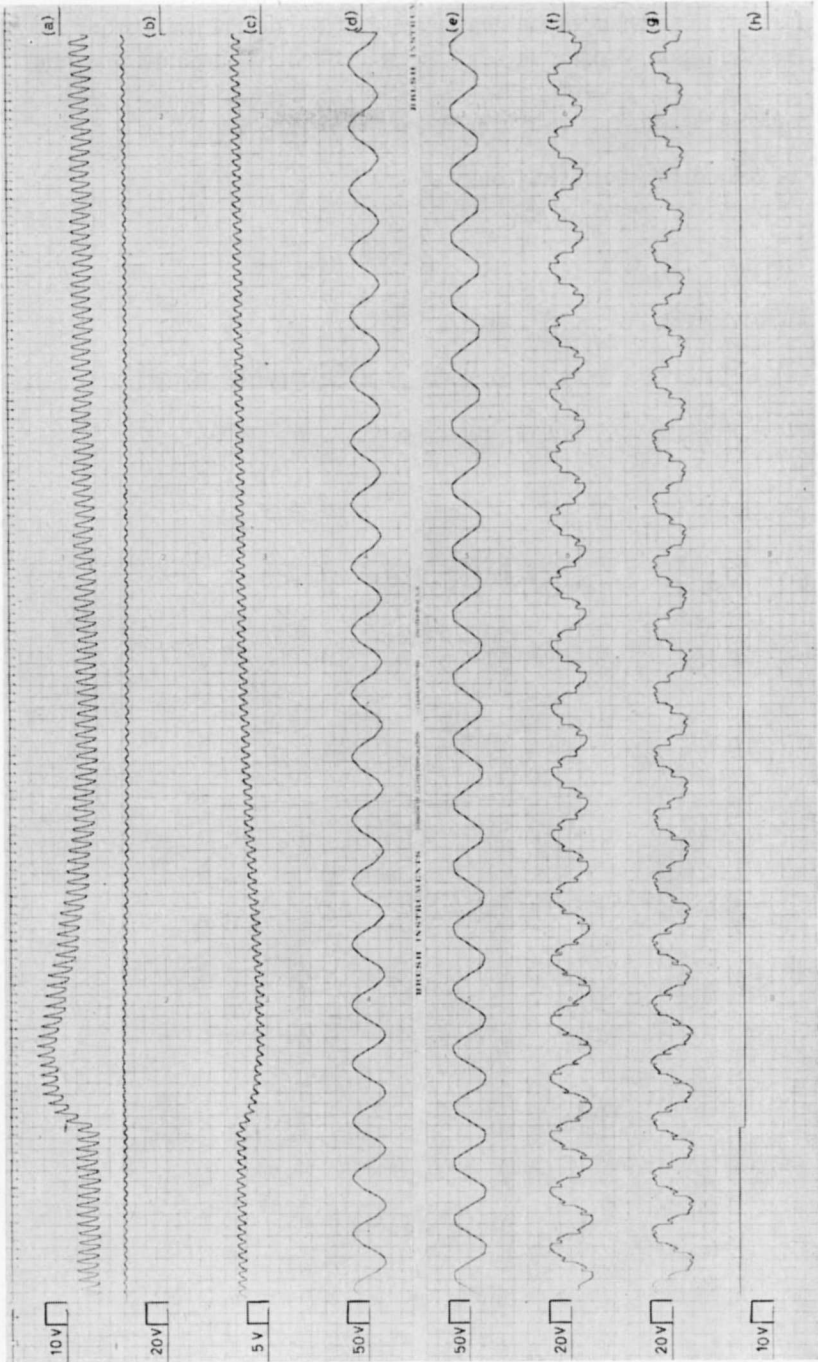


Fig. 43 iv

Fig. 44 The effect of sudden increase of the mechanical torque M_a^r on the oscillograms of the three-phase controlled synchronous machine

$$U_f^r = 1 \quad \alpha' = 170^\circ \quad U_d^r = 1.3$$

M_a^r is suddenly increased from 0.4 to 0.7

Fig. 44 i

$$\begin{array}{lll} \text{(a)} = 0.1 i_1^r & \text{(d)} = 0.25 u_1^r & \text{(g)} = 5 i_D^r \\ \text{(b)} = 0.1 i_2^r & \text{(e)} = 0.25 i_f^r & \text{(h)} = 0.25 M_a^r \\ \text{(c)} = 0.1 i_3^r & \text{(f)} = 2 i_D^r & \end{array}$$

Fig. 44 ii

$$\begin{array}{lll} \text{(a)} = 0.1 i_a^r & \text{(d)} = 0.5 i_q^r & \text{(g)} = 0.05 \frac{d i_1^r}{d t_c} \\ \text{(b)} = 0.1 i_\beta^r & \text{(e)} = 0.05 \frac{d i_d^r}{d t_c} & \text{(h)} = 0.25 M_a^r \\ \text{(c)} = 0.5 i_d^r & \text{(f)} = 0.05 \frac{d i_q^r}{d t_c} & \end{array}$$

Fig. 44 iii

$$\begin{array}{lll} \text{(a)} = 0.25 u_a^r & \text{(d)} = 0.25 u_q^r & \text{(g)} = 0.25 \frac{d \psi_a^r}{d t_c} \\ \text{(b)} = 0.25 u_\beta^r & \text{(e)} = 0.25 u_{v1}^r & \text{(h)} = 0.25 M_a^r \\ \text{(c)} = 0.25 u_d^r & \text{(f)} = 0.25 \frac{d \psi_d^r}{d t_c} & \end{array}$$

Fig. 44 iv

$$\begin{array}{lll} \text{(a)} = 0.25 M_a^r & \text{(d)} = 0.5 \psi_a^r & \text{(g)} = 0.25 \frac{d \psi_a^r}{d t_c} \\ \text{(b)} = 0.25 M_e^r & \text{(e)} = 0.5 \psi_\alpha^r & \text{(h)} = 0.25 \frac{d \psi_\beta^r}{d t_c} \\ \text{(c)} = 0.5 \psi_d^r & \text{(f)} = 0.5 \psi_\beta^r & \end{array}$$

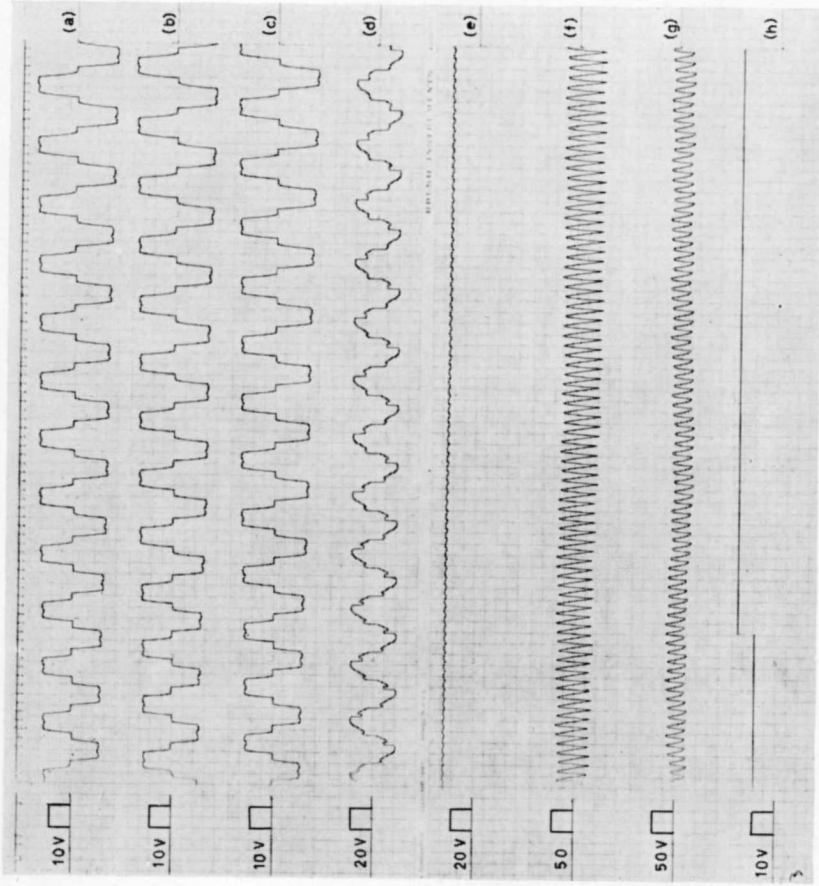


Fig. 44 i

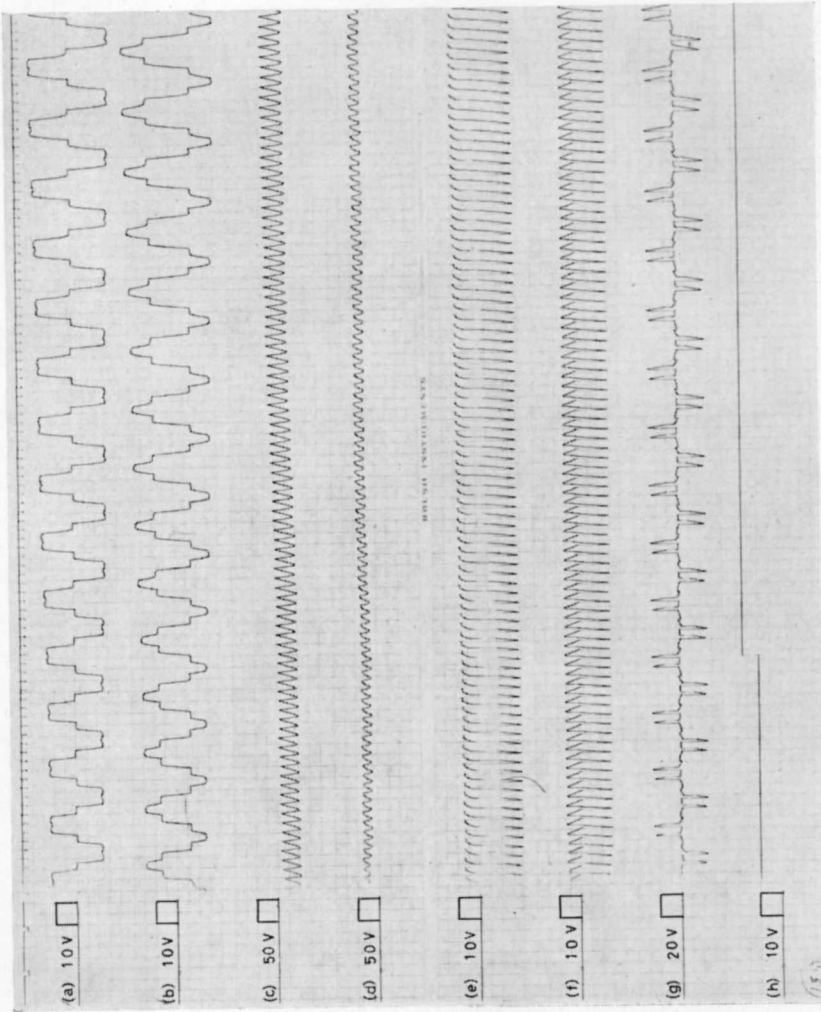


Fig. 44 ii

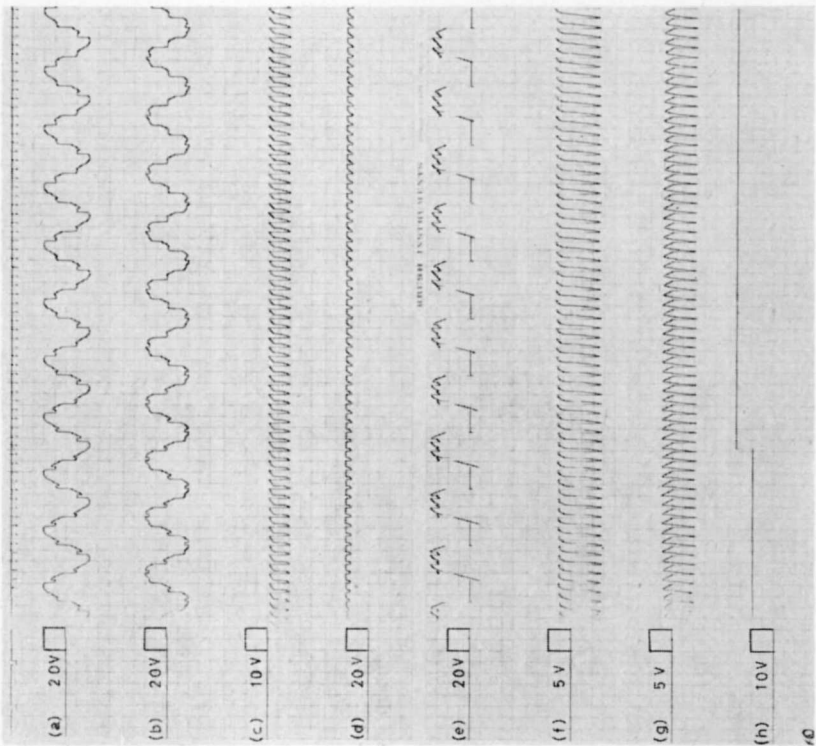


Fig. 44 iii

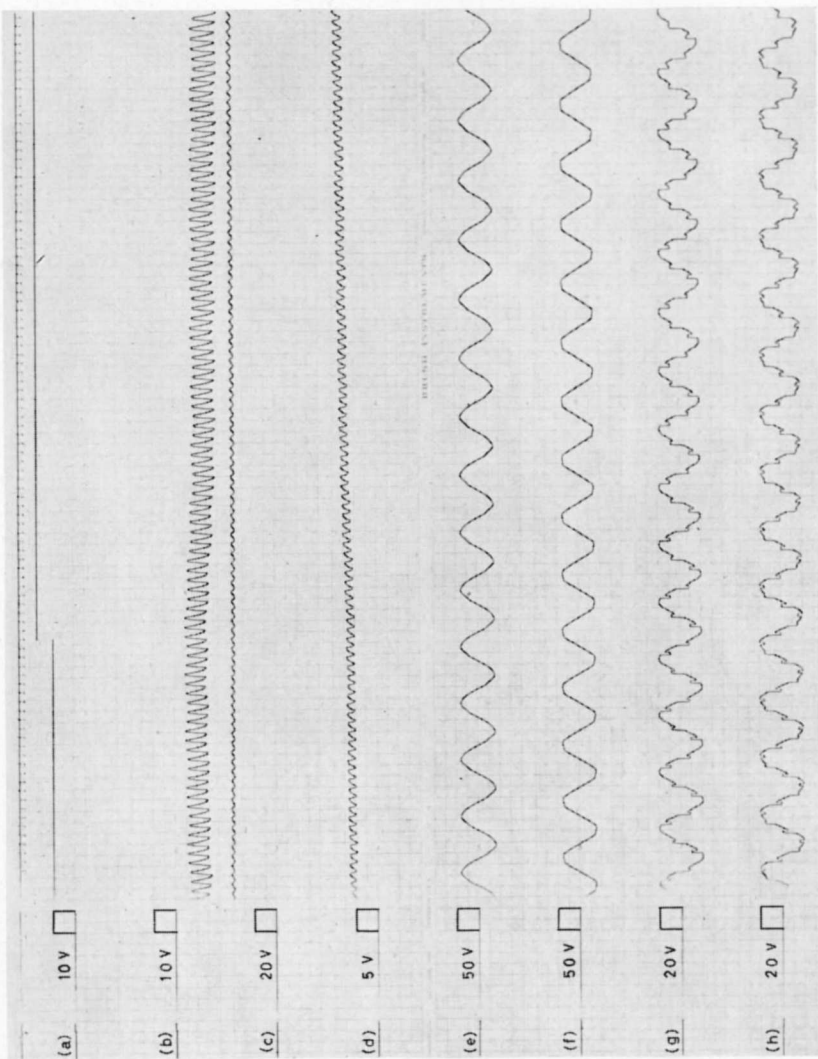


Fig. 44 iv

10. SUMMARY AND CONCLUSION

This thesis deals with the investigation of a thyatron controlled synchronous motor.

The motor was examined experimentally, but it was found that the measurements made directly on the machine do not give a complete picture of its behaviour, e.g. it was not possible to measure the instantaneous value of the electromagnetic torque, or the currents in the damper windings. It is possible to investigate the behaviour of each quantity belonging to the machine if it is mathematically analyzed. Since the synchronous machine is in general complicated, and since the insertion of the thyatrons or silicon-controlled rectifiers in its stator increases this complexity, it was found more convenient to use an analog computer as a means of solving this problem.

The system was solved for the single- and the three-phase cases. The stator currents, voltages and fluxes were transformed at first on the (α, β) stationary axes and then on the (d, q) moving axes. Thus the whole transformation was separated into a linear and a nonlinear one. This has the advantage of greatly reducing the necessary number of multipliers. It was then possible to take oscillograms for all the quantities of interest, especially the currents flowing in both the damper windings in the transient and the steady states. Oscillograms were also taken for the instantaneous value of the electromagnetic torque and for the voltage across the thyatrons in both the transient and steady states.

The external characteristic curves were calculated, also the loci of the fundamental component of the stator currents were plotted against that of the stator voltage with α' as a parameter. The behaviour of the air gap flux vector was studied for a certain operating point and the armature reaction flux vector was deduced. This was drawn once with respect to the stationary axes and another with respect to the moving axes. The effect of the sudden variation of the applied voltage on the different oscillograms was shown. The oscillograms show how the motor functions as a generator for a short time and then back to the motor action through the sudden decrease of the applied d.c. voltage U_d . This is most obvious when the oscillograms of the electromagnetic torque and that of the current i_q are considered. The effect of the sudden variation of the mechanical torque was also studied.

The pulses controlling the synchronous machine in our case were obtained from voltages taken from a tachometer mounted on the shaft of the machine. It is proposed that these pulses may be obtained from a separate source, so that the speed may be varied by varying the frequency of that source.

In the publication made by Prof. ED. GERECKE [21], the problem was calculated after making some simplifications. All the resistances in the a.c. side were neglected and the inductance in the d.c. side was assumed to be infinitely large. However, an agreement to a great extent can be noted between the oscillograms obtained in this thesis and those got in the mentioned paper. The angle α' in this thesis equals $(60 + \psi)$ in that paper. The simulation of the motor in this thesis was executed on two types of computers, the first on a "Donner" type and the second on a PACE one. The simulation on the Donner computer demanded the building of a circuit simulating the thyatron effect. This contained 18 gates, 15 bistable multivibrators, 15 Schmitt triggers and two saw tooth generators.

The comparators already built in the PACE analog computer were made use of to simulate the thyratrons.

ZUSAMMENFASSUNG

Untersuchung eines kommutatorlosen Gleichstrommotors, bestehend aus einer Drehstrom-Synchronmaschine und einem Wechselrichter, durch Simulation auf einem Analogrechner.

Zweck der Arbeit ist die Untersuchung aller Ströme und Spannungen sowie des Drehmomentes eines kollektorlosen Gleichstrommotors. Dieser besitzt eine normale dreiphasige, in Stern geschaltete Statorwicklung und ein Polrad mit ausgeprägten Polen, einer Erregerwicklung und zwei in der Längs- bzw. Querachse angeordneten Dämpferwicklungen. Die Speisung erfolgt von einer Gleichspannungsquelle aus über eine Glättungsinduktivität und über eine dreiphasige, mit sechs steuerbaren Ventilen (Thyatronen oder Thyristoren) ausgerüstete Brückenschaltung. Zunächst wurde ein 4-kW-Motor experimentell untersucht. Die Steuerung der Ventile erfolgte von einem auf der Motorwelle angebrachten dreiphasigen Tachogenerator aus. Es wurden die Oszillogramme aller zugänglichen Ströme und Spannungen im Ein- und Dreiphasenbetrieb aufgenommen und ferner das Drehmoment elektronisch gemessen. Ferner wurden alle für die anschließenden Berechnungen nötigen Daten der Maschine ermittelt.

Für die theoretische Untersuchung wurde zunächst das Dreiphasensystem des Stators in ein ruhendes Zweiphasensystem umgewandelt und dieses nach der Zweiachsentheorie in ein mit dem Polrad synchron rotierendes Zweiachsensystem übergeführt. Über die Kurvenform der Ströme und Spannungen wurden keine Annahmen gemacht. Ferner wurden der Erregerstrom sowie die beiden Dämpferströme in die Rechnung einbezogen. Zudem waren die Verschiedenheit des magnetischen Widerstandes in der Längs- und Querachse sowie die verschiedenen Streuungen und eine veränderliche Drehzahl zu berücksichtigen. Es handelt sich also um ein hochgradig nichtlineares System, weshalb die Laplace-Transformation nicht verwendet werden konnte. Für die Koordinatentransformationen wurden die benötigten Matrizen ermittelt. Ferner mußten die Schaltbedingungen der Ventile formuliert werden.

Die Nachbildung wurde alsdann auf total sechs kleinen Analogrechnern (Donner, Kalifornien) vorgenommen. Da die Zahl der Multiplikatoren auf acht beschränkt war, mußte die Programmierung unter Verwendung

der vorhandenen Mittel durchgeführt werden, was Differentiationen bedingte. Für die Erzeugung der Zündimpulse wurde ein transistorisierter sechsphasiger Impulsgenerator gebaut. Es gelang dann, sowohl im Einphasen- wie im Dreiphasenbetrieb die Oszillogramme aller Spannungen und aller Ströme, ja sogar der beiden Dämpferströme, aufzunehmen. Die Übereinstimmung mit den experimentell ermittelten war befriedigend, jedoch zeigten sich zufolge der Differentiation einige Unschönheiten.

Daher wurde das Problem nochmals auf dem von der ETH inzwischen angeschafften großen Analogrechner «PACE 231-R» programmiert, wobei es durch Umformung des Gleichungssystemes gelang, ohne irgendwelche Differentiationen auszukommen. Es ergaben sich nun sehr saubere Oszillogramme aller Ströme und Spannungen sowie des elektromagnetischen Drehmomentes. Dieses zeigt neben dem konstanten Wert einen mit der dreifachen Statorfrequenz leicht pulsierenden Anteil. Ferner wurden alle Oszillogramme ebenfalls bei transienten Zuständen, wie plötzlichem Belasten, bei plötzlicher Änderung des Lastmomentes und bei schrittweiser Veränderung der speisenden Gleichspannung, ermittelt. Es zeigte sich dabei, daß die Maschine kurzzeitig als Generator arbeitet und Gleichstrom an die Speisequelle zurückliefert.

LITERATURE

- [1] PARK, R. H.: Two-reaction theory of synchronous machines, generalized method of analysis. Part I. AIEE Transactions, vol. 48, 1929, pp. 716-727.
- [2] CONCORDIA, C.: Synchronous machines, theory and performance. John Wiley and Sons, Inc., New York 1951.
- [3] LAIBLE, T.: Die Theorie der Synchronmaschine im nichtstationären Betrieb. Springer-Verlag, 1952.
- [4] WHITE and WOODSON: Electromechanical energy conversion. John Wiley and Sons, Inc., New York 1959.
- [5] KOVÁCS, K. P., und RÁCZ, I.: Transiente Vorgänge in Wechselstrommaschinen. Band I. Verlag der ungarischen Akademie der Wissenschaft, Budapest 1959.
- [6] HANNAKAM, L.: Dynamisches Verhalten von synchronen Schenkelpolmaschinen bei Drehmomentstößen. Archiv für Elektrotechnik, Band XLIII, Heft 6, 1958, S. 402-426.
- [7] AIEE Test codes for synchronous machines, No. 503, June 1945.
- [8] WARING, M. L., and CRARY, S. B.: Operational impedances of a synchronous machine. General Electric Review, 35, 1932, p. 578.
- [9] NÜRNBERG, W.: Die Prüfung elektrischer Maschinen. Berlin 1940.
- [10] BADR, H.: Primary-side thyatron controlled three-phase induction machine. Diss. No. 3060, ETH, Zurich.
- [11] COROLLER, P.: Simulation of a synchronous machine with an analogue computer. Brown Boveri Review, vol. 46, No. 5, 1959, pp. 299-306.
- [12] WILLEMS, P.: Sur la stabilité dynamique des réseaux interconnectés. Une Thèse de Doctorat en Sciences appliquées, Université Libre de Bruxelles, 1956.
- [13] FIFER, S.: Analogue computation. McGraw-Hill, Inc., New York 1961.
- [14] JOHNSON: Analog computer techniques. McGraw-Hill, Inc., New York 1956.
- [15] KORN and KORN: Electronic analog computers. McGraw-Hill, Inc., New York 1952.
- [16] MILLMAN and TAUB: Pulse and digital circuits. McGraw-Hill, Inc., New York 1956.

- [17] PRESSMAN, A.: Design of transistorized circuits for digital computers. John F. Rider, Inc., New York 1959.
- [18] SEV 0192, 1959: Regeln und Leitsätze für Buchstabensymbole und Zeichen, 4. Auflage, 1959.
- [19] International Electrotechnical Commission (IEC), Recommendations for mercury arc converters, Publication 84, 1957.
- [20] BAUMGARTNER: Dynamisches Verhalten von Regelkreisen und reaktiven Verstärkermaschinen mit Begrenzungs- und Hysterese-gliedern. ETH Zürich, Promotionsarbeit Nr. 2916, 1959.
- [21] GERECKE, ED.: Synchronmaschine mit Stromrichterbelastung. Neue Technik 3, 11, 758–766 (1961).

CURRICULUM VITAE

I was born in Alexandria, Egypt, on the 25th of September 1933. I attended the primary school during the years 1942–1946 and the secondary school during the years 1946–1951, both in Alexandria. I passed the maturity examination in July 1951. In October 1951, I began my studies at the Faculty of Engineering, Alexandria University, and in June 1956, I was awarded the B.Sc. degree in Electrical Engineering. From October 1956 until February 1958, I have worked at the Ministry of Industry in Cairo. In April 1958, I began my studies at the Institute of Automatic Control and Industrial Electronics of the Swiss Federal Institute of Technology at Zurich under the supervision of Prof. ED. GERECKE. In November 1959, I passed the admission examination to the doctorate work. This thesis was carried out during the period from 1960 until June 1963. I passed the doctorate degree examination on the 19th of July 1963.